NAVAL POSTGRADUATE SCHOOL
Monterey, California

THESIS

USE OF USCG DIFFERENTIAL GPS BEYOND NOMINAL RANGE

by

Daniel W. Valascho

September 2002

Thesis Co-Advisors:	James R. Clynch
	James N. Eagle
Second Reader:	Lyn Whitaker

Approved for public release; distribution unlimited

THIS PAGE INTENTIONALLY LEFT BLANK

REPORT DOCUMENTATION PAGE		*Form Approved OMB No. 0704-0188*
Public reporting burden for this collection of information is estimated to average 1 hour per response, including the time for reviewing instruction, searching existing data sources, gathering and maintaining the data needed, and completing and reviewing the collection of information. Send comments regarding this burden estimate or any other aspect of this collection of information, including suggestions for reducing this burden, to Washington headquarters Services, Directorate for Information Operations and Reports, 1215 Jefferson Davis Highway, Suite 1204, Arlington, VA 22202-4302, and to the Office of Management and Budget, Paperwork Reduction Project (0704-0188) Washington DC 20503.		
1. AGENCY USE ONLY *(Leave blank)*	**2. REPORT DATE** September 2002	**3. REPORT TYPE AND DATES COVERED** Master's Thesis
4. TITLE AND SUBTITLE: The Use Of USCG Differential GPS Beyond Nominal Range		**5. FUNDING NUMBERS**
6. AUTHOR(S) Daniel W. Valascho		
7. PERFORMING ORGANIZATION NAME(S) AND ADDRESS(ES) Naval Postgraduate School Monterey, CA 93943-5000		**8. PERFORMING ORGANIZATION REPORT NUMBER**
9. SPONSORING /MONITORING AGENCY NAME(S) AND ADDRESS(ES) N/A		**10. SPONSORING/MONITORING AGENCY REPORT NUMBER**
11. SUPPLEMENTARY NOTES The views expressed in this thesis are those of the author and do not reflect the official policy or position of the Department of Defense or the U.S. Government.		
12a. DISTRIBUTION / AVAILABILITY STATEMENT Approved for public release; distribution unlimited		**12b. DISTRIBUTION CODE**

13. ABSTRACT *(maximum 200 words)*

The United States Coast Guard makes Differential GPS available to all maritime vessels in US coastal and inland waters to ensure 10 meter (2drms) horizontal accuracy. The Coast Guard guarantees this accuracy if the maritime user is within nominal range of the beacon transmitter. Maritime user's can often receive the differential correction beyond the nominal range, but the accuracy begins to degrade as baseline distance increases. After gathering differential corrections from varying distances, at different times of the day, at different latitudes, and different signal strengths, operational statistics have been calculated to describe the Differential GPS accuracy beyond the USCG's nominal range.

14. SUBJECT TERMS Differential Global Positioning System GPS DGPS USCG maritime positioning			**15. NUMBER OF PAGES** 127
			16. PRICE CODE
17. SECURITY CLASSIFICATION OF REPORT Unclassified	**18. SECURITY CLASSIFICATION OF THIS PAGE** Unclassified	**19. SECURITY CLASSIFICATION OF ABSTRACT** Unclassified	**20. LIMITATION OF ABSTRACT** UL

i

THIS PAGE INTENTIONALLY LEFT BLANK

USE OF USCG DIFFERENTIAL GPS BEYOND NOMINAL RANGE

Daniel W. Valascho
Lieutenant, United States Navy
B.S., United States Naval Academy, 1995

Submitted in partial fulfillment of the
requirements for the degree of

MASTER OF SCIENCE IN OPERATIONS RESEARCH

from the

NAVAL POSTGRADUATE SCHOOL
September 2002

Author: Daniel W. Valascho

Approved by: James R. Clynch
                    Thesis Co-Advisor

                    James N. Eagle
                    Co-Advisor

                    Lyn Whitaker
                    Second Reader

                    James N. Eagle
                    Chairman, Department of Operations Research

THIS PAGE INTENTIONALLY LEFT BLANK

ABSTRACT

The United States Coast Guard makes Differential GPS available to all maritime vessels in US coastal and inland waters to ensure 10 meter (2drms) horizontal accuracy. The Coast Guard guarantees this accuracy if the maritime user is within nominal range of the beacon transmitter. Maritime user's can often receive the differential correction beyond the nominal range, but the accuracy begins to degrade as baseline distance increases. After gathering differential corrections from varying distances, at different times of the day, at different latitudes, and different signal strengths, operational statistics have been calculated to describe the Differential GPS accuracy beyond the USCG's nominal range.

THIS PAGE INTENTIONALLY LEFT BLANK

TABLE OF CONTENTS

LIST OF FIGURES

THIS PAGE INTENTIONALLY LEFT BLANK

LIST OF TABLES

THIS PAGE INTENTIONALLY LEFT BLANK

LIST OF ABBREVIATIONS, ACRONYMS, SYMBOLS

2drms	twice distance root mean square
AOC	Area of Coverage
BCE	Broad Cast Ephemeris
C2CEN	Command and Control Center
COMDTINST	Commandant Instruction
CONUS	Continental United States
DGPS	Differential Global Positioning System
DOP	Dilution of Precision
drms	distance root mean square
FOC	Full Operational Capability
FRP	Federal Radionavigation Plan
GDOP	Geometric Dilution of Precision
GPS	Global Positioning System
HDOP	Horizontal Dilution of Precision
HHA	Harbor and Harbor Approach
HTDP	Horizontal Time Dependent Positioning
IPP	Ionospheric Pierce Point
MCS	Master Control Station
MDGPS	Maritime Differential Global Positioning System
MF	Medium Frequency
NAD-83	North American Datum (1983)
NAVSTAR	Navigation System using Timing and Ranging
NDGPS	Nationwide Differential Global Positioning System
OCS	Operational Control Segment
PDOP	Position Dilution of Precision
PE	Precise Ephemeris
PRN	Pseudo-Random Noise
SV	space vehicle
TEC	Total Electron Content
TDOP	Time Dilution of Precision
URA	User Range Accuracy
USCG	United States Coast Guard
UTC	Coordinated Universal Time
VDOP	Vertical Dilution of Precision
WGS-84	Worldwide Geodetic System (1984)

THIS PAGE INTENTIONALLY LEFT BLANK

ACKNOWLEDGMENTS

THIS PAGE INTENTIONALLY LEFT BLANK

EXECUTIVE SUMMARY

Differential Global Positioning System (DGPS) uses corrections from a reference station to improve the accuracy provided by the positioning of a normal GPS signal. This study gathered DGPS correction data from a ship off the west coast of the United States. These corrections were then post-processed to determine the effects of the time-of-day, baseline distance from the reference station and latitude on positioning accuracy. Additional results were obtained concerning the shape of the bivariate distribution of the horizontal DGPS position errors. Also, some support was provided for the National Geodetic Survey (NGS) Horizontal Time Dependent Position (HTDP) model of tectonic plate motion. All accuracy measures are reported as twice distance root mean square (2drms), which is two standard deviations of the radial horizontal error.

Time-of-day. The effect of time-of-day and distance from the reference station can be summarized with four categories plus one aggregated category. At *Night* (2300-0500 local), the observed positioning accuracy was 1.9 meters (2drms) plus one meter for each additional 400 kilometers. During *Twilight* (1800-2300 local), the observed positioning accuracy was 1.5 meters (2drms) plus one meter for each additional 200 kilometers of baseline distance. During the *Day* (1000-1800 local), the observed positioning accuracy was 2.7 meters (2drms) plus one meter for each 185 kilometers of baseline distance. At *Dawn* (0500-1000 local), the observed positioning accuracy was 3.4 meters (2drms) plus one meter for each additional 550 kilometers. The *Dawn* and *Twilight* categories were combined into a new category, *Transition* (0500-1000 & 1800-2300 local), which had an observed positioning accuracy of 2.5 meters (2drms) plus one meter for each additional 300 kilometers of baseline distance.

Latitude Difference. The effect of latitude difference between the mobile user and the reference station was notable but was strongly correlated to the distance to the reference station in this study. At close latitudes, the observed accuracy was 2.5 meters (2drms). At farther latitudes (-6º to +10º), the accuracy was 5 meters (2drms).

Error Ellipses. For the bivariate normal (BVN) distribution, the 95% error ellipse is the smallest area that contains the user's horizontal position 95% of the time. For each reference station used in this study, a best-fit BVN 95% horizontal error ellipse was created. The size and shape of these error ellipses was unique to each reference station. This error ellipse's orientation was strongly correlated to the bearing of the reference station. The semimajor axis and the eccentricity of the error ellipses were moderately correlated to the average distance from the reference station. These two statistics describe how the horizontal accuracy degrades with distance. As distance from the reference station increased, so did the semimajor axis and eccentricity of the 95% error ellipse. In general, the semimajor axis pointed from the mobile user to the reference station.

Support of NGS HTDP Model. Of the many functions of the National Geodetic Survey (NGS), one is to study the movements of the Earth's tectonic plates. NGS has developed a model to predict the plate motions as a function of time; it is called the Horizontal Time Dependent Positioning (HTDP) model.

The NGS HTDP model was employed in this study. This study provided some experimental evidence to support the validity of the HTDP model. The predictions of the HTDP model corrected the reference station location for the plate motion. By shifting the reference datum per the output of the HTDP model, systematic errors in the data were reduced, which in turn, reduced biases in the position solutions.

I.   INTRODUCTION

A.   PURPOSE

The Federal Radionavigation Plan (FRP) (DoD/DoT, 2001) defines the accuracy requirements of the Global Positioning System. The United States Coast Guard implemented a coastal and inland waterway Maritime Differential GPS to achieve Full Operational Capability on 15 September 1999. Accuracy of 10 meters (2drms)* is mandated within the Area of Coverage (AOC) of any DGPS reference station. The accuracy begins to degrade as the mobile user moves outside the AOC. The purpose of this thesis is to investigate the degradation of accuracy outside the AOC.

B.   BACKGROUND

The Navigation System using Timing and Ranging (NAVSTAR) Global Positioning System (GPS) has a space, control, and user segment. The space segment is made up of a constellation 28 space-vehicles in orbit approximately 20,200 km above the Earth at an inclination relative to the equator of 55°. The control segment is composed of ground tracking stations to measure distances to the space vehicles and maintain the ephemeris data. The user segment equipment differs depending upon the application using GPS. A more detailed discussion of GPS is in APPENDIX A. GPS FUNDAMENTALS.

---

* "Twice distance root mean squared" (2drms) is a measurement of horizontal positional variability. It is twice the square root of the sum of the variances in the east and north directions; i.e.,

$$2 \cdot \mathrm{drms} = 2 \cdot \sqrt{\sigma_e^2 + \sigma_n^2} \ .$$
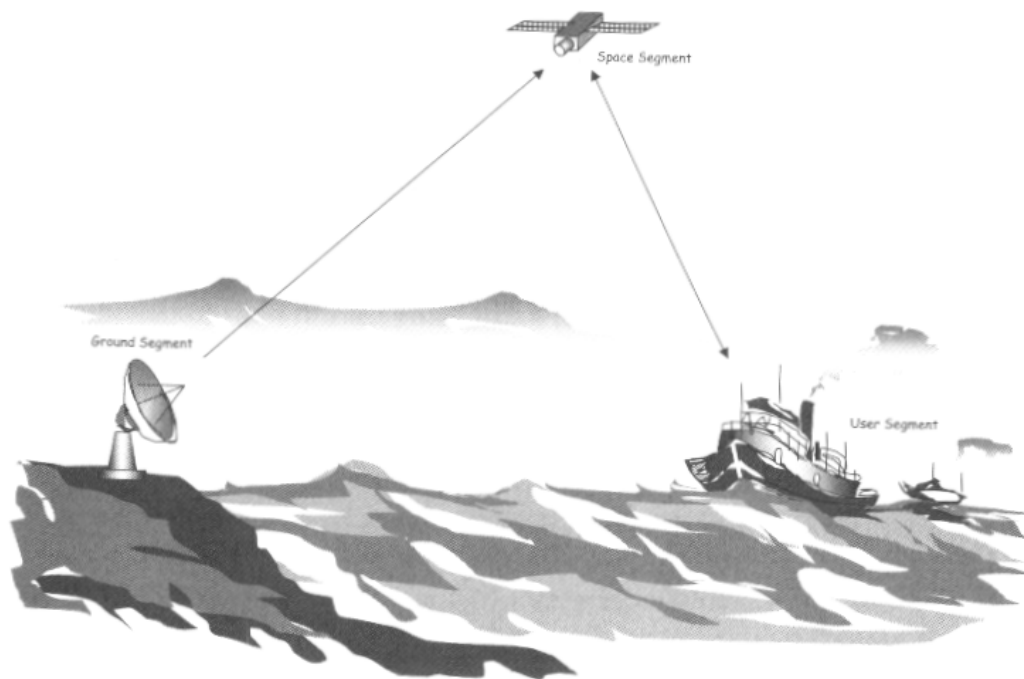
Figure 1   GPS Segments (From Monroe and Bushy, 1998)

1.   Differential GPS

Differential GPS is made possible by placing a receiver on an accurately surveyed location and then measuring the distances to the observable satellites. The surveyed location of the GPS receiver antenna is called the reference station. In theory, the reference station and mobile user are measuring the same observed satellites. The reference station compares the theoretical distances with the actual measurements to the observed satellites. The difference between the theoretical and measured distances represents the pseudorange error. This error comes from inaccurate measurements from each observed satellite and other sources. These pseudorange errors are now called corrections. In a generic sense, these corrections must be available to a mobile user to be effective. So a one-way data link must be established from the reference station to the mobile user to communicate the corrections.
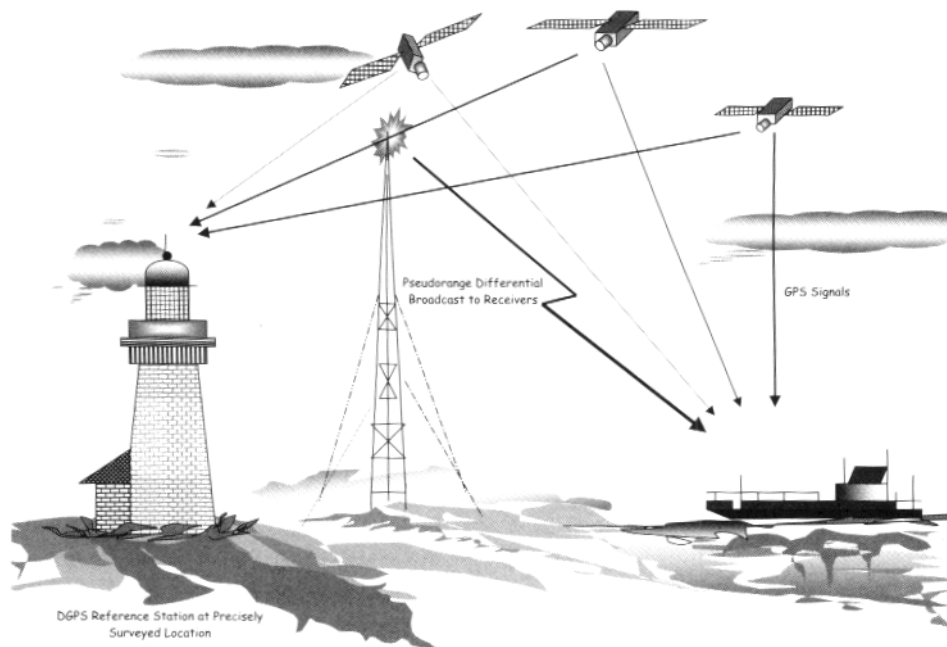
Figure 2   Differential GPS (From Monroe and Bushy, 1998)

The USCG broadcasts the corrections to mobile users using *medium frequency* (MF) transmitters (see Figure 2). The mobile user then adds the corrections to their measurements of the observed satellites. Once the mobile user has this correction information, an updated solution is calculated, providing position with a higher accuracy. This technique removes the common errors experienced by both the mobile user and the reference station.

The USCG defines the Area of Coverage (AOC) as the region near the reference station where a mobile user can reliably receive the communication signal. So there are two separate discussions when referring to USCG DGPS:

- quality of the correction information,
- quality of the data link.

The quality of the correction information refers to the accuracy of the correction signals provided by the reference station. The quality of the data link refers to the ability of the mobile user to receive the corrections from the reference station. In this study, these two quality issues will be considered separately.

2.   Datums

Any discussion of positioning requires an explanation of datums. Local areas, including country boundaries, but also continents and tectonic plates, are surveyed very carefully. The resulting surveys yield maps or datum-planes. These datums are often based upon oblate spheroids, which model the sea level based upon the Earth's gravity and rotation. Typically these local datums are accurate only for a single area. The chosen local datum for the United States is the North American Datum 1983 (NAD-83). The engineers who designed the GPS needed a global datum. The accuracy possible using a local datum is sacrificed when switching to a global datum. The chosen global datum is the Worldwide Geodetic System 1984 (WGS-84). The USCG uses NAD-83 for all reference stations. Although the mobile user is on WGS-84, once the differential corrections are made, the datum shifts to NAD-83. The differences between the two datums are negligible for purposes of this study.

3.   Errors

The word *error* as used in this study has several different meanings. *Error* is the difference between a specific value and the correct value. *Accuracy* is the degree of conformance with the correct value, while *precision* is a measure of consistency of a value. *Systematic errors* are those, which follow some rule by which they can be predicted. *Random errors* are unpredictable. The laws of probability govern random errors. (Bowditch, 1995)

If both systematic and random errors are present in a process, increasing the number of data points decreases the average residual random error but does not decrease the systematic error. If a systematic error is combined with a random error, the probability density plots of the residuals will have the correct shape but will have an offset from zero. (Bowditch, 1995) This offset is called a *bias*.

4.   Pseudorange Errors

The discussion will now focus on the quality of the DGPS correction information. An important distinction in the discussion of errors is the difference between measurement space and solution space. Pseudorange errors are associated with

measurement space. More details of the measurement and timing relationship can be found in APPENDIX B. PSEUDORANGE AND TIMING.

a.   *Dilution of Precision*

The geometry of the observable satellite constellation has a significant effect on the error in position. This effect is measurable and is called Dilution of Precision (DOP). In theory, the best geometry comes from measurements with one satellite directly overhead and three others at the elevation mask angle of the receiver on evenly separated azimuths. Since the satellites below the elevation mask angle of the receiver are subject to increased delays, they are generally not used in calculations of position. Additionally, the satellites that are cutout by the Earth cannot be used in the solution because their signal cannot reach the receiver. DOP is divided into five subcategories: GDOP, PDOP, HDOP, VDOP, and TDOP; for geometric, position, horizontal, vertical, and time. DOP is then used as a scaling factor to describe the geometric effect on the error of the GPS position. This relationship can be approximated by (Kaplan, 1996):

$$\left(\text{error in GPS solution}\right) = \left(\text{geometry factor}\right) \times \left(\text{pseudorange error factor}\right), \quad (1.1)$$

$$\sqrt{\sigma_{east}^2 + \sigma_{north}^2 + \sigma_{up}^2 + \sigma_{ct_b}^2} = GDOP \times \sigma_{UERE}, \quad (1.2)$$

where σ_{UERE} is the User Equivalent Range Error, typically a constant, and σ_{east}^2, σ_{north}^2, σ_{up}^2, and $\sigma_{ct_b}^2$ are the variance of error in the east direction, north direction, up direction and time bias, respectively.

b.   *Atmospheric Delay*

The navigation and ranging data transmitted by each GPS satellite must pass through the Earth's atmosphere to reach the users. As the signal propagates through the atmosphere toward the Earth, it experiences a delay before reaching the receiver antenna. This delay appears as a pseudorange error and must be accounted for in the measurement offset.

The ionosphere is the upper region of the Earth's atmosphere. It is important to understand the effect this layer has on the operation of the GPS. The total

5

electron content (TEC) of the ionosphere is dependent upon the sun. The ionosphere is different during the day than at night as illustrated in Figure 3 and Figure 4. Most modern receivers model the pseudorange errors incorporating the ionospheric delay. The delay is dependent upon the TEC at the *ionospheric pierce point* (IPP). This can be modeled by knowing the slant angle between the user and satellite and the time-of-day (see Figure 5).
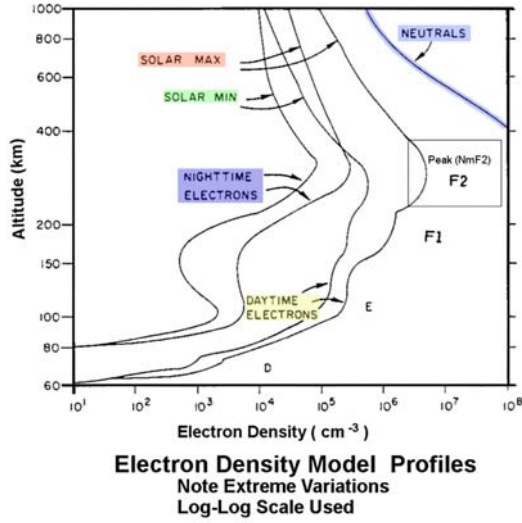
Figure 3   Ionosphere Profile (After Valley, 1965)
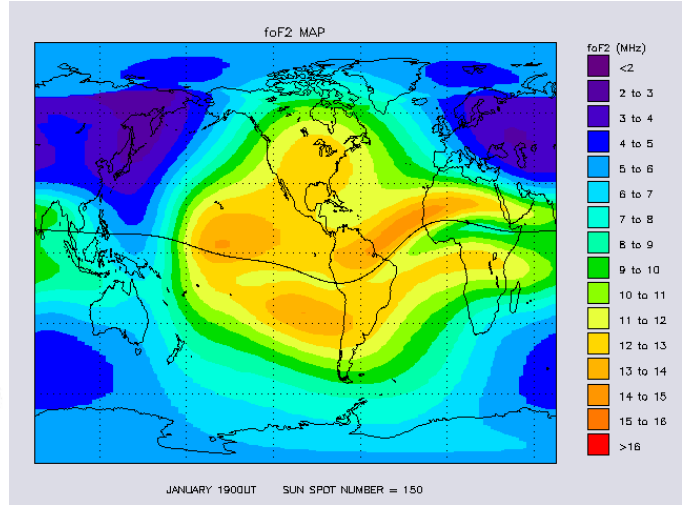
Figure 4   NASA GSFC Ionosphere Model (From NASA GSFC, 2001)

The peak electron density in Figure 3, NmF2, is related to the peak plasma frequency in Figure 4, foF2, by

$$\left(\mathrm{foF2}\right)^2 \cdot 1.24 \times 10^{10} = \mathrm{NmF2}. \tag{1.3}$$
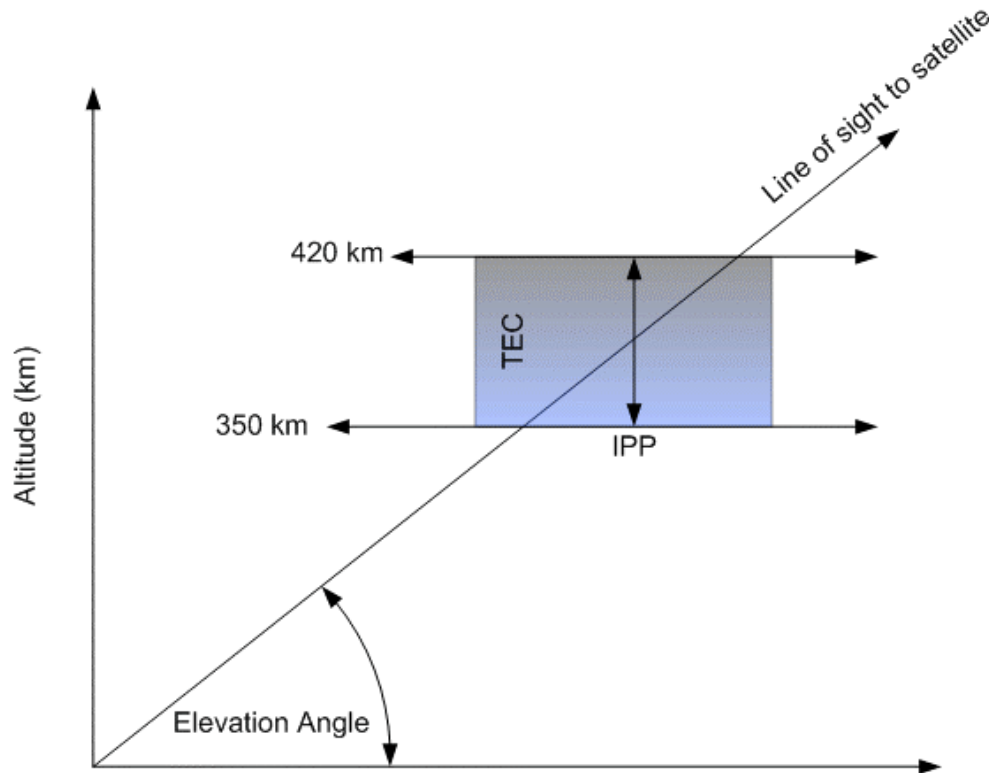
Figure 5   TEC Modeled by IPP for GPS Measurements

The troposphere is the region of the Earth's atmosphere just beneath the ionosphere. Tropospheric errors in GPS also refer to and include effects from the troposphere, tropopause, stratosphere, stratopause, mesosphere and mesopause. Radio wave propagation is attenuated by three major factors in the troposphere; scintillation, absorption, and delay. Scintillation is the effect of the radio waves spreading through the medium. Absorption represents losses due directly to collisions of the radio wave with molecules in the atmosphere. Delay is a combination of effects on radio waves that come from bending and refraction and are dependent upon the elevation angle to the satellite. Low elevation angle paths experience more delay effects than do high elevation angle paths.

Modern GPS receivers model the effects of the troposphere with many different techniques. Robust models can effectively anticipate the error associated with the troposphere. In differential GPS, the tropospheric error is negated because it is assumed common to the user and reference site.

c. Deliberate Errors

The United States government designed GPS for military applications. Inherent in the design, the GPS signal can be heard by anyone with receiver capabilities. Since the receivers are passive, there is no way for the U.S. government to limit access to the signal. To allow U.S. military forces high accuracy while denying the enemy the same requires some additional design considerations. Selective Availability (SA) provides a solution.

Selective Availability adds a signal to the measurement noise of an observed satellite. This signal varies randomly in frequency and magnitude. Hundreds of meters of inaccuracy can be added to the solution of a non-military user with SA on. For civilian users, this represents the largest error in a position. For U.S. government and military receivers using the encrypted Precise Positioning Service (PPS), the effects of SA are ignored.

In May 1995, by order of Presidential Directive, SA was turned off. Although currently off, the capability to turn SA back on still exists. For purposes of this study, the effects of SA will not be examined. In general, differential GPS users can ignore the effects of SA because the errors are common to both the user and reference station.

d. Satellite Clock Errors

Each GPS satellite has an onboard atomic clock. Satellite range data used in the GPS solution is reliant upon the accuracy of this clock. The data transmitted by the GPS satellite includes a predicted clock time bias for each satellite. Knowing this time bias allows the user to account for the difference between clocks and calculate position with higher accuracy. Although satellite clock error is unique to each satellite, it is common to both the user and reference station and cancels in differential GPS.

e. Ephemeris Errors

Ephemeris errors are also called orbit errors. They occur when the satellite's position is not accurately reported to the GPS user. Since GPS satellites are in orbit around the Earth, the along-track error is largest, with the cross-track and radial errors typically smaller. As the satellite moves across the sky, the radial distance

associated with that satellite changes slowly over time for a user on the Earth. The along-track position of a fast moving satellite may change quickly; however, its direction of change is nearly parallel to the surface of the Earth and therefore the resulting errors are relatively small for GPS users on the Earth.

f.   Multipath Errors

Multipath errors come from reflections of the GPS satellite navigation data off nearby obstacles including buildings, bridges, trees, and other structures.   This reflected information can confuse the receiver and result in inaccurate positioning.

Techniques exist to minimize or eliminate the effects of multipath interference.   Some of these techniques are only useful to static users.   They include antenna positioning, receiver elevation mask angle settings, and the operating location. One other technique to minimize multipath effects is a feature of modern GPS receivers; it is called *narrow correlator*.   With a *narrow correlator* receiver, any multipath reflections that arrive outside the interval of time between the two correlated reference carriers are ignored. *Narrow correlator* receivers remove the effects of any potential multipath objects farther than 300 meters from the antenna. Most high performance C/A-code receivers incorporate this technique.

Multipath effects are different for each receiver and therefore do not cancel in differential GPS.   Conditions that could generate significant multipath effects are noted during the data collection portion of this study.   Specifically, whenever the mobile user is within approximately 400 meters of the span of a bridge, the data is tagged as being suspected of excessive multipath.

g.   Receiver Clock Errors

It would be prohibitively expensive and impractical to use atomic clocks on every GPS receiver. Instead, modern GPS receivers use inexpensive and small quartz clocks. Since the errors associated with quartz clocks are large compared to atomic clocks, a solution technique is used to calculate the clock bias and incorporate it into the position solution. Pseudorange measurements to three satellites give the GPS user an estimate of position in a region defined by the intersection of three spheres.   With a measurement from one additional satellite, a common bias can be added to the spheres

generating the user's position, thereby improving the accuracy of the solution. This bias is the *receiver clock error*. To always have the bias available, GPS receivers require a minimum of four observable satellites to solve for a position. If more than four satellites are observed, then the position solution is over determined. In modern GPS receivers, all available observed satellites are used to calculate the position.

h.   Hardware Errors

The noise and resolution capability associated with the user's equipment has an effect on the pseudorange error. For accurate surveying using differential GPS, reliable hardware is needed. Careful choice of receiver equipment can make for more accurate positioning.

4.   Solution Errors

The solution space error associated with a GPS position refers to one-, two- and three-dimensional errors. One-dimensional errors represent the individual components of latitude, longitude, and height. Two-dimensional errors are formed from the latitude and longitude components together to describe a horizontal plane. Three-dimensional errors use the components of latitude, longitude, and height to describe a sphere.

In a maritime application of DGPS, it is common to represent the accuracy of a position in the horizontal plane. In aircraft and spacecraft applications, a three-dimensional representation of accuracy is used. In this study, the horizontal error will be examined.

5.   Ionospheric Absorption

The discussion now returns to the quality of the data link. The ionosphere affects radio wave propagation inside the Earth's atmosphere. Of particular interest to this study is how the ionosphere affects the *medium frequency* (MF) band on which the USCG transmits correction data. A combination of radio waves can reach mobile users near a broadcast antenna. The *ground wave* is the portion of the broadcast that propagates along the surface of the Earth. The ionosphere does not affect the ground wave; its primary attenuation is caused by the conductivity of the surface material. The *sky wave*, shown in Figure 6, reflects off the ionosphere and bounces back to mobile users on the surface.

For a mobile user attempting to receive the USCG broadcasts, one of four mutually exclusive situations can occur:

1. *The ground* wave alone is received.
2. A combination of *ground* and *sky wave* is received.
3. The *sky wave* alone is received.
4. Neither the *ground wave* nor the *sky wave* is received.

Since the ionosphere absorption is greatly reduced during the night, it is possible to receive the signal at much greater distances than during the day. Quantifiable measures of exactly how far away the signal could be received were not gathered during the experiment. During the night, usable USCG DGPS signals were received from over 1200 kilometers away from Appleton, Washington and Point Loma, California.
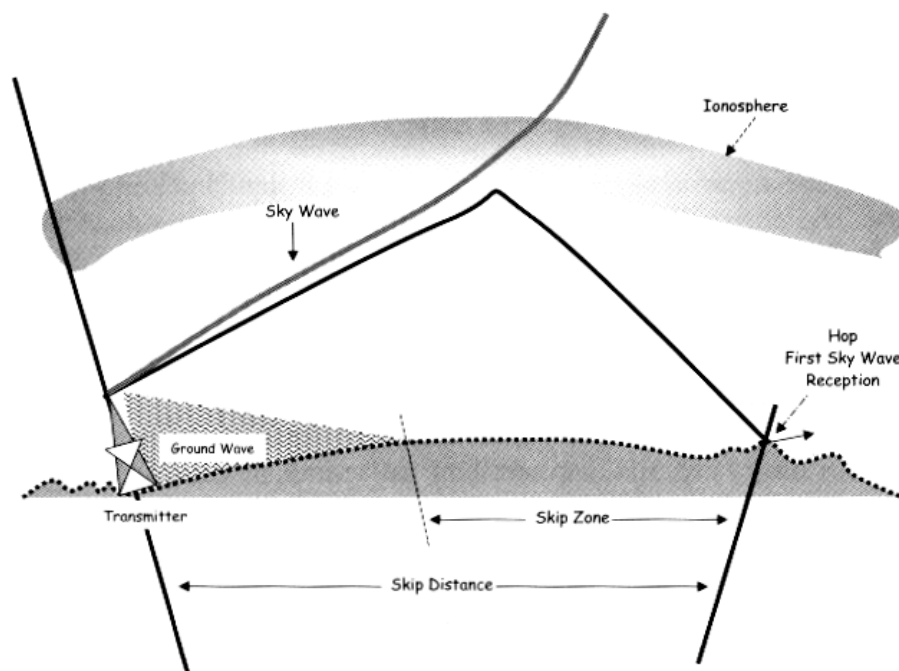
Figure 6   Radio Signal Propagation (From Monroe and Bushy, 1998)

C.   EXISTING WORK

A model exists to describe the behavior of the position accuracy as distance from the DGPS reference station increases. The Broadcast Standard for the USCG DGPS Navigation Service COMDTINST M16577.1 proposed a reasonable approximation of achievable accuracy. This approximation starts with a typical error at a short baseline

(approximately 0.5 meters) from the reference station, adds an additional meter of error for each 150 kilometers of separation between the mobile user and the reference station, and finally adds an additional 1.5 meters of error for the user equipment. (COMDTINST M16577.1, 1993)

D.   PROPOSED WORK

The general purpose of this thesis is to further a scientific investigation into the degradation of accuracy beyond the Area of Coverage. To this end, some specific questions need to be answered. What is the effect of distance from the reference station on accuracy? What is the effect of transmitter power on the accuracy? What is the effect of the ionosphere on the daytime accuracy of the differential correction? Thus in the next chapter we describe an experiment designed to answer these questions by simulating the use of USCG DGPS by a typical mobile user. Analyses of the results of this experiment are given in Chapter IV. Finally, conclusions and recommendations are given in Chapters V and VI respectively.

II.   DYNAMIC EXPERIMENT

A.   DESIGN

An experiment was devised to discover the answers to the proposed questions of accuracy of the USCG DGPS beyond nominal range. Data is collected from a marine mobile user in a controlled environment. The criteria selected for the experiment design is important for proper data analysis later. To simulate a typical marine civilian mobile user, the single frequency SPS data and USCG DGPS correction data are needed. Lindy, 2002 uses the same mobile user data to answer related questions about the use of dual frequency DGPS for military applications. The focus of this study is civilian maritime usage. The number of observations that can be generated is limited by current computing power and storage media capabilities. A variety of environmental factors, which can potentially affect the data analysis need to be mitigated or documented. Since the answer is a matter of describing positional error, data needs to be collected to provide an assumed true position.

Figure 7   RV Point Sur

B. IMPLEMENTATION

With limited funding available, an experiment was added to the Research Vessel POINT SUR's agenda for the scheduled underway time in late November and early December of 2001. Using the POINT SUR (see Figure 7) for the experiment would closely mimic the operations of a typical USCG DGPS marine mobile user. The proposed course of the POINT SUR's was known in advance. It was clear that the ship's path would never leave the closest USCG DGPS reference station's AOC. As a control to the experiment, gathering data from the closest reference station and two others exploited knowledge of the ship's plans. To accomplish this control, three DGPS beacon receivers would be needed with three separate data loggers. To simulate using reference stations beyond the AOC, data was purposely gathered from distant operational USCG beacons. The plan called for collecting data 24 hours a day for nine continuous days in or around the Monterey Bay of California. Since the data logger could only temporarily record about a day and a half of information, the data stream was stopped at midnight UTC (1600 local) to store it on removable media. The data collection went well and nearly all criteria of the experiment were met. All data collected was post-processed.

III.   DATA ANALYSIS

A.   POST-PROCESSING

The raw data was collected for three USCG DGPS beacon stations, two ASHTECH Z12 DGPS receivers, and the ship's GPS attitude. This data was in binary format and required reformatting to begin mathematical calculation of position and error. The DGPS receiver on board the POINT SUR simulated the marine mobile user for the experiment.   Post-processing the three separate USCG DGPS reference station's correction data through the DGPS receiver data tripled the useable data.
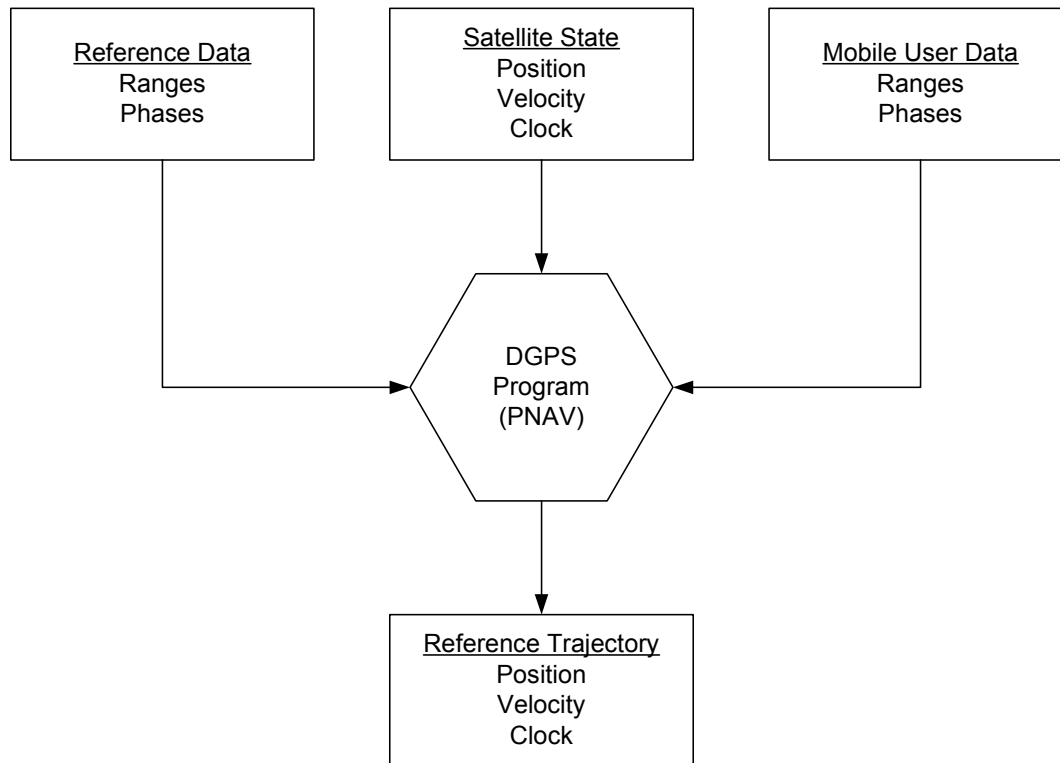
Figure 8   Post-Processed Reference DGPS Kinematic Solution (After Clynch, 2001)

Figure 8 illustrates, in very general terms, how the reference or "truth" trajectory was developed. *Reference Data* comes from a benchmarked GPS receiver. *Mobile User Data* comes from the GPS receiver onboard the vessel.   In general, *Satellite State* information comes from the ephemeris data.   Ephemeris data can either be collected dynamically from the observable satellites or downloaded later; these two are called

Broadcast Ephemeris (BCE) and *Precise Ephemeris* (PE) respectively. The BCE is the position of each satellite's orbital path and comes in the navigation data from the satellite. One example of a PE is based upon the International GPS Service (IGS) tracking and data holdings. The PE is calculated from raw data collected from permanent tracking stations to develop a raw orbit for the entire GPS constellation.   For real-time processing, typically only the BCE is available. For this study, only the BCEs are used.
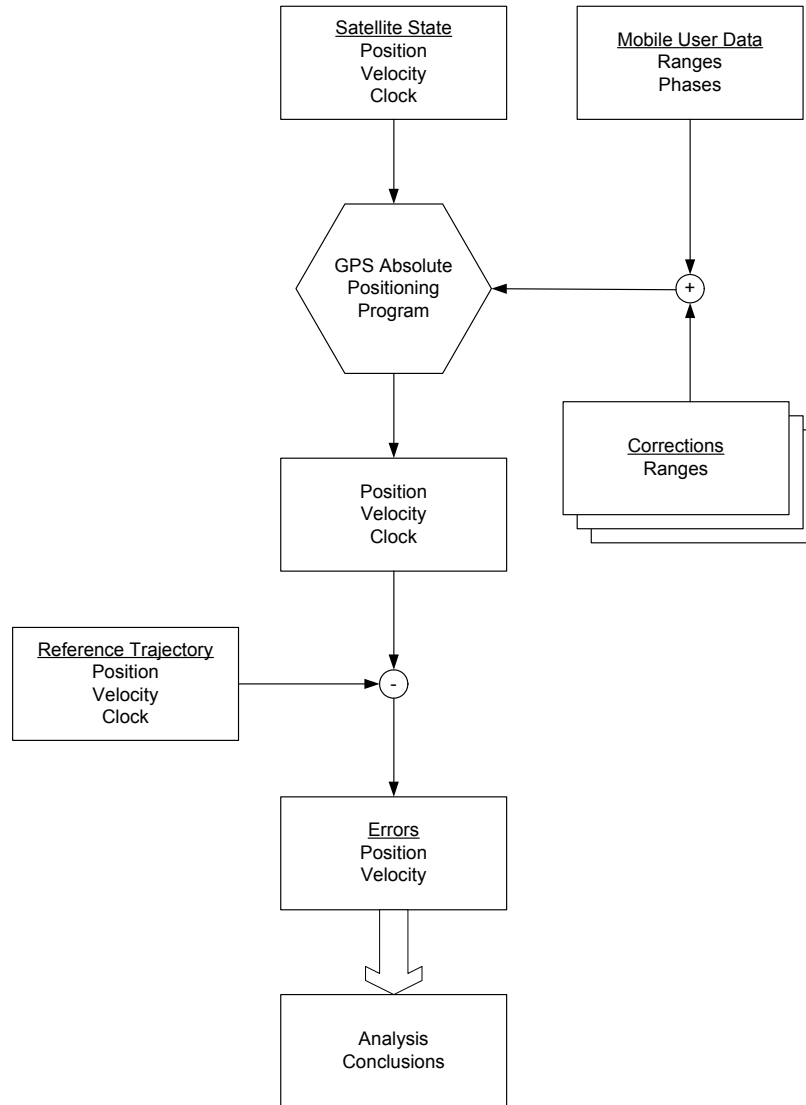
Figure 9   Post-Processing Using Position (From Clynch, 2001)

There are two methods for implementing the process described in Figure 8. The data can be post-processed using positions as described in Figure 9 or using the residual errors as described in Figure 10. Both methods give the same results.

16
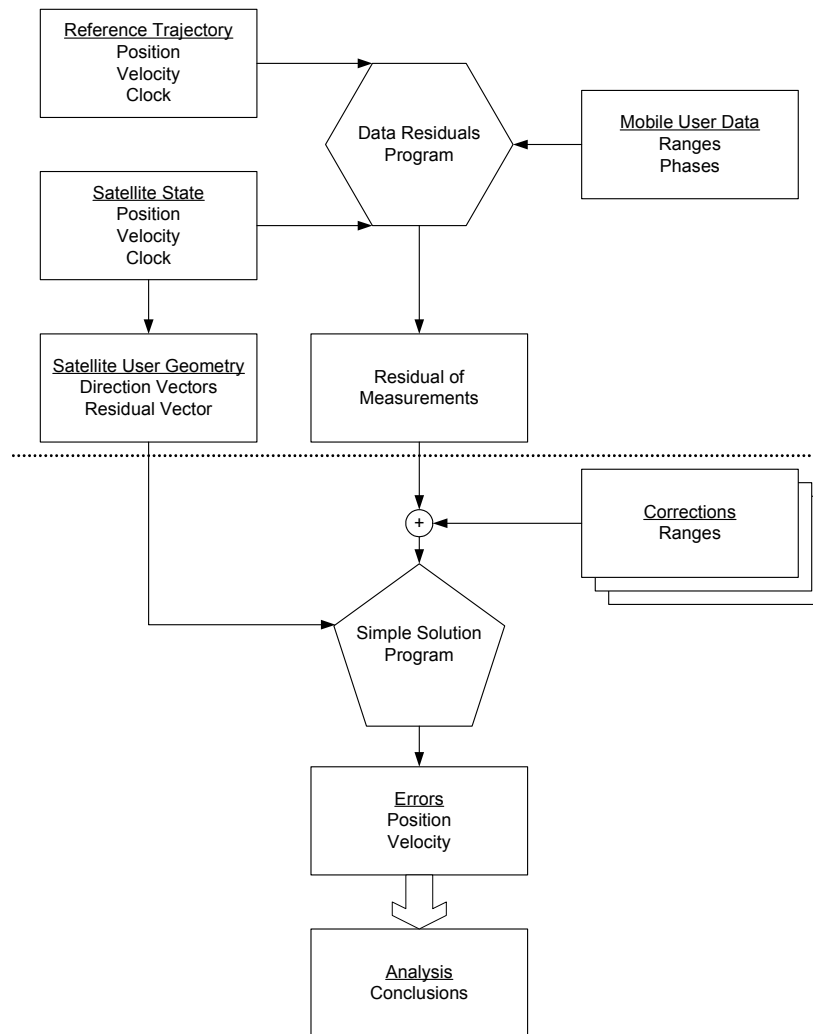
Figure 10   Post-Processing Using Residual Errors (From Clynch, 2001)

Although post-processing using the positions is a simpler concept to understand, it is more advantageous to use the residual errors. Since the coordinate system used by GPS is an Earth Centered Earth Fixed X,Y,Z frame (ECEF-xyz), all distances are calculated from the center of the Earth. Pseudorange measurements from the satellites to the user's position are compared to theoretical distances based upon the ECEF-xyz frame. To employ Differential GPS, it is necessary to add the correction information before solving for position. Common to all pseudorange measurements are the errors inside the user's GPS receiver. The magnitude of the receiver clock errors is much larger than the next closest error. Since receiver clock error is the same for each observed satellite and of such great magnitude compared to the other errors, it can be removed from the solution

17

and recorded later as a time bias common to all positions. Now the data processing is concerned only with the errors of small magnitude, whose accuracy would have been lost if the time bias was included in the pseudorange measurements. Therefore, all post-processing in this study was done using the residual errors method as shown in Figure 10.

1.   USCG DGPS Beacons

Seven USCG DGPS reference stations transmissions were collected over the duration of the ship's operations. The shaded red area in Figure 11 is the test area of the ship for the experiment. The USCG DGPS beacons are denoted as red stars in Figure 11.

> Appleton, Washington
> Cape Mendocino, California
> Chico, California
> Pigeon Point, California
> Point Blunt, California
> Lompoc, California
> Point Loma, California
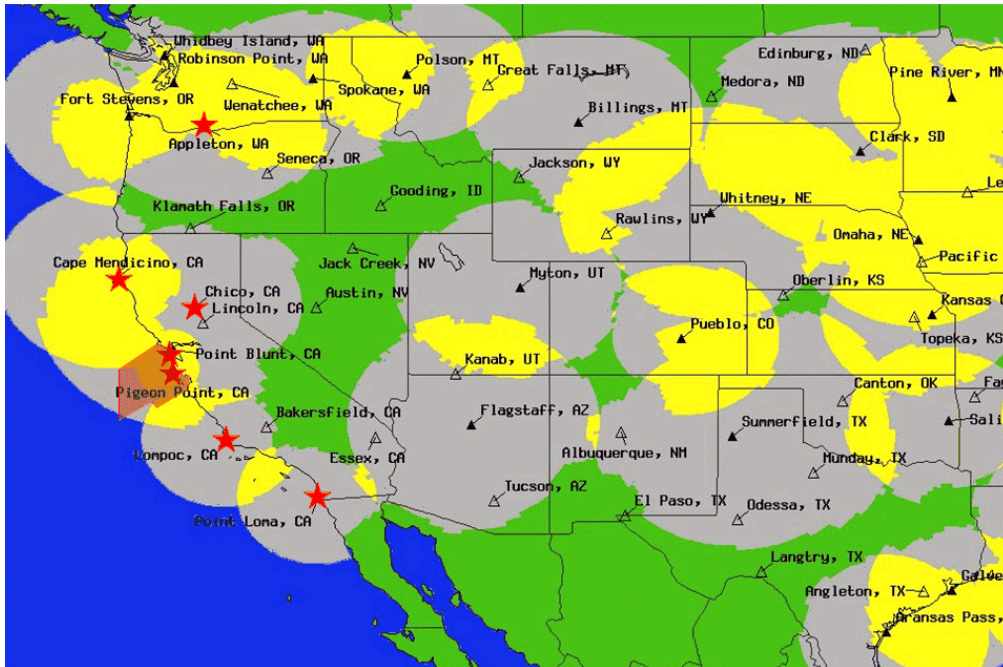
Figure 11   USCG DGPS Coverage Plot – West Coast. (After NAVCEN 2002)

Each USCG DGPS transmitter uses a *medium frequency* (MF) band (~300 KHz) to send the corrections to mobile users within their AOC. In Figure 11, the gray shaded arcs represent the AOC for each displayed DGPS reference station. The yellow shaded

patches represent double or triple coverage by more than one DGPS reference station. It is within either of these colored arcs that the USCG guarantees better than 10 meters (2drms) accuracy to SPS users.

Each DGPS reference station uses an ASHTECH Z12 reference receiver. After finding the pseudorange corrections from observed satellites, the reference station then broadcasts them to DGPS-capable mobile users within their AOC. Because of the nature of MF band in the Earth's atmosphere, mobile users well beyond the reference station's AOC can often receive this correction broadcast. The USCG has designed this system to improve GPS for safety of navigation to Harbor and Harbor Approach (HHA) sea-lanes. But mobile users are able to receive the DGPS corrections beyond the nominal ranges because of the propagation behavior of the MF band. How relevant is this information if the mobile user is beyond the guaranteed AOC?

2. DGPS Receivers

In order to post-process the data gathered during the dynamic experiment, high quality ASHTECH Z12 receivers were simultaneously used onboard the POINT SUR and on top of Spanagel Hall at the Naval Postgraduate School in Monterey, California. This allowed a dedicated reference solution to test the accuracy of the USCG DGPS correction data. One-second data was gathered continuously for twelve days of operation.
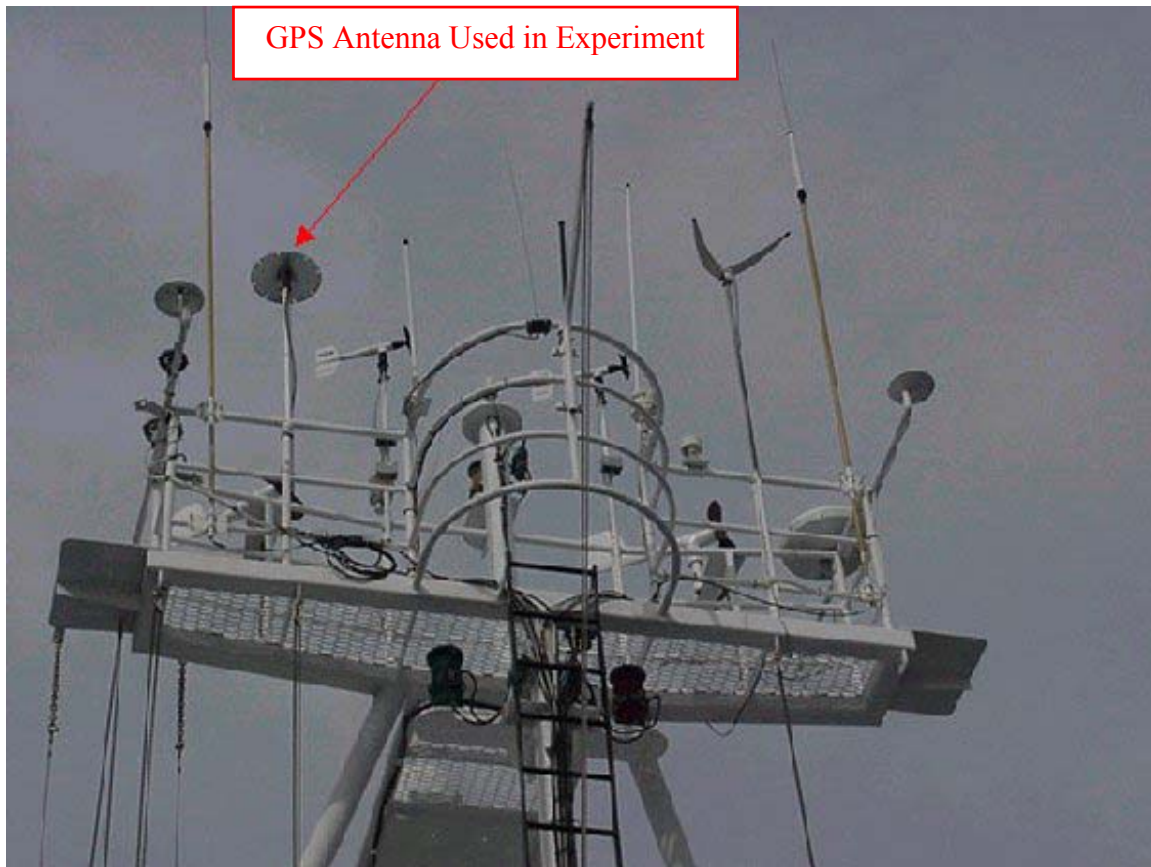
Figure 12   Arrangement of GPS Receiver Antenna on POINT SUR's Mast.

B.   DATA CLASS SELECTION

From the twelve days of collected data, 1.76 million positions were calculated. The data set was trimmed to handle outliers based upon two criteria. Any data points with a Position Dilution of Precision (PDOP) as defined in Chapter I, greater than 6.0 was removed. A PDOP greater than 6.0 represented a poor geometry for timing and ranging solutions. Whenever the truth trajectory root mean square residuals of fit exceeded 0.5 meters, the data points for that time were trimmed. These trimming criteria yielded a final data set of 1.71 million positions, which was 97.2% of the original data. Call this trimmed data set U for future reference in this study.
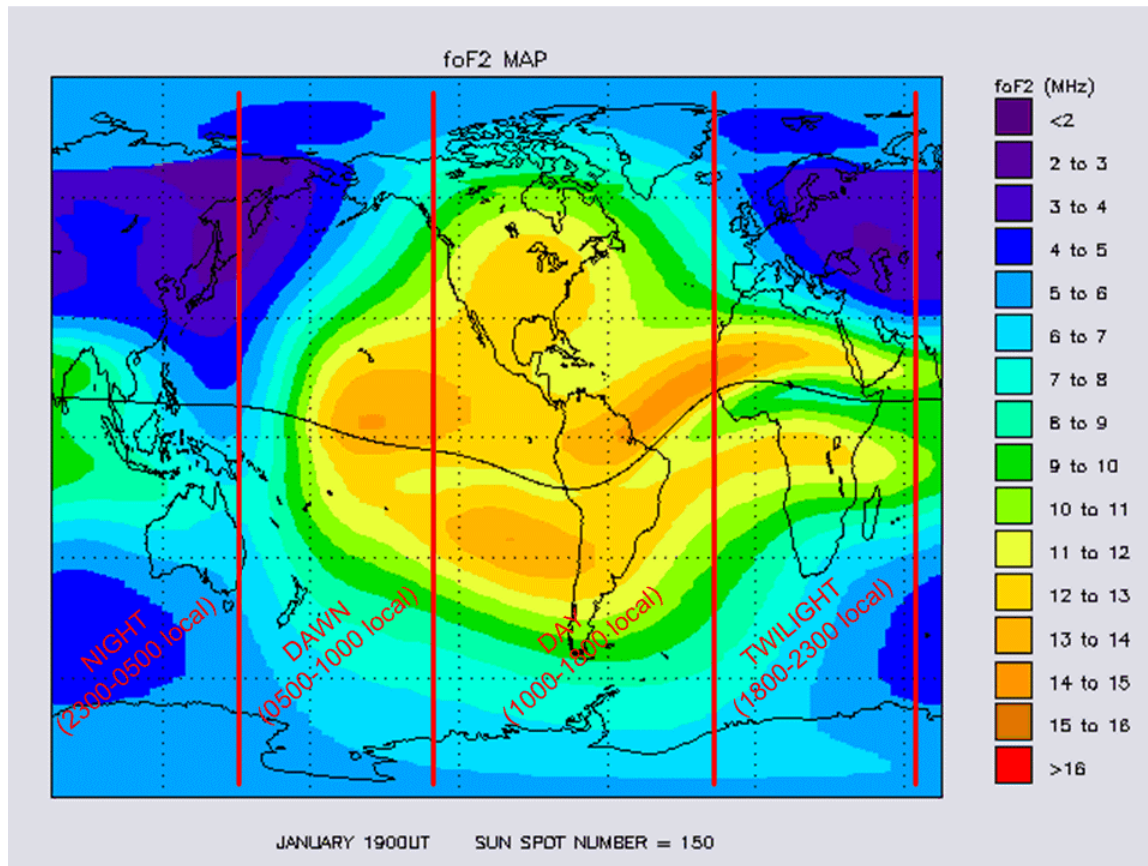
Figure 13   NASA GSFC Ionosphere Model January at 1900 UTC and Sun Spot Number 150
(After NASA GSFC, 2001)

1. Time-of-Day

The data set *U* was tagged with four categories to represent local time-of-day. These break points were based upon models of the Total Electron Content (TEC) in the ionosphere. In Figure 13, the NASA GSFC ionosphere model shows the TEC around the globe during different local times.   The quality of the data link, which carries the correction data, is influenced by absorption from the TEC in the ionosphere. As the TEC increases during the local daylight hours, so do the absorption effects upon the MF band. Time-of-day categories were chosen to directly address the question of ionospheric effects upon the quality of the USCG DGPS correction data. The categories were:

Dawn	(0500-1000 local)
Day	(1000-1800 local)
Twilight	(1800-2300 local)
Night	(2300-0500 local)

21

During the *Dawn* period, solar radiation begins to increase the TEC and degrades propagation in the MF band. During the *Day* period, the TEC is highest and which causes absorption of the MF band to be highest. During the *Twilight* period, the TEC in the ionosphere begins to decline to zero, but the effects of absorption on the MF band are still present. During the *Night*, the TEC is negligible, and has no effect on the absorption of the MF band. Figure 14 illustrates these effects with a plot of signal strength versus time-of-day for a MF band signal.
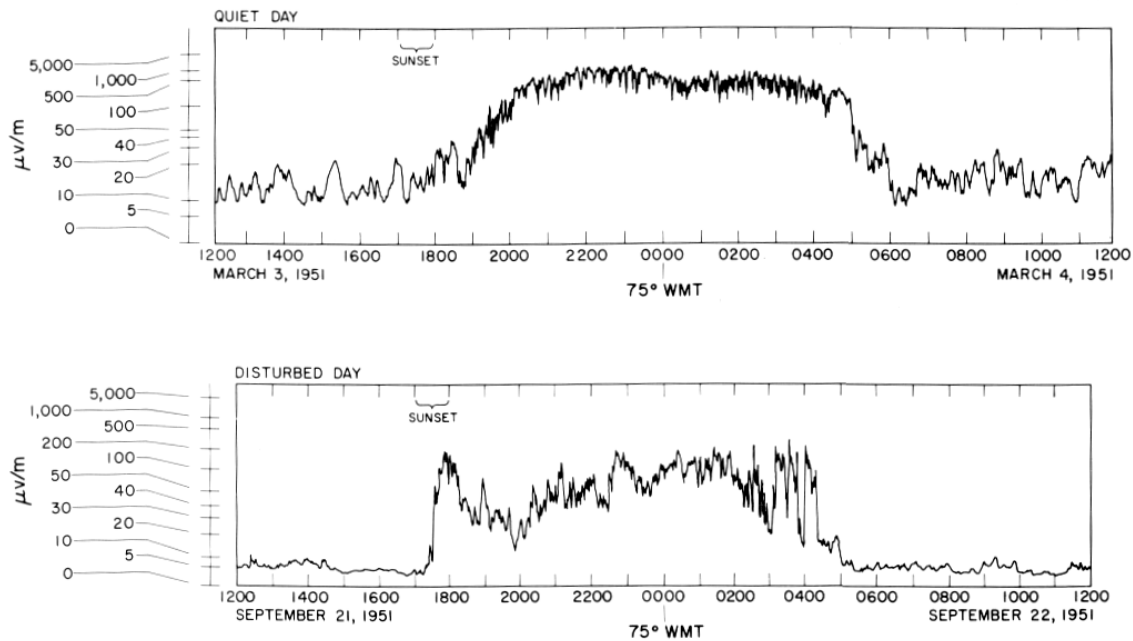
Figure 14   Diurnal Variations of the Signal Strength of 700 kHz, 50kW Signals from Cincinnati to Baltimore (665 km) on a Quiet Day and on a Disturbed Day (From Davies, 1990)

2.   Distance from Reference Station

The data set *U* was separated into three bins depending on distance to the reference station; *Short* Range, *Medium* Range, and *Long* Range. *Short* Range was defined as positions within the USCG DGPS AOC. *Medium* Range was defined as positions between one and two time the standard AOC range. *Long* Range was defined as positions between two and three times the AOC range.

3. Magnetic Latitude

The data set included geographic latitude. Since MF wave propagation is dependent upon magnetic latitude, this quantity was computed using

$$\sin \Phi = \sin \phi \sin \phi_0 + \cos \phi \cos \phi_0 \cos(\lambda - \lambda_0), \text{ where} \qquad (3.1)$$

ϕ_0 and $\lambda_0 \equiv$ geographic latitude and longitude of the north dipole pole,

ϕ and $\lambda \equiv$ geographic coordinates, and

$\Phi \equiv$ dipole latitude.
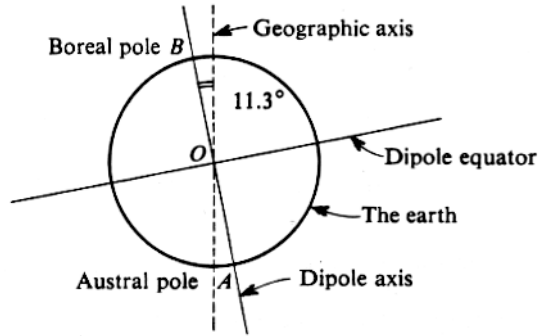
Figure 15   Earth's Dipole Field Showing the North (B) and South (A) Dipole Poles and the Dipole Equator. (From Davies, 1990)

When the experiment was conducted, the values for ϕ_0 and λ_0 were approximately 79.0°N and 105.1°W. These coordinates are the magnetic north pole or Boreal pole as illustrated in Figure 15. The true position of the Boreal pole can only be approximated to one tenth of a degree. Many variables are needed to predict the position of the Earth's magnetic field. An accurate position of the Boreal pole is necessary to predict the effects of the Earth's magnetic field. During the experiment, the research vessel's position varied by only three degrees of geographic latitude. The reference stations used during the experiment varied by as much as 17° of latitude. The data set U was tagged with the difference in latitude of the mobile user and the USCG reference station.

4. Reference Trajectory

The ASHTECH program, PNAV, and ASHTECH Z12 receivers on the roof of Spanagel Hall at the Naval Postgraduate School in Monterey, California, and onboard the research vessel POINT SUR were used to develop a reference trajectory. From this

"truth", all DGPS positions were differenced. The ASHTECH program, PNAV, used these two receivers to solve for a reference solution. PNAV also computed an estimated error for each calculated position.

5.   Transmitter Power

Each USCG beacon antenna transmits the correction signal in the MF band. The USCG reports a receivable power as a function of distance from the antenna. This value was available from the NAVCEN web page (http://www.navcen.uscg.gov/) and was reported as power per distance (μV/m). Both the power at nominal range and distance guaranteed by the USCG were tagged on the data set *U*.

C.   RESULTS

The data set *U* was imported into the statistical software package *S-Plus 2000.* To answer the proposed questions of the study, the reference trajectory was subtracted from the observed trajectory to yield the residual errors. Horizontal 2drms error is the principle quality used to measure the positional accuracy. This is derived from the components of the standard deviation and mean of the residual errors.

The following is an explanation of the mathematical definition of 2drms. Let *ΔEast* and *ΔNorth* represent the random independent residual errors in the east and north directions, respectively. *Horizontal$_{rms}$* (3.2) is calculated by taking the square root of the sum of variances (σ^2) and squared means (μ^2) of *ΔEast* and *ΔNorth*. There is only one *Horizontal$_{rms}$* value for the data set (or subset of the data set being examined). *HDOP* (3.3) is calculated by taking the square root of first two terms of the trace of the covariance matrix used to calculate the position solution. There are *HDOP* calculations for each data point within the data set. The σ_{UERE} (3.4), User Equivalent Range Error, is calculated by dividing the *Horizontal$_{rms}$* by the *HDOP*. The value of 2drms is defined by equation (3.5).

$$Horizontal_{rms} = \sqrt{\sigma_{east}^2 + \sigma_{north}^2 + \mu_{east}^2 + \mu_{north}^2} \, , \qquad (3.2)$$

$$HDOP = \sqrt{\sigma_{E_u}^2 + \sigma_{N_u}^2} \, , \qquad (3.3)$$

$$\sigma_{UERE} = \frac{Horizontal_{rms}}{HDOP} \, , \qquad (3.4)$$

$$2\text{drms} = 2 \cdot HDOP \cdot \sigma_{UERE} \tag{3.5}$$

$$= 2 \cdot Horizontal_{rms}.$$

1. The Effect of Distance

Analysis of the effect of baseline distance on accuracy was done two ways. The first analysis involved a simple linear regression of 2drms error versus baseline distance for all the data. The second analysis was done using summary statistics on the data separated into three categories based upon *Short*, *Medium*, and *Long* range. Both of these results were averaged over time-of-day.

Based on plots of 2drms versus distance, the relationship between baseline distance and 2drms error appears approximately linear. The linear regression predicted that with a baseline distance from zero to ~250 kilometers, the positioning accuracy is to be 2.5 meters (2drms). To predict the positioning accuracy as the baseline distance increases from ~250 to ~1100 kilometers, the linear regression adds 2.5 meters (2drms) and to an additional one meter for each additional 300 kilometers of baseline distance.

Analysis of the summary statistics in Table 1 indicates that *Short* Range and *Medium* Range errors appear about the same. *Long* Range shows an increase in the magnitude and variability of 2drms error. This data supports the postulation that distance does affect positional accuracy when using DGPS.

The 2drms column in Table 1 shows the radial error variability. It is clear that as the distance from the reference station increases, so does the 2drms error.

Category	Δ*North* (meters)	Δ*East* (meters)	2drms (meters)	# satellites	Horizontal DOP	σ_{UERE} (meters)
Short Range (~0-350 km)	$\hat{\mu}$=-0.46 $\hat{\sigma}$ = 1.54	$\hat{\mu}$= 0.17 $\hat{\sigma}$ = 1.26	4.10	$\hat{\mu}$= 7.2 $\hat{\sigma}$ = 1.2	$\hat{\mu}$ = 1.3 $\hat{\sigma}$ = 0.4	$\hat{\mu}$ = 1.1 $\hat{\sigma}$ = 1.1
Medium Range (~350-700 km)	$\hat{\mu}$=-0.30 $\hat{\sigma}$ = 1.82	$\hat{\mu}$= 0.08 $\hat{\sigma}$ = 1.12	4.32	$\hat{\mu}$= 7.4 $\hat{\sigma}$ = 1.3	$\hat{\mu}$ = 1.2 $\hat{\sigma}$ = 0.4	$\hat{\mu}$ = 1.7 $\hat{\sigma}$ = 0.9
Long Range (~700-1100 km)	$\hat{\mu}$=-0.25 $\hat{\sigma}$ = 3.69	$\hat{\mu}$= 1.69 $\hat{\sigma}$ = 2.66	9.72	$\hat{\mu}$= 6.3 $\hat{\sigma}$ = 1.2	$\hat{\mu}$ = 1.6 $\hat{\sigma}$ = 0.6	$\hat{\mu}$ = 2.1 $\hat{\sigma}$ = 2.1

Table 1   Distance Summary Statistics

2. The Effect of Time-of-Day

Outside the Area of Coverage the ionosphere absorbs most of the USCG DGPS signal during the hours of daylight. Even when the data link can be received, the effects of the ionosphere at the reference station are often different than near the mobile user.

The effect of time-of-day on accuracy is illustrated in Table 2. At *Dawn* (0500-1000 local)*,* the accuracy is 5.1 meters (2drms). During the *Day* (1000-1800 local)*,* the accuracy is 5.2 meters (2drms). As the sun sets during the *Twilight* (1800-2300 local)*,* the accuracy is 3.5 meters (2drms). At *Night* (2300-0500), the accuracy is 3.1 meters (2drms). The union of *Dawn* and *Twilight*, called *Transition* (0500-1000 & 1800-2300 local) has an accuracy of 4.6 meters (2drms).

The data in Table 2, suggests that time-of-day does have an effect on the accuracy of the USCG DGPS position. A key assumption made by the Radio Technical Commission For Maritime Services (RTCM) committee is that the ionosphere would be the same at the reference station and the mobile user's position. (RTCM 104, 1998) The data set *U* supports that assumption. At short baseline distances (< 350 km) the ionospheric effects appear muted or non-existent.

The data collected was taken from reference stations in a mostly north-south direction. This might have influenced the results because large changes in the ionosphere at *Dawn* and *Twilight* could be observed looking longitudinally, but might be rather small looking latitudinally. More data is needed to explore this question.

Category (all times local)	ΔNorth (meters)	ΔEast (meters)	2drms (meters)	# satellites	Horizontal DOP	σ_{UERE} (meters)
Dawn (0500-1000)	$\hat{\mu}$=-0.79 $\hat{\sigma}$ = 1.87	$\hat{\mu}$=-0.14 $\hat{\sigma}$ = 1.75	5.37	$\hat{\mu}$ = 7.0 $\hat{\sigma}$ = 1.2	$\hat{\mu}$ = 1.3 $\hat{\sigma}$ = 0.4	$\hat{\mu}$= 1.4 $\hat{\sigma}$ = 1.3
Day (1000-1800)	$\hat{\mu}$= -0.69 $\hat{\sigma}$ = 2.07	$\hat{\mu}$= 0.12 $\hat{\sigma}$ = 1.54	5.35	$\hat{\mu}$ = 6.7 $\hat{\sigma}$ = 1.0	$\hat{\mu}$ = 1.4 $\hat{\sigma}$ = 0.4	$\hat{\mu}$= 1.4 $\hat{\sigma}$ = 1.5
Twilight (1800-2300)	$\hat{\mu}$= 0.08 $\hat{\sigma}$ = 1.26	$\hat{\mu}$= 0.62 $\hat{\sigma}$ = 1.23	3.74	$\hat{\mu}$ = 7.1 $\hat{\sigma}$ = 1.2	$\hat{\mu}$ = 1.2 $\hat{\sigma}$ = 0.3	$\hat{\mu}$= 1.0 $\hat{\sigma}$ = 0.9
Night (2300-0500)	$\hat{\mu}$=-0.20 $\hat{\sigma}$ = 1.36	$\hat{\mu}$= 0.45 $\hat{\sigma}$ = 0.77	3.28	$\hat{\mu}$ = 7.8 $\hat{\sigma}$ = 1.2	$\hat{\mu}$ = 1.3 $\hat{\sigma}$ = 0.5	$\hat{\mu}$= 1.0 $\hat{\sigma}$ = 0.6
Transition (0500-1000,1800-2300)	$\hat{\mu}$=-0.38 $\hat{\sigma}$ = 1.67	$\hat{\mu}$= 0.22 $\hat{\sigma}$ = 1.57	4.67	$\hat{\mu}$ = 6.9 $\hat{\sigma}$ = 1.1	$\hat{\mu}$ = 1.3 $\hat{\sigma}$ = 0.4	$\hat{\mu}$= 1.2 $\hat{\sigma}$ = 1.3

Table 2   Time-of-Day Summary Statistics

3. Aggregation of Distance and Time-of-day Effects

The data used to create Table 1 and Table 2 can be examined in more detail by separating the data into sub-categories as shown in Table 3. Now we can attempt to analyze any correlation between distance and time-of-day. As expected, improvements in accuracy are seen at shorter baselines. Additionally, accuracy improvements are seen in the data collected at night. By combining the effects of distance and time-of-day, it is clear that accuracy at night is better than during other times, and reducing the distance between reference station and mobile user improved the accuracy in position. Shorter baselines consistently improved accuracy regardless of time-of-day.

Category (all times local)	Sub-category	$\Delta North$ (meters)	$\Delta East$ (meters)	2drms (meters)	# satellites	Horizontal DOP	σ_{UERE} (meters)
Day (1000-1800)	*Short* Range	$\hat{\mu}$=-0.65 $\hat{\sigma}$=1.78	$\hat{\mu}$=-0.01 $\hat{\sigma}$=1.28	4.57	$\hat{\mu}$= 7.1 $\hat{\sigma}$= 1.2	$\hat{\mu}$= 1.3 $\hat{\sigma}$= 0.4	$\hat{\mu}$= 1.28 $\hat{\sigma}$=1.15
	Medium Range	$\hat{\mu}$=-0.64 $\hat{\sigma}$=1.87	$\hat{\mu}$=-0.03 $\hat{\sigma}$=1.37	4.81	$\hat{\mu}$= 7.4 $\hat{\sigma}$= 1.1	$\hat{\mu}$= 1.2 $\hat{\sigma}$= 0.3	$\hat{\mu}$= 1.98 $\hat{\sigma}$=0.89
	Long Range	$\hat{\mu}$=-1.55 $\hat{\sigma}$=5.03	$\hat{\mu}$= 2.69 $\hat{\sigma}$=3.13	13.38	$\hat{\mu}$= 6.1 $\hat{\sigma}$= 1.0	$\hat{\mu}$= 1.6 $\hat{\sigma}$= 0.5	$\hat{\mu}$= 3.10 $\hat{\sigma}$=2.73
Transition (0500-1000,1800-2300)	*Short* Range	$\hat{\mu}$=-0.43 $\hat{\sigma}$=1.53	$\hat{\mu}$= 0.15 $\hat{\sigma}$=1.46	4.33	$\hat{\mu}$= 6.9 $\hat{\sigma}$= 1.1	$\hat{\mu}$= 1.3 $\hat{\sigma}$= 0.3	$\hat{\mu}$= 1.14 $\hat{\sigma}$=1.26
	Medium Range	$\hat{\mu}$=-0.23 $\hat{\sigma}$=1.90	$\hat{\mu}$= 0.11 $\hat{\sigma}$=1.04	4.36	$\hat{\mu}$= 7.2 $\hat{\sigma}$= 1.3	$\hat{\mu}$= 1.2 $\hat{\sigma}$= 0.4	$\hat{\mu}$= 1.56 $\hat{\sigma}$=0.89
	Long Range	$\hat{\mu}$= 0.31 $\hat{\sigma}$=3.07	$\hat{\mu}$= 1.78 $\hat{\sigma}$=3.01	9.33	$\hat{\mu}$= 6.1 $\hat{\sigma}$= 1.1	$\hat{\mu}$= 1.6 $\hat{\sigma}$= 0.5	$\hat{\mu}$= 2.10 $\hat{\sigma}$=2.10
Night (2300-0500)	*Short* Range	$\hat{\mu}$=-0.28 $\hat{\sigma}$=1.09	$\hat{\mu}$= 0.43 $\hat{\sigma}$=0.65	2.74	$\hat{\mu}$= 7.8 $\hat{\sigma}$= 1.2	$\hat{\mu}$= 1.2 $\hat{\sigma}$= 0.4	$\hat{\mu}$= 0.87 $\hat{\sigma}$=0.53
	Medium Range	$\hat{\mu}$= 0.09 $\hat{\sigma}$=1.52	$\hat{\mu}$= 0.19 $\hat{\sigma}$=0.77	3.43	$\hat{\mu}$= 7.9 $\hat{\sigma}$= 1.3	$\hat{\mu}$= 1.17 $\hat{\sigma}$= 0.30	$\hat{\mu}$= 1.37 $\hat{\sigma}$=0.74
	Long Range	$\hat{\mu}$= 0.19 $\hat{\sigma}$=2.71	$\hat{\mu}$= 0.90 $\hat{\sigma}$=1.37	6.35	$\hat{\mu}$= 6.7 $\hat{\sigma}$= 1.2	$\hat{\mu}$= 1.69 $\hat{\sigma}$= 0.75	$\hat{\mu}$= 1.38 $\hat{\sigma}$=0.84

Table 3   Distance and Time-of-Day Summary Statistics

Analysis of the effects of baseline distance and time-of-day on accuracy was done three ways. The first analysis was done using summary statistics on the data separated into fifteen categories based upon *Day*, *Transition* and *Night* time-of-day conditioned over *Short*, *Medium*, and *Long* range. The second analysis was a simple linear regression

of each time-of-day category. The third analysis was a more robust locally weighted regression of each time-of-day category.

The summary statistics in Table 3 are computed from the category of time-of-day separated into sub-categories of baseline distance. Cumulative Distribution Functions for each of theses fifteen plots can be found in APPENDIX D. HORIZONTAL ERROR BASED ON DISTANCE AND TIME-OF-DAY.

The linear regression of the effect of time-of-day can be summarized with four categories plus one aggregated category. At *Night* (2300-0500 local), the positioning accuracy is 1.9 meters (2drms) plus one meter for each additional 400 kilometers. During *Twilight* (1800-2300 local), the positioning accuracy is 1.5 meters (2drms) plus one meter for each additional 200 kilometers of baseline distance. During the *Day* (1000-1800 local), the positioning accuracy is 2.7 meters (2drms) plus one meter for each 185 kilometers of baseline distance. At *Dawn* (0500-1000 local), the positioning accuracy is 3.4 meters (2drms) plus one meter for each additional 550 kilometers. The *Dawn* and *Twilight* categories are combined into a new category; *Transition* (0500-1000 & 1800-2300 local), which has a positioning accuracy of 2.5 meters (2drms) plus one meter for each additional 300 kilometers of baseline distance.

	Coefficients	
	a	*b*
	(meters)	(meters/kilometer)
Time of Use (all times local)	(2drms)	
Night (2300-0500)	1.9	0.0025
Twilight (1800-2300)	1.5	0.0050
Day (1000-1800)	2.7	0.0054
Dawn (0500-1000)	3.4	0.0018
Transition (0500-1000 & 1800-2300)	2.5	0.0033

Table 4   2drms Prediction Coefficients Based on Time of Use

These predictions can also be computed from the coefficients provided by Table 4 using

$$2\text{drms} \approx a + b \cdot \left(\text{baseline distance (km)} \right). \qquad (3.6)$$

The lines plotted in Figure 16 are based upon Robust Locally Weighted Regression and Smoothing. The fitted line is based on an iterative method to solve a

polynomial fit using weighted least squares where the weight is large if the data point is close to the prediction and small if it is not. (Cleveland, 1979) The fitted lines in Figure 16 where calculated using the `lowess` function in *S-Plus 2000*. These effects have also been separated into their respective time-of-day categories and are plotted in APPENDIX C. 2DRMS VS. BASELINE PLOTS.

There are four notable observations in Figure 16. First, the horizontal error increases as baseline distance increases. Second, the time-of-day effects are ordered; *Night* offers the best accuracy, then *Twilight & Dawn*, and finally *Day*. Third, beyond about 300 kilometers, the error appears to be linearly increasing with baseline distance. Fourth, using DGPS with baseline distances up to approximately 700 kilometers always does better than standard non-differential GPS. Only during the *Day* at baseline distance of 700-1100 kilometers does it make sense to use non-differential GPS, as the differential corrections are actually increasing the horizontal error.
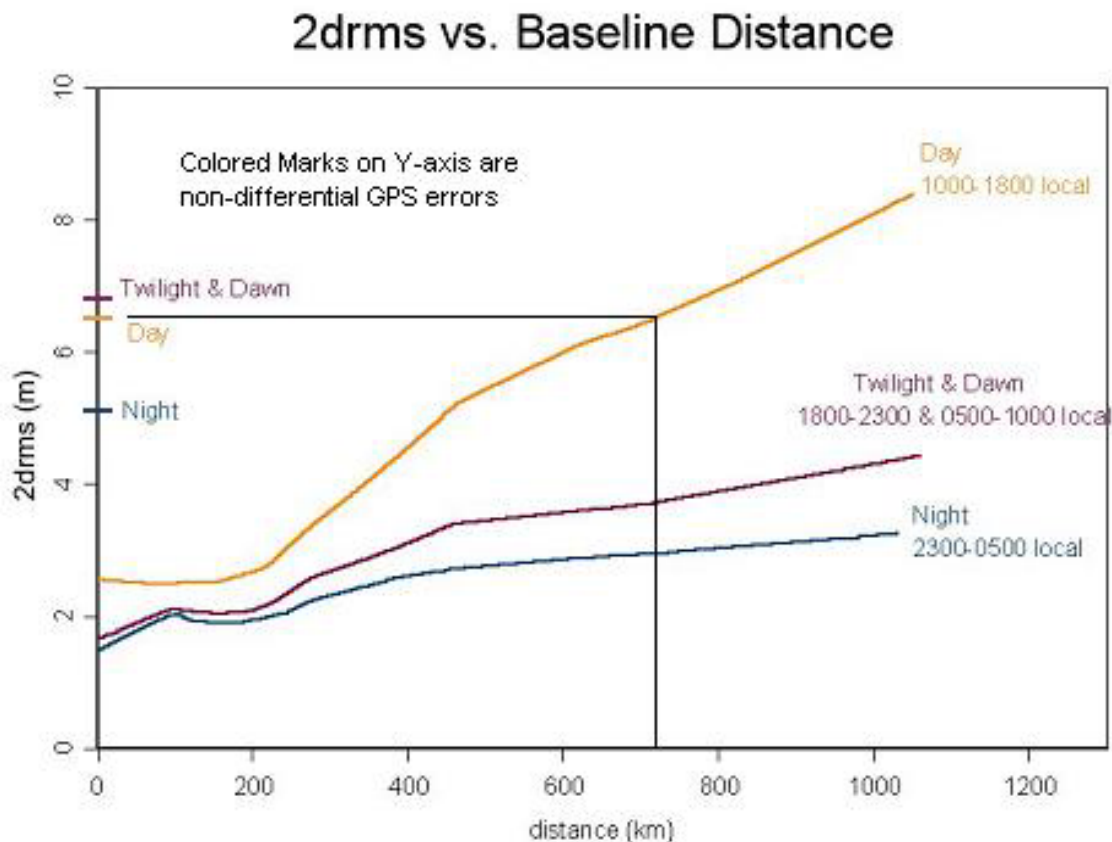
Figure 16   DGPS from USCG, 2drms vs. Baseline Distance Based on Time-of-Day Effects

29

4.   The Effect of Latitude

The latitude of the USCG DGPS station relative to the mobile user may have an effect on accuracy. For the data analyzed here, there was a strong correlation between the difference in latitude and baseline distance. So it is not clear that latitude alone caused the degradation in accuracy. To answer this question may require more data collection and further study.

Figure 17   Comparison of the Frequency Contour from each USCG DGPS Reference Station

5.   Elliptical Contours

For each reference station all north-south and east-west residual errors were used to develop two-dimensional histograms. For all seven reference stations, the errors were

modeled as bivariate normal (BVN). For each reference station, the best-fit BVN distribution was computed together with the semimajor axis, semiminor axis and semimajor axis orientation of the 95% error ellipse. As the baseline distance between the mobile user and reference station increased, so did the size of the 95% error ellipse. Also the semimajor axis consistently pointed in the direction of the reference station.
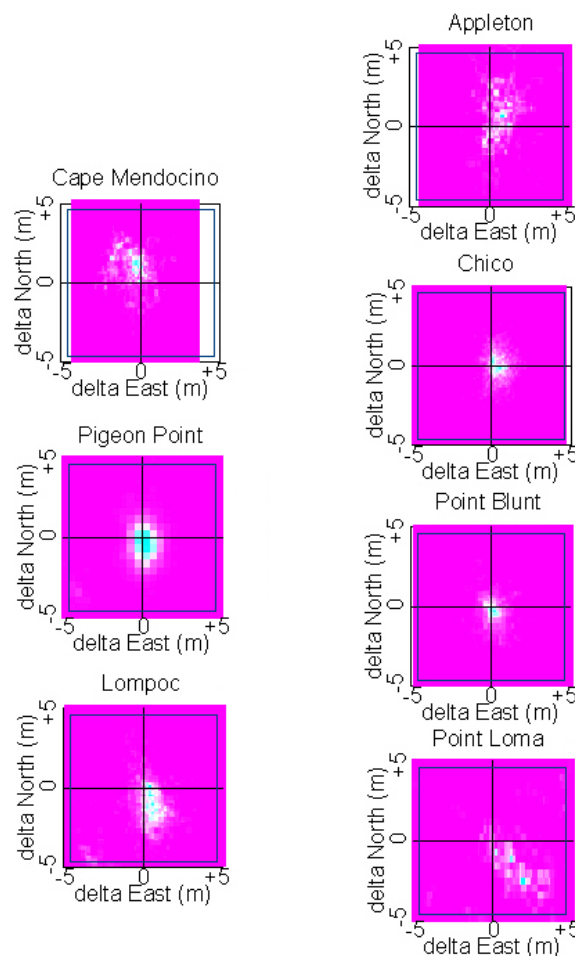
Figure 17 shows the two-dimensional histogram of the residual errors for each reference station. The number of data points and the intensity scales vary from plot-to-plot, but the general BVN shape is apparent. Scaled plots of higher resolution appear in APPENDIX E. CONTOUR PLOTS AND CORRELATIONS FOR USCG DGPS REFERENCE STATIONS.

It should be noted that the reference stations were largely to the north or south of the mobile user in this study. Because of differences between the north-south and east-west structure of the ionosphere, it is not known whether BVN assumption would also hold for reference stations distributed mainly east-west relative to the mobile user.

For each of the seven reference stations, sample variances and covariance statistics were computed. These values were used to estimate the orientation and size of the best-fit 95% BVN horizontal error ellipse. Specifically, to estimate α, the azimuth of the semimajor axis, sample quantities replaced corresponding parameters in the following equation

$$\tan 2\alpha = \frac{2 \cdot \hat{\sigma}_{EN}}{\hat{\sigma}_N^2 - \hat{\sigma}_E^2}, \text{ where} \qquad (3.7)$$

$\hat{\sigma}_E^2 = \hat{\sigma}_{east}^2 \equiv$ sample variance of the east error residual

$\hat{\sigma}_N^2 = \hat{\sigma}_{north}^2 \equiv$ sample variance of the north error residual

$\hat{\sigma}_{EN} \equiv$ sample covariance of the east and north error residual

The standard deviations a and b of the semimajor and semiminor axes respectively of the BVN error ellipse are given by the eigenvalues of the covariance matrix:

31

$$a = \sqrt{\frac{1}{2} \cdot \left\{ \sigma_E^2 + \sigma_N^2 + \sqrt{\left(\sigma_E^2 - \sigma_N^2\right)^2 + 4 \cdot \left(\sigma_{EN}\right)^2} \right\}}, \qquad (3.8)$$

$$b = \sqrt{\frac{1}{2} \cdot \left\{ \sigma_E^2 + \sigma_N^2 - \sqrt{\left(\sigma_E^2 - \sigma_N^2\right)^2 + 4 \cdot \left(\sigma_{EN}\right)^2} \right\}}. \qquad (3.9)$$

For the BVN distribution, the lengths of the 95% (2.45σ) semimajor and semiminor axes are obtained by multiplying a and b by 2.45. Once the semimajor and minor axes are known, we solve for eccentricity, e, of the error ellipse using (3.10).

$$e = \sqrt{1 - \frac{b^2}{a^2}} \qquad (3.10)$$

The α in (3.7) represents the *orientation* of the error ellipse. The average distance and azimuth to each USCG reference station can be calculated from the data set U.

$$\text{average distance} \equiv \overline{distance} \qquad (3.11)$$

$$\text{average azimuth} \equiv \overline{azimuth} \qquad (3.12)$$

In Table 5, *orientation* and $\overline{azimuth}$ are strongly related. Additionally, *eccentricity* and *semimajor axis* are moderately related to $\overline{distance}$.

Reference Station	1σ Semi-major axis (meters)	1σ Semi-minor axis (meters)	*Eccentricity*	*Orientation* (˚True)	$\overline{azimuth}$ (˚True)	$\overline{distance}$ (km)
Appleton	2.10	1.08	0.86	009.8	009.7	1020.4
Cape Mendocino	1.20	0.90	0.66	341.1	333.2	425.5
Chico	0.99	0.65	0.75	001.9	028.5	234.7
Pigeon Point	1.64	1.27	0.63	209.4	168.3	080.5
Point Blunt	1.27	0.91	0.70	171.0	081.9	023.8
Lompoc	1.92	1.18	0.79	211.2	149.3	296.7
Point Loma	4.79	3.11	0.76	152.9	129.5	731.3

Table 5   Data Set *Contour*, USCG DGPS Reference Stations's 1σ Error Ellipses Summary

The correlation coefficient between *eccentricity* and $\overline{distance}$ is 0.7. The correlation coefficient between *orientation* and $\overline{azimuth}$ is 0.9, supporting the visual

32

results in Figure 17. A summary of the correlation tables and more detailed plots of the contours are in APPENDIX E. CONTOUR PLOTS AND CORRELATIONS FOR USCG DGPS REFERENCE STATIONS.

To validate the error ellipses definition, the Appleton, Washington data was plotted against the derived ellipses from equations (3.8) and (3.9). Each data point was checked to see if it fell within the 1σ ellipse or outside the ellipse.

$$\frac{19123 \text{ data points inside the ellipse}}{48859 \text{ total data points}} = 0.39139 \approx 39\% \tag{3.13}$$

The resulting ratio was 0.39, consistent with a 1σ error ellipse. For a bivariate normal random variable, the $x \cdot \sigma$ error ellipse contains $1 - e^{\left(-x^2/2\right)}$ of the probability mass. So the 1σ ellipse should contain $1 - e^{\left(-1^2/2\right)} \approx 0.393$.
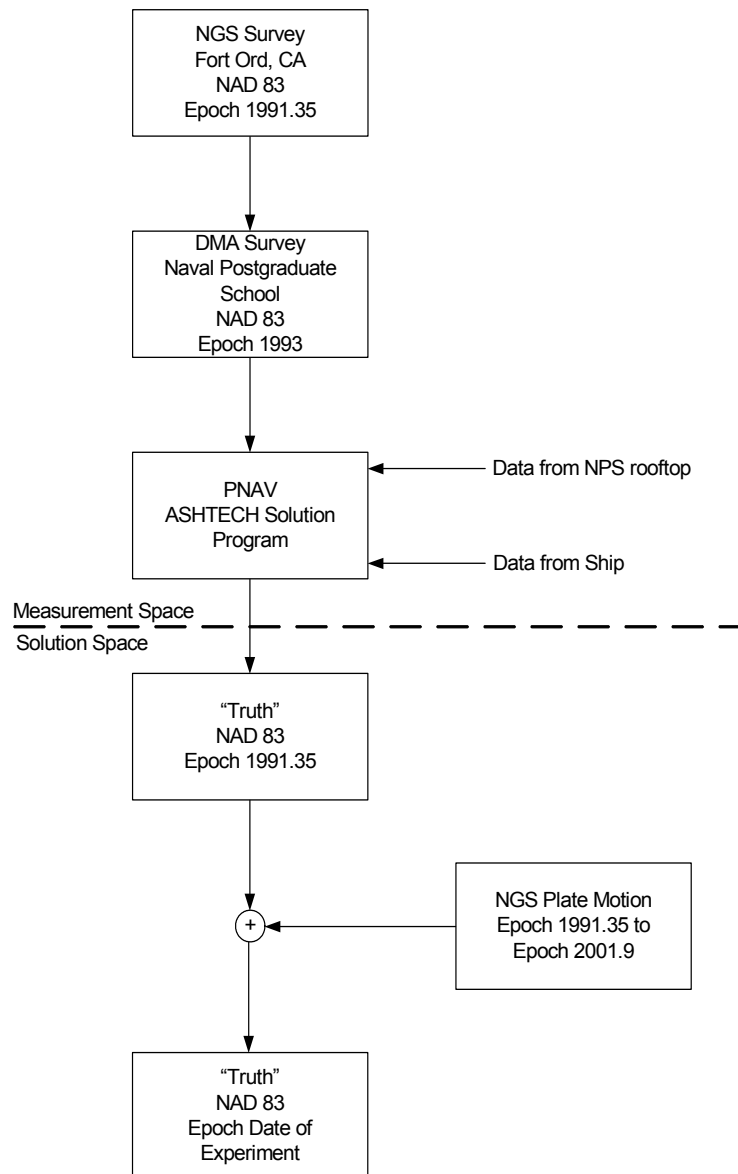
Figure 18   Application Diagram for NGS HTDP Plate Motion Model (After Clynch, 2002)

6.   Support of the National Geodetic Survey Plate Motion Model

The National Geodetic Survey has a plate motion model program on their website at   http://www.ngs.noaa.gov/TOOLS/Htdp/Htdp.html.   This software is called the Horizontal Time Dependent Positioning (HTDP) program.   It allows the user to interactively supply a starting date, ending date, and geographic position.   The HTDP

software then calculates the effects of the plate motion in the north and east directions. The model follows the illustration in Figure 19.

To attain an accurate truth trajectory for calculating the position differences in this study, the HTDP model of plate motion was used (see Figure 18). The base reference station for the reference solution was last surveyed off an NGS data sheet in Epoch 1991.35. Using HTDP (version 2.6), the Naval Postgraduate School's Spanagel Hall roof top benchmarks were displaced 0.398 meters northward and 0.277 meters eastward. When these displacements were added to the biases of the data set, the resulting means were within 9-10 centimeters of zero. The DGPS position solution is zero-mean based. Those 9-10 centimeters are small enough in magnitude to be below the threshold of potentially skewing the resulting analysis.
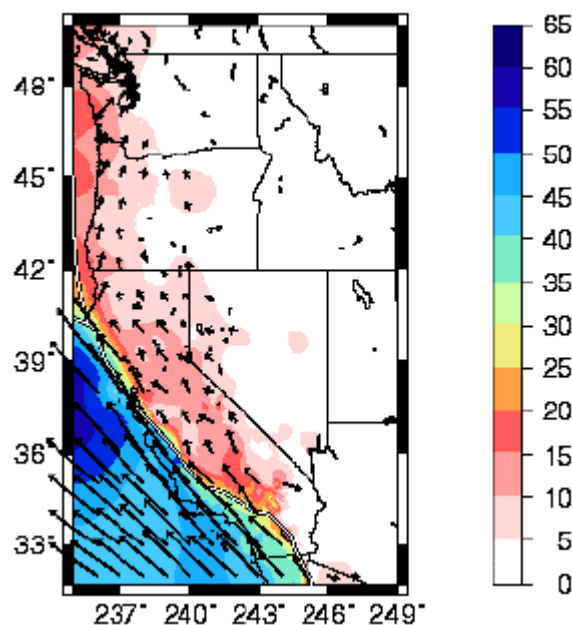

Figure 19   National Geodetic Survey (NGS) - Horizontal Time Dependent Positioning (HTDP) Model in Millimeters per Year (From NGS, 2002)

7.   Equivalent Small Changes in Datum for Measurement and Solution Space

The purpose of this section is to explain the equivalence between measurement space and solution space for small changes in datums. The datum of the reference station becomes the datum of the mobile user when using Differential GPS. In the case of the USCG DGPS, the datum is North American Datum 1983 (NAD-83). The datum used for

the reference trajectory, on top of the Naval Postgraduate School's Spanagel Hall, had to be carefully reconciled to NAD-83. Since differential corrections are actually made in measurement space, before any position solution is calculated, it was important to assess the consequences of making small changes in datum in solution space.

a. USCG Datum

The datum used by the USCG for DGPS is NAD-83. The NAVCEN web page, which lists all USCG reference station's status, also states NAD-83 as the datum in use. A visit to the USCG Differential GPS reference station at Pigeon Point, California also confirmed the datum was NAD-83. More details can be found in APPENDIX H. PIGEON POINT VISIT. The data collected for the experiment came from seven different USCG reference stations from the west coast of the contiguous 48 United States. Each station reported and appeared to be using NAD-83, the correct datum.

b. Naval Postgraduate School Datum

The datum used by the rooftop benchmarks on Spanagel Hall at the Naval Postgraduate School in Monterey, California is NAD-83. The reference trajectory was solved using a GPS receiver on the roof of Spanagel Hall. Any differences between the datum of the USCG DGPS and the "truth" had to be carefully reconciled. The rooftop benchmarks were traced back to a National Geodetic Survey (NGS) of April 8, 1991. The majority of the data was processed using the correct benchmark.

c. Datum Shift

Some of the data was processed using an incorrect location about six meters away. This offset was discovered during analysis of the data set U. To correct it, an experiment was conducted to analyze the differences between the reference trajectory based upon two different benchmarks, one in measurement space and the other in solution space. Since GPS measurements are made from the center of the Earth, small changes in a solved position on the surface would be negligible when translated back to measurement space. Experimental data suggested small changes in position (on the order of a few meters or less) are equivalent to simply adding a bias. So the data set was adjusted for this offset and all reference stations were placed on the same datum.

IV. CONCLUSION

A. SUMMARY

Differential GPS has provided a valuable service to marine users within the USCG's Area of Coverage (AOC). Although mobile users may not be within the AOC, the beacon signal is still receivable and relevant. The correction data improves the accuracy of the position as a function of distance and time-of-day. The USCG DGPS is more accurate than absolute GPS positioning in a 0 to ~700 kilometer baseline during the *Day* (1000-1800 local) and in 0 to ~1100 kilometer baselines during all other times (1800-1000 local). As long as the marine mobile user understands the degradation of accuracy when using the correction data outside of the AOC, there should be no harm in using the signal. If this predictable loss of accuracy is unacceptable, alternative solutions to maintain high accuracy are available, but require additional equipment and financial support.

1. Baseline Distance Affects Accuracy

Baseline distance affects the accuracy of USCG DGPS. With a baseline distance from zero to ~250 kilometers, the positioning accuracy is 2.5 meters (2drms). To find the positioning accuracy as the baseline distance increases from ~250 to ~1100 kilometers, take 2.5 meters (2drms) and add an additional one meter (2drms) for each additional 300 kilometers. This result is averaged over time-of-day.

2. Time-of-Day Affects Accuracy

The time-of-day affects the accuracy of USCG DGPS. At *Night* (2300-0500 local), the positioning accuracy is 1.9 meters (2drms) plus one meter for each additional 400 kilometers. During *Twilight* (1800-2300 local), the positioning accuracy is 1.5 meters (2drms) plus one meter for each additional 200 kilometers of baseline distance. During the *Day* (1000-1800 local), the positioning accuracy is 2.7 meters (2drms) plus one meter for each 185 kilometers of baseline distance. At *Dawn* (0500-1000 local), the positioning accuracy is 3.4 meters (2drms) plus one meter for each additional 550 kilometers. The *Dawn* and *Twilight* categories are combined into a new category;

Transition (0500-1000 & 1800-2300 local), which has a positioning accuracy of 2.5 meters (2drms) plus one meter for each additional 300 kilometers of baseline distance.

3.   Error Ellipses

For the bivariate normal (BVN) distribution, the 95% error ellipse is the smallest area that contains the user's horizontal position 95% of the time. For each reference station used in this study, a best-fit BVN 95% error ellipse was created. The size and shape of these error ellipses was unique to each reference station. The error ellipse's orientation was strongly correlated to the bearing of the reference station. The semimajor axis and the eccentricity of the error ellipses were moderately correlated to the average distance from the reference station. These two statistics describe how the horizontal accuracy degrades with distance. As distance from the reference station increased, so did the semimajor axis and eccentricity of the 95% error ellipse. In general, the semimajor axis pointed from the mobile user to the reference station.

B.   FURTHER STUDIES

This study has addressed some of the issues and questions about Differential GPS beyond nominal range. It has also prompted new speculation and potential further work on this topic. The relevance to marine positioning and potential military applications cannot be understated.

1.   Effects of Latitude on Accuracy

The data collected in the experiment to support this study only examined small changes in latitude's effect on accuracy. More detailed analysis could further explain the effects of the magnetic equator and relationship to the southern and northern hemispheres.

2.   Effects of Longitude and Time-of-Day on Accuracy.

The data collected for this study was gathered from reference stations with predominantly North-South azimuths. There is not enough statistical support in the data set to make any conclusions about the effects of longitude and East-West azimuths on the DPGS accuracy. Because of the sharp increase in the Total Electron Content (TEC) at dawn as seen in Figure 13 and the assumption made by the RTCM Committee that the

ionosphere is the same everywhere within the range of the beacon signal, more data is needed to explore the East-West azimuth effects.

THIS PAGE INTENTIONALLY LEFT BLANK

V. RECOMMENDATIONS

A.   STRATEGIES FOR USE OF CURRENT SYSTEM

To obtain more reliably accurate positioning outside the Area of Coverage (AOC) when using the USCG DGPS, it is recommend to survey at night (2300-0500 local), or to minimize survey operations during transition periods between night and day (0500-1000 & 1800-2300 local), when the effects of the ionosphere are changing. At baseline distances from approximately zero to 700 kilometers, USCG DGPS is providing better positioning than standard GPS during the day (1000-1800 local). During all other times (1800-1000 local), USCG DGPS with baselines less than approximately 1100 kilometers always does better than standard GPS. A developed understanding of the forces that affect the accuracy beyond nominal range led to this recommendation.

B.   ADDITION OF MORE REFERENCE STATIONS

Adding a reference station near the area of operation requiring highly accurate positioning is recommended. Sub-meter accuracy has been obtained at short baselines using real-time and post-processing kinematic solutions. Short baseline data in this study also endorses this recommendation. Positioning accuracy was 4.0 meters (2drms) when within the USCG DGPS AOC. In the current fiscal atmosphere, adding more reference stations may not be a viable course of action.

C.   USE OF A WEIGHTED SOLUTION

If more than one DGPS correction signal can be received, apply a system of weights to the solutions to improve the accuracy of the position. If more than one USCG beacon signal is receivable, apply a system of mathematical weights to the corrections to give a more robust correction. This technique could be accomplished in real time, given additional beacon receivers and software capable of including a weighting system. Accuracy of 7.5 meters (2drms) has been achieved using this technique. (Abousalem, 1996)

This technique is often referred to as Wide Area Differential GPS (WADGPS). It involves one of three algorithms; measurement domain, solution domain, or state-space domain algorithms. (Abousalem, 1996) Measurement domain involves weighting the

pseudorange corrections and then calculating a solution position. Solution domain algorithms calculate solutions and then apply a weighting scheme to the solutions to provide combination of the positions based on the geographic centroid of the reference stations. State-space domain algorithms use atmospheric models, predictions of accuracy, and other techniques to apply the weighting in the solution processing. (Abousalem, 1996). Each of these techniques has advantages and disadvantages. Before deciding to employ any of these systems, the financial and logistical requirements must be determined. Perhaps simply buying better equipment is not possible.

D. USE OF EXTENDED DGPS

Subscribe to a satellite communication link that provides Extended DGPS corrections out to a baseline of approximately 1600 kilometers from CONUS with eight meter (2drms) accuracy. Extended DGPS uses many disparate reference stations to create an ionospheric and tropospheric model and a prediction of the ephemeris error to improve accuracy over long baselines distances as shown in Figure 20. (Brown, 1989)
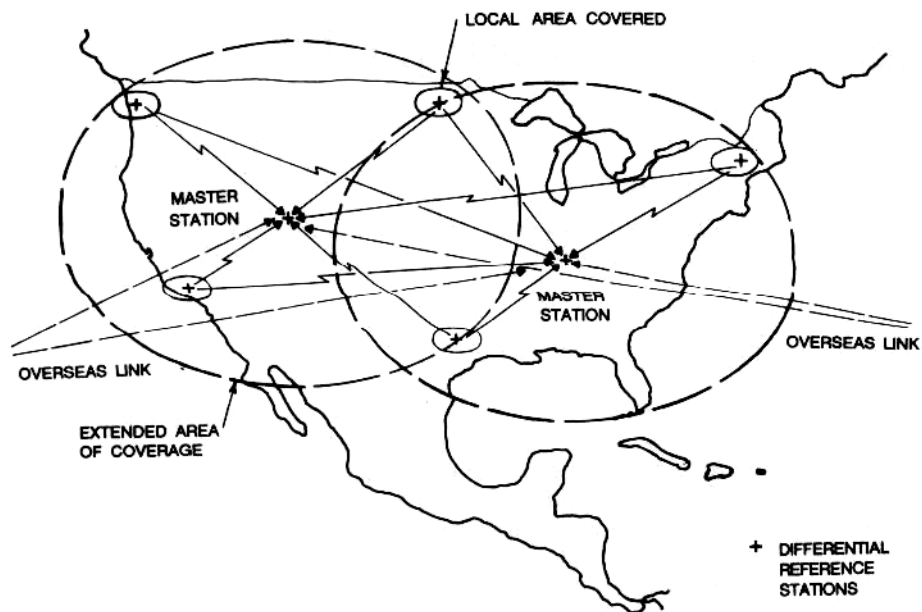

Figure 20   Extended GPS Network (From Brown, 1989)

E. USE OF WIDE AREA AUGMENTATION SYSTEM (WAAS)

The Wide Area Augmentation System (WAAS) was originally devised for precision aircraft landing systems. It involves using two geostationary satellites to broadcast the Differential GPS correction information to the North American continent. Additional navigation data is involved in the transmission to the mobile user, similar to the USCG Differential GPS. It includes an integrity monitor, to notify the mobile user that the correction information is suspect. Although designed for aircraft, it could prove effective to marine users within the broadcast range of the correction signal from space.

THIS PAGE INTENTIONALLY LEFT BLANK

APPENDIX A. GPS FUNDAMENTALS

A.   SPACE SEGMENT

The space segment includes all of the deployed satellites, placed in precise orbits via unmanned booster rockets or the space shuttle. Precise spacing of the satellites in orbit is arranged such that a minimum of four satellites are in view to a user at any given time on a worldwide basis. The 24 satellites are in six semi-synchronous orbital planes with four satellites per plane. At any given time, 21 of the satellites are active, with three in use as spares. Each space vehicle completes an orbit approximately once every 12 hours.

There are two signals transmitted continuously by each space vehicle. The modulated spread spectrum signals come on two L-band frequencies, 1575.42 MHz (L1) and 1227.6 MHz (L2). The transmissions are pseudo-random noise (PRN), sequence modulated radio signals. Both a coarse acquisition code (C/A code) and precision code (P code) are transmitted on the L1 band, but only the P code is transmitted on the L2 band. Because both the C/A and P code are transmitted on L1 band, the PRN is unique for each satellite. Using the PRN sequence is how a satellite is identified when the GPS control system communicates with users about a particular GPS satellite. In addition to the PRN, there is navigation information super-imposed on the codes that contain satellite ephemeris data, atmospheric propagation information, the satellite clock bias, and satellite health data.

B.   CONTROL SEGMENT

The Earth-based tracking stations that monitor the satellite's orbits and provide corrective information to the system are called the operational control segment (OCS). The control segment consists of a master control station (MCS), a number of monitor stations, and ground antennas located throughout the world. The MCS located in Colorado Springs, Colorado, consists of equipment and facilities required for satellite monitoring, telemetry, tracking, commanding, control, uploading, and navigation message generation. The monitor stations, located in Hawaii, Colorado Springs, Kwajalein, Diego Garcia, and Ascension Island, passively track the satellites,

accumulating ranging data from the satellites' signals and relaying them to the MCS. The MCS processes this information to determine very precise satellite position and signal data accuracy, updates the navigation message of each satellite and relays this information to the ground antennas. The ground antennas then transmit the position and data accuracy information to the satellites.

C.   USER SEGMENT

The third component is the receiver segment, consisting of government provided or commercially available receiving units. The user segment is designed for different requirement of various users. These receivers can be used in high, medium, and low dynamic applications. The user segment can consist of stand-alone receivers or equipment that is integrated into another navigation system. The user equipment is designed to receive and process signals from four or more orbiting satellites either simultaneously or sequentially.

To describe the accuracy of the calculated position, a meaningful vocabulary is needed. User range accuracy (URA) is a statistical indicator of the ranging accuracies obtainable with a specific space vehicle (SV). URA is a one-sigma estimate of the user range errors in the navigation data for the transmitting satellite. It includes all errors for which the space and control segment are responsible. It does not include any errors introduced in the user set or the transmission media.

APPENDIX B. PSEUDORANGE AND TIMING
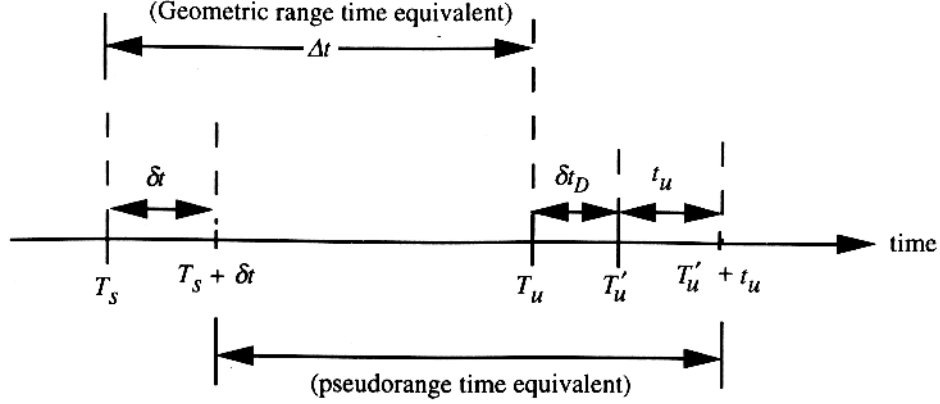
Figure 21   Range Measurement Timing Relationships. (From Kaplan, 1996)

The timing relationships are shown in Figure 21, where

Δt = geometric range time equivalent

T_s = system time at which the signal left the satellite

T_u = system time at which the signal would have reached the user receiver without δt_D (theoretical)

T_u' = system time at which the signal reached the user receiver with δt_D

δt = offset of the satellite clock from system time (advance is positive; retardation (delay) is negative)

$$\delta t_D = \delta t_{atm} + \delta t_{noise\&res} + \delta t_{mp} + \delta t_{hw} + \delta t_{SA} \qquad (5.1)$$

δt_{atm} = delays due to the atmosphere

$\delta t_{noise\&res}$ = receiver noise and resolution offset

δt_{mp} = multipath offset

δt_{hw} = receiver hardware offsets

δt_{SA} = SA degradation (Kaplan, 1996)

THIS PAGE INTENTIONALLY LEFT BLANK

APPENDIX C. 2DRMS VS. BASELINE PLOTS

This appendix has each time-of-day effect plotted separately as a function of baseline distance. The colored solid line is the robust locally weighted least squares regression and smoothing of a polynomial fit ($\hat{y}_i$) to the data. The colored dashed line represents $\hat{y}_i \pm 1\sigma$ (the prediction at the i-th point plus and minus one standard deviation). The black solid straight line is the mean (μ) of the absolute GPS position without using any differential corrections. The black dashed lines are the $\mu \pm 1\sigma$ (the mean plus and minus one standard deviation). The fourth plot includes all three categories of time and their respective 1σ prediction intervals.
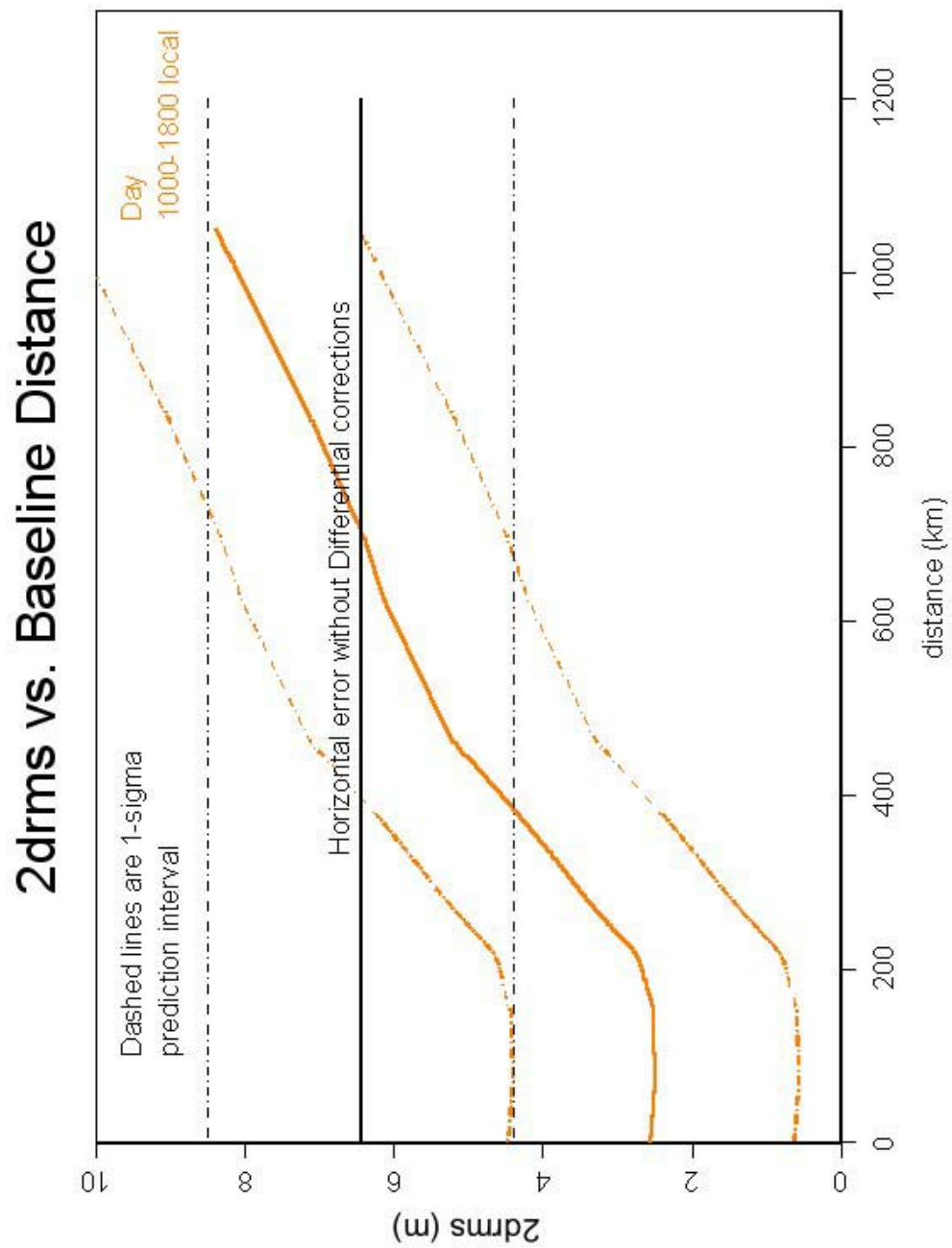
Figure 22 2drms *vs.* Baseline Distance during *Day*
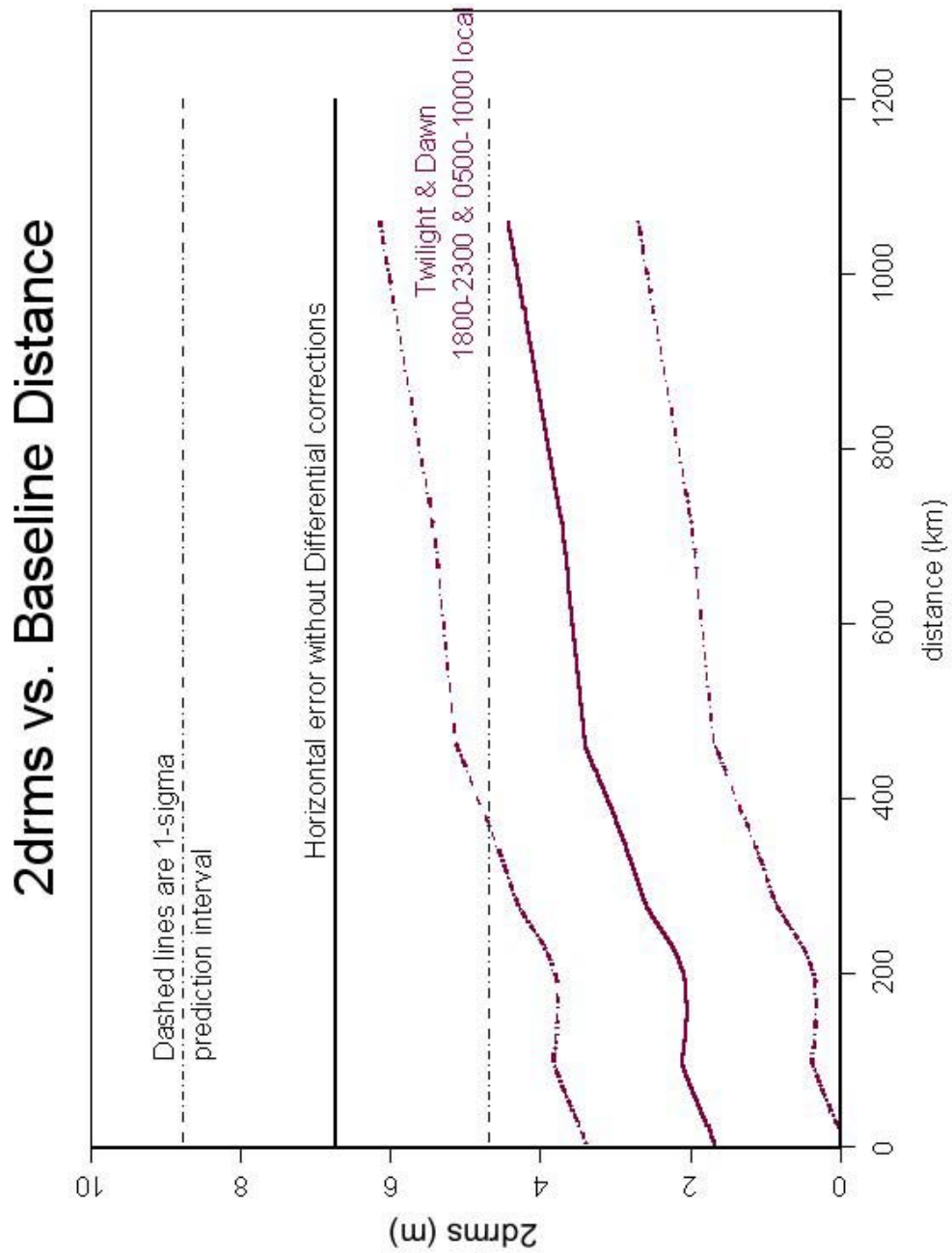
Figure 23   2drms *vs.* Baseline Distance during *Dawn* and *Twilight*
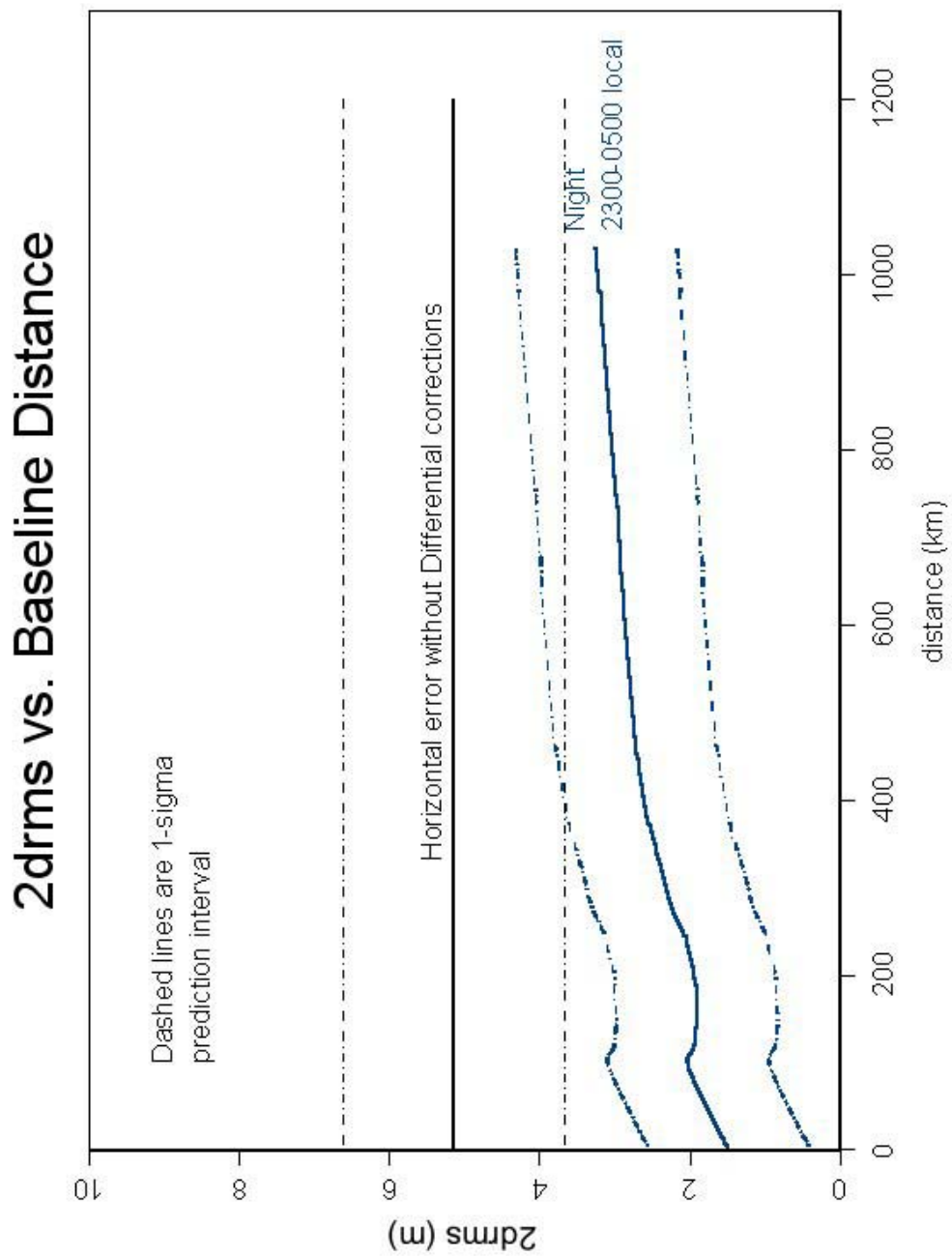
Figure 24   2drms *vs.* Baseline Distance during *Night*
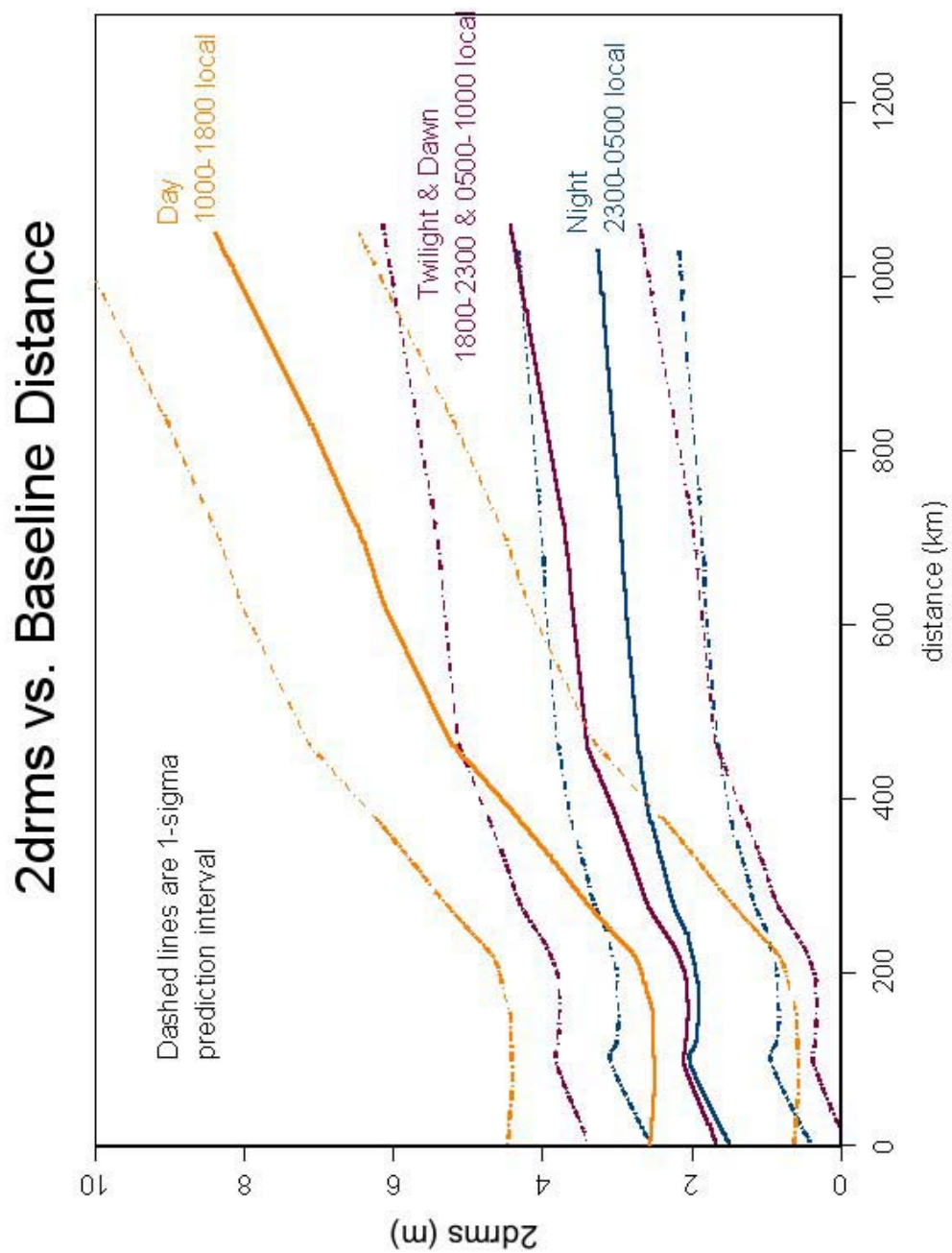
Figure 25   2drms vs. Baseline Distance with Time-of-Day and 1σ Prediction Intervals

THIS PAGE INTENTIONALLY LEFT BLANK

APPENDIX D. HORIZONTAL ERROR BASED ON DISTANCE AND TIME-OF-DAY
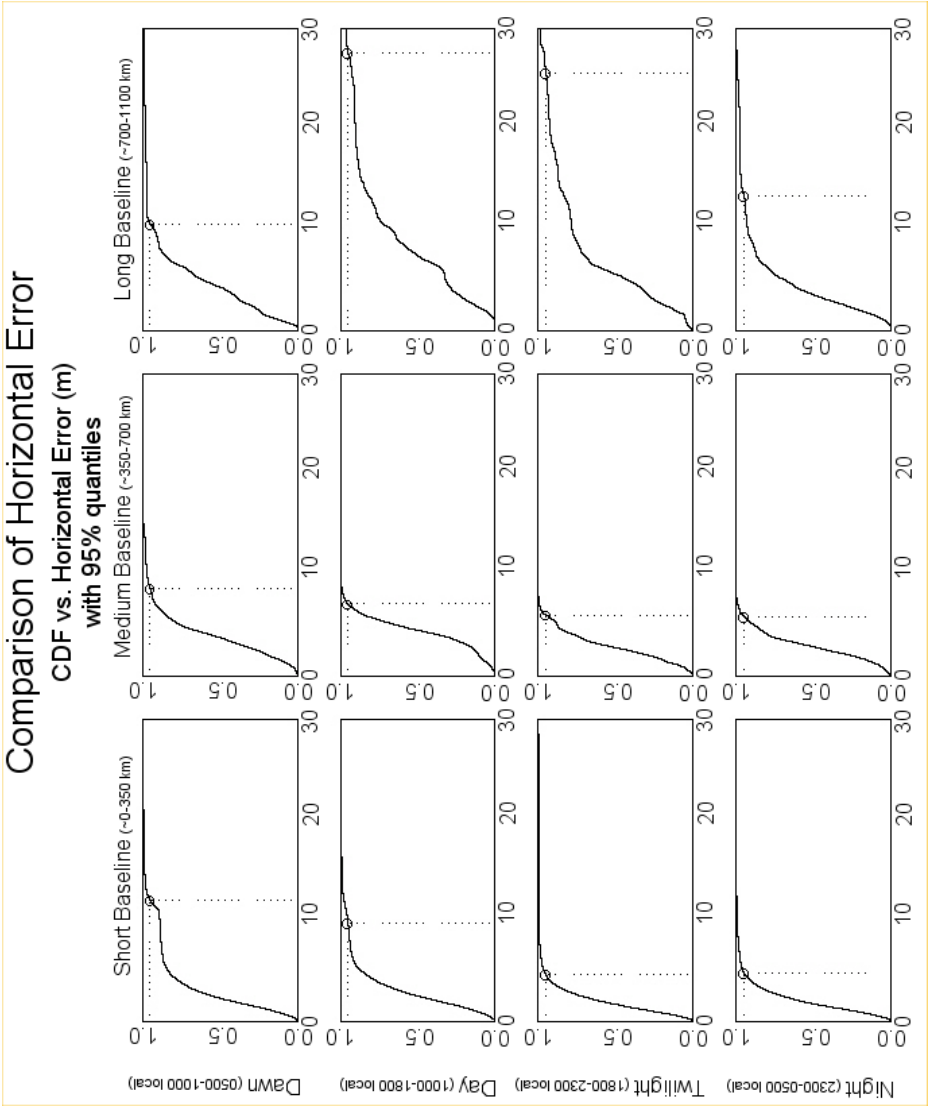
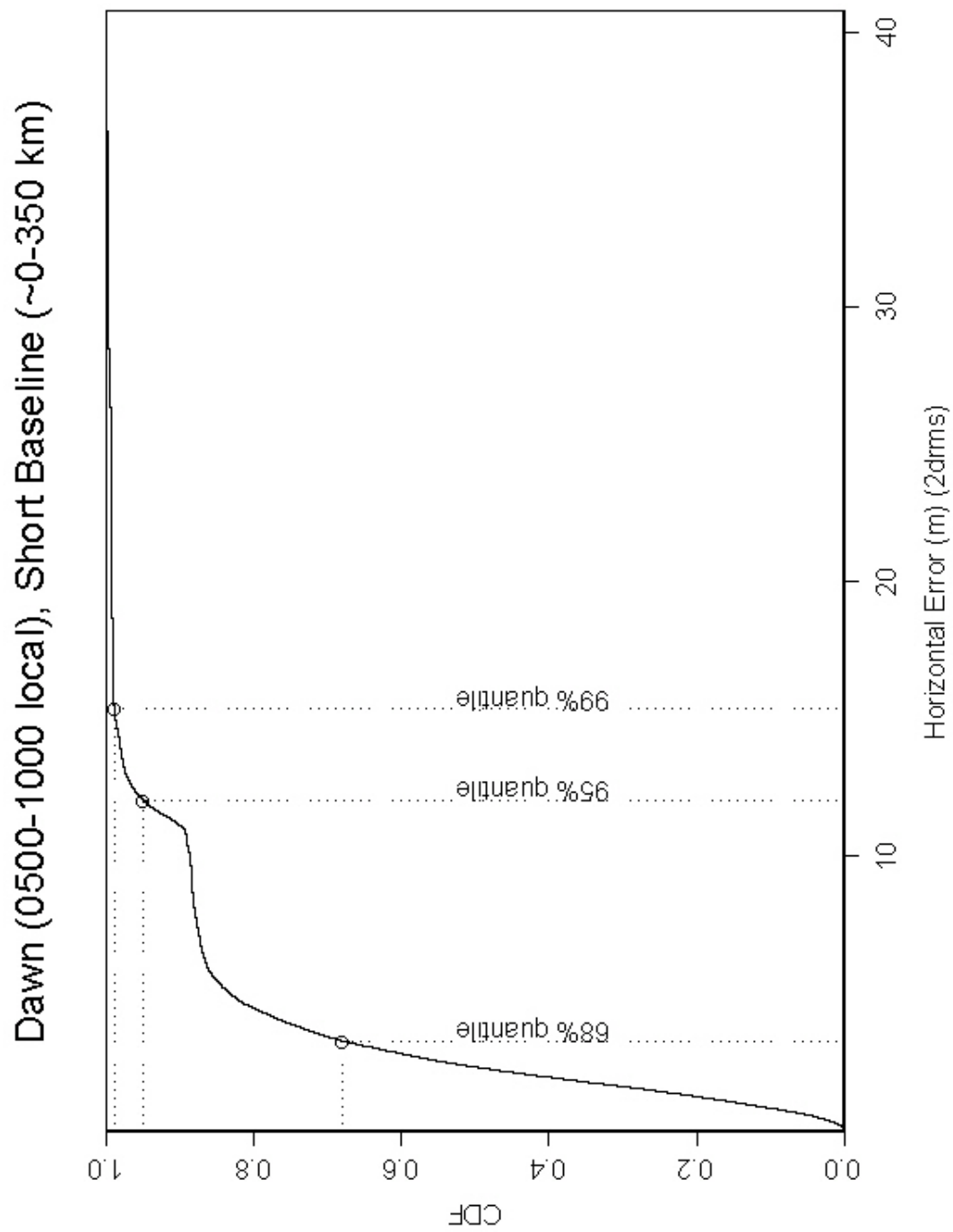Figure 26   Comparison of Horizontal Error Based on Baseline Distance and Time-of-Day

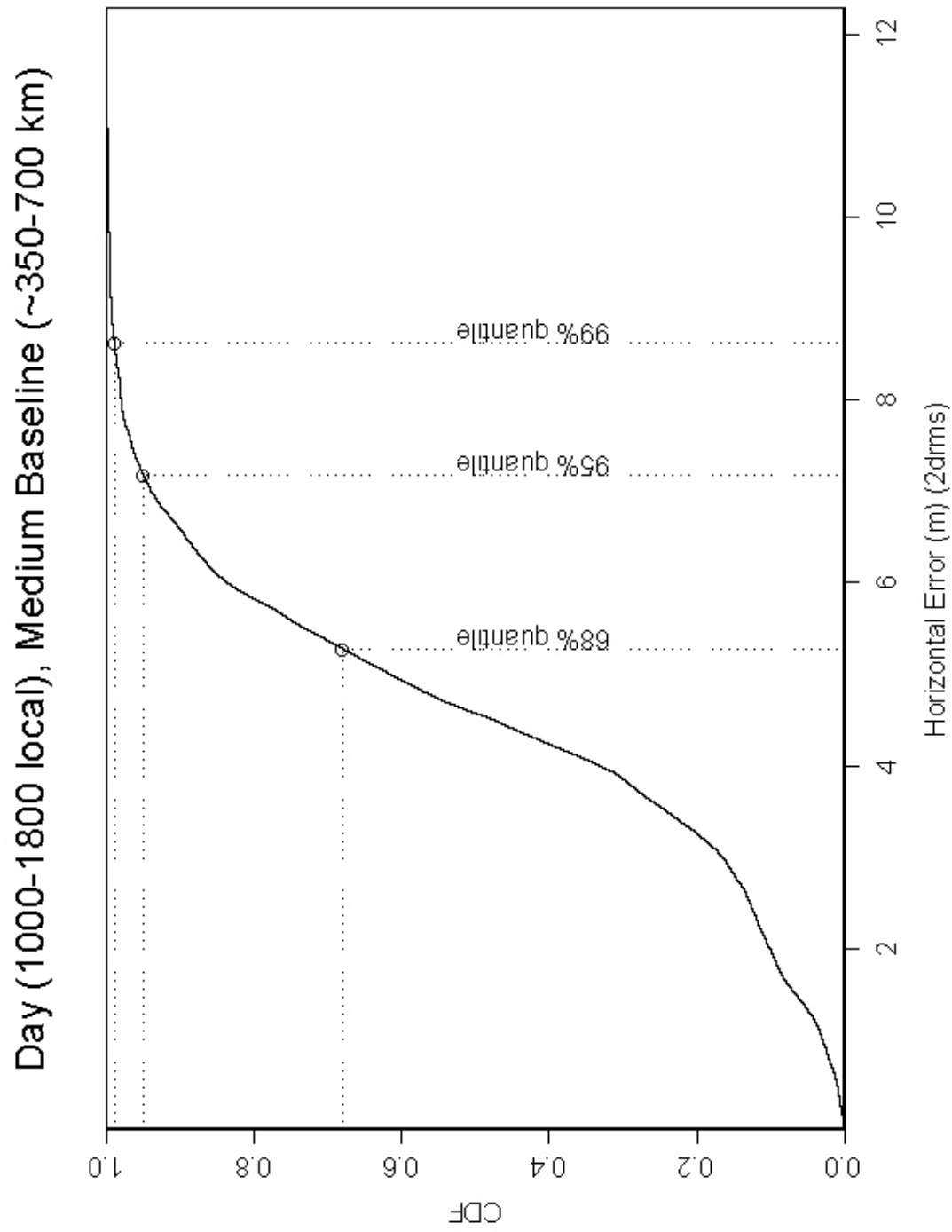Figure 27   Horizontal Error – CDF during *Dawn* with a *Short* Baseline
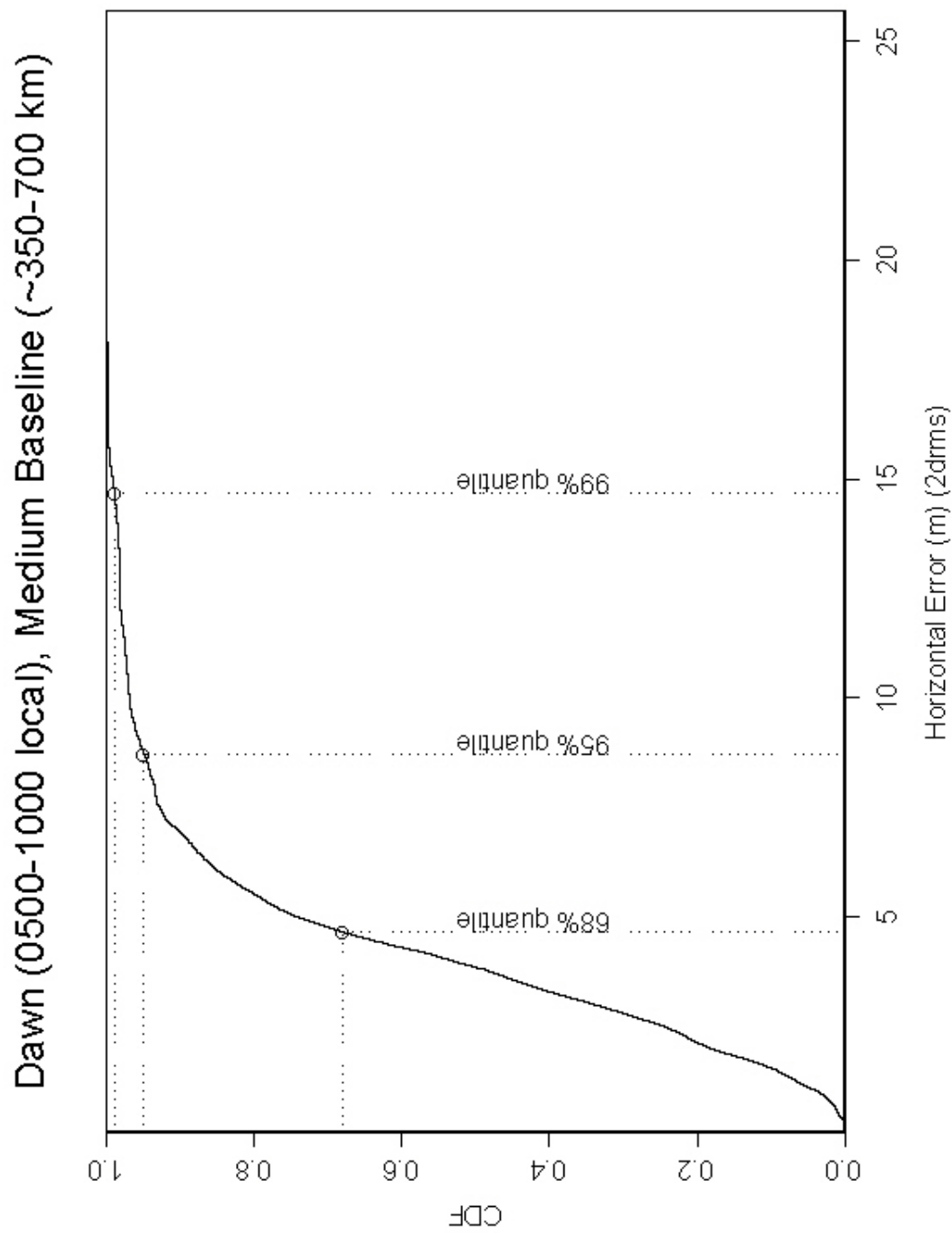
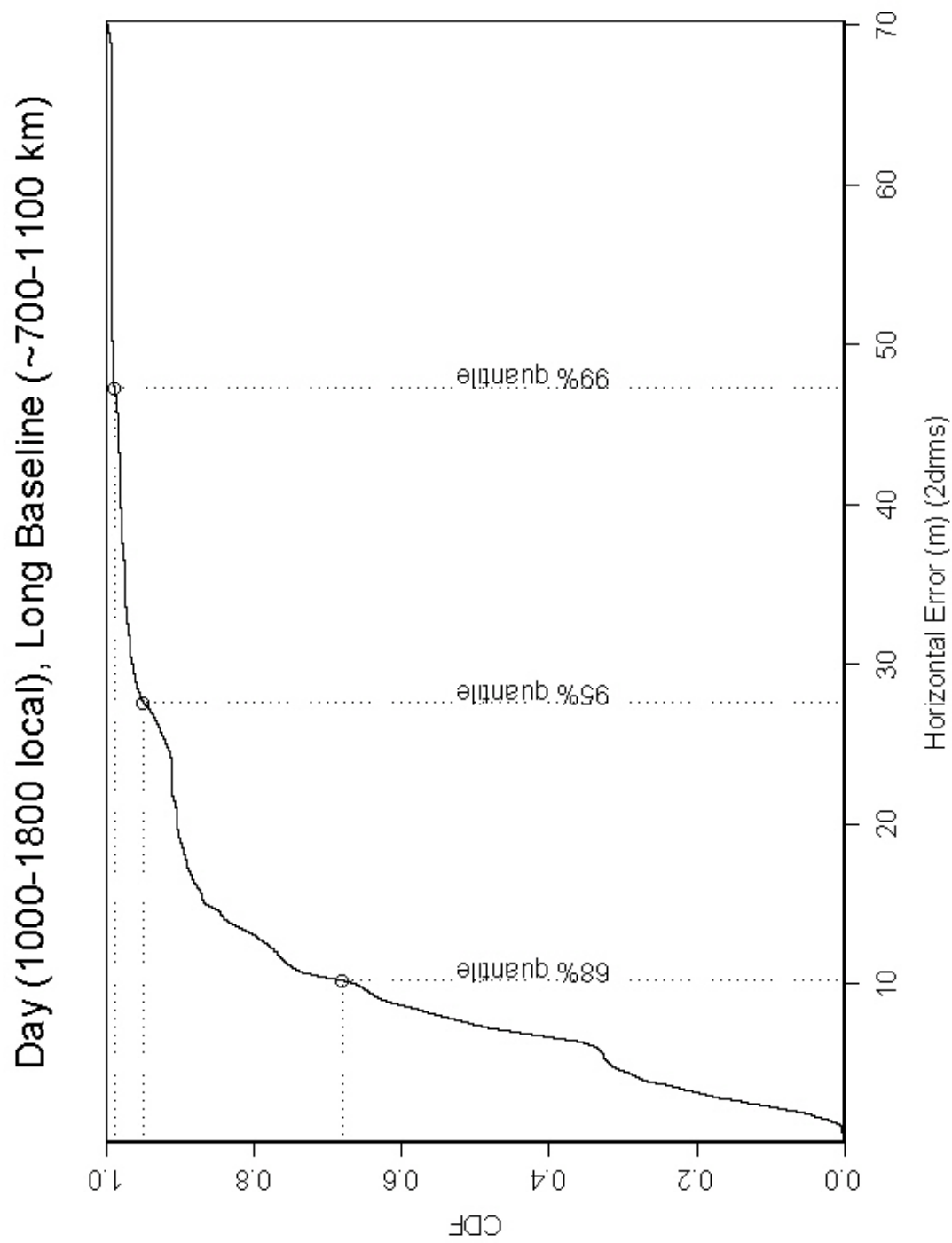Figure 28   Horizontal Error – CDF during *Dawn* with a *Medium* Baseline

57
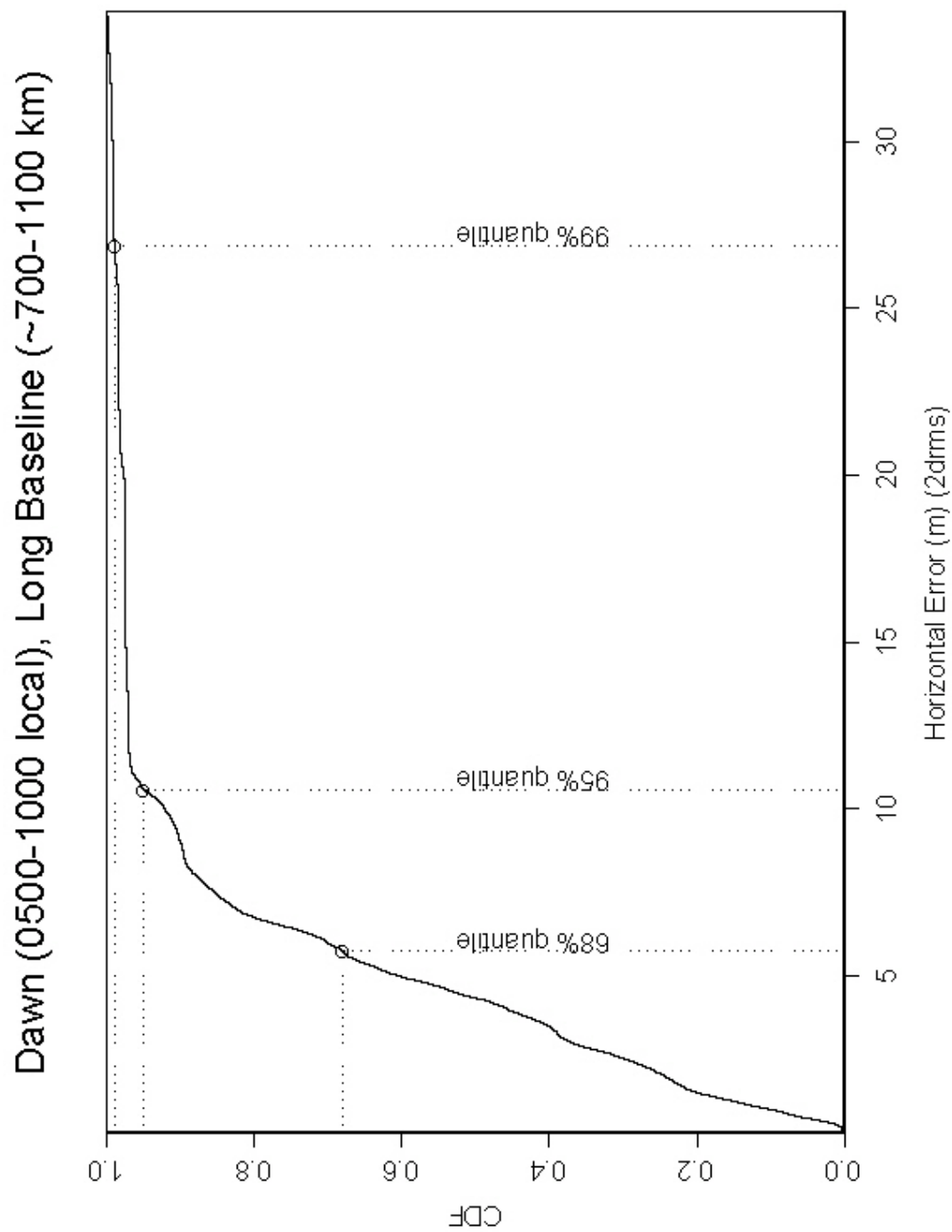
Figure 29   Horizontal Error – CDF during *Dawn* with a *Long* Baseline

Day (1000–1800 local), Short Baseline (~0–350 km)

68% quantile

95% quantile

99% quantile

Horizontal Error (m) (2drms)

CDF
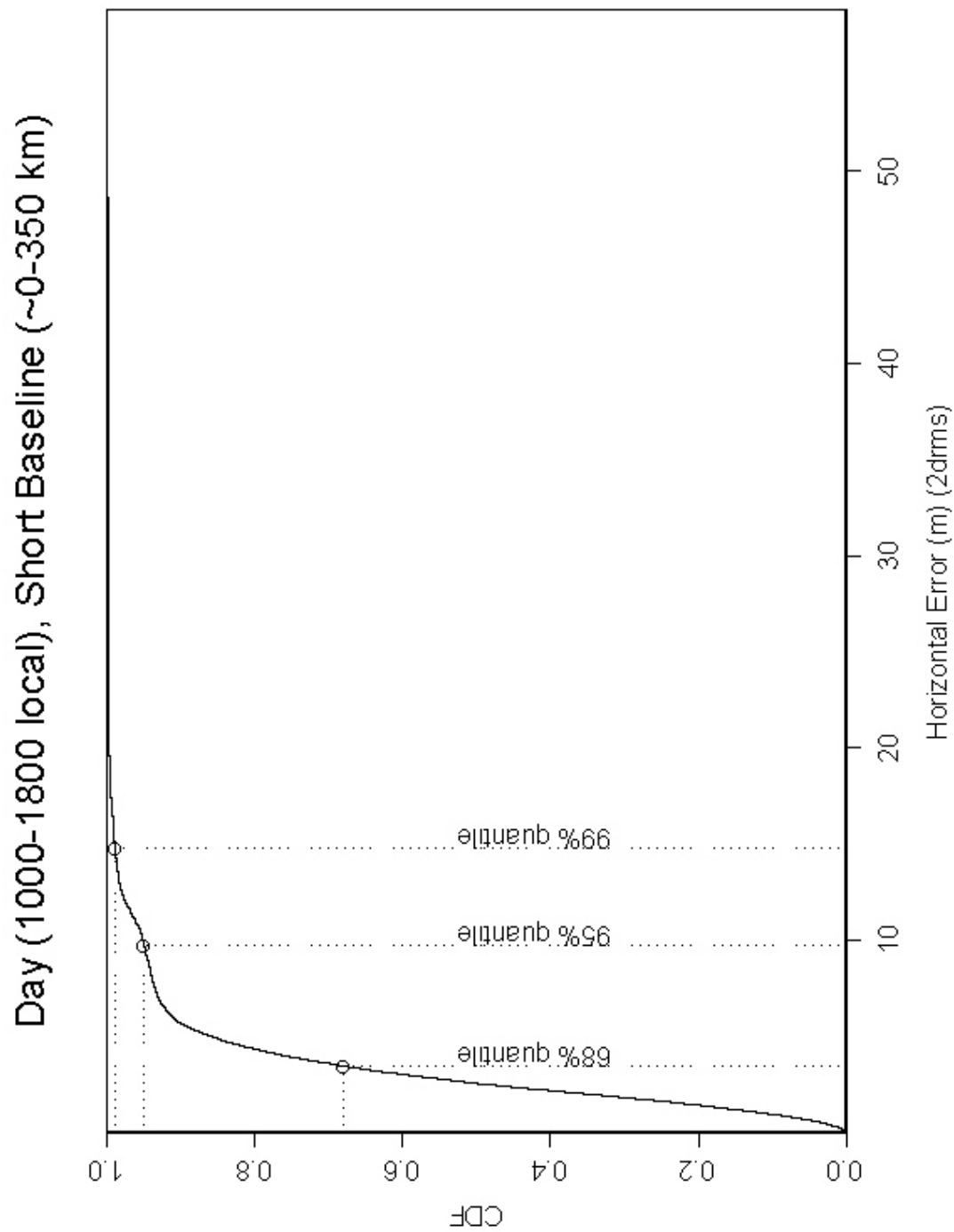
Figure 30   Horizontal Error – CDF during *Day* with a *Short* Baseline

59

Figure 31   Horizontal Error – CDF during *Day* with a *Medium* Baseline

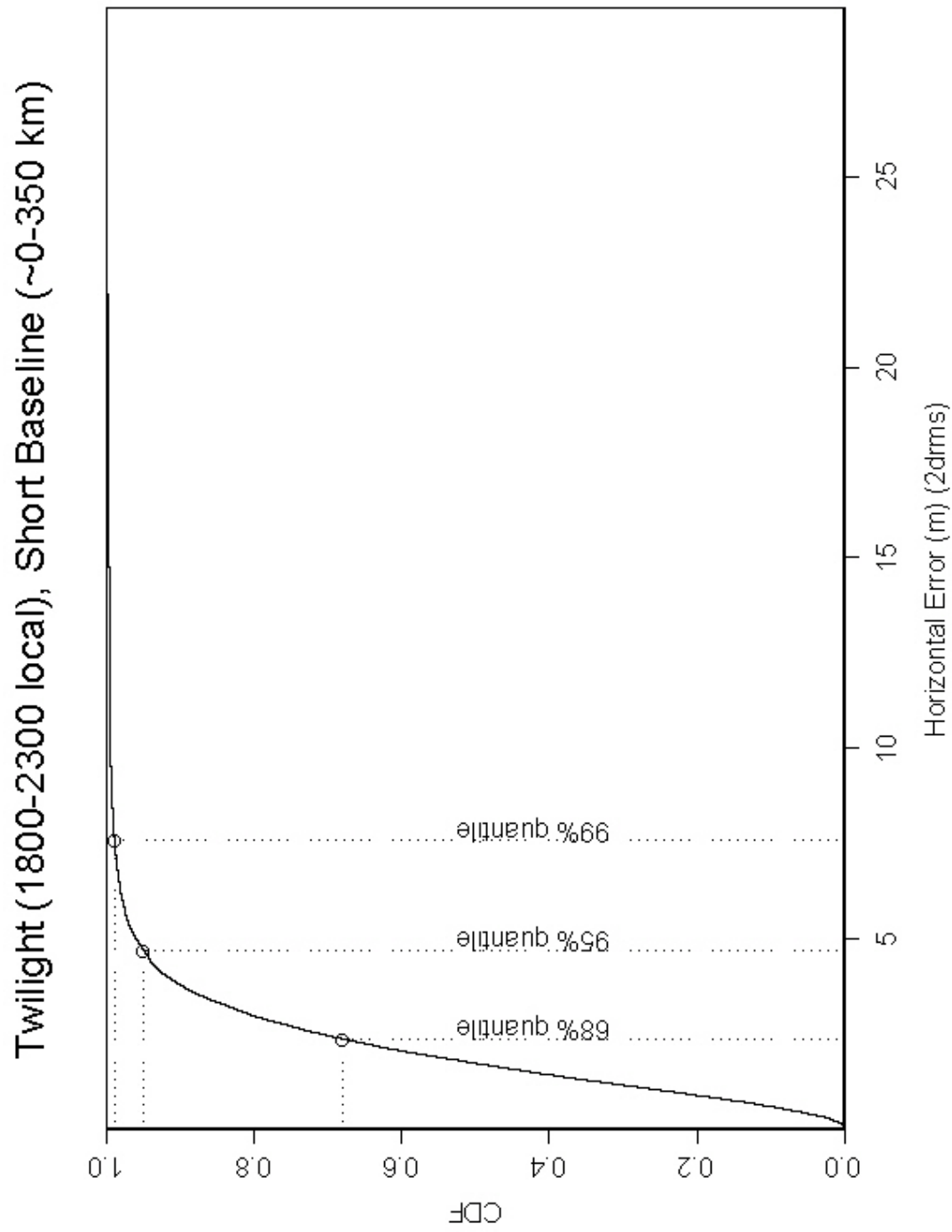Figure 32 Horizontal Error – CDF during *Day* with a *Long* Baseline

61

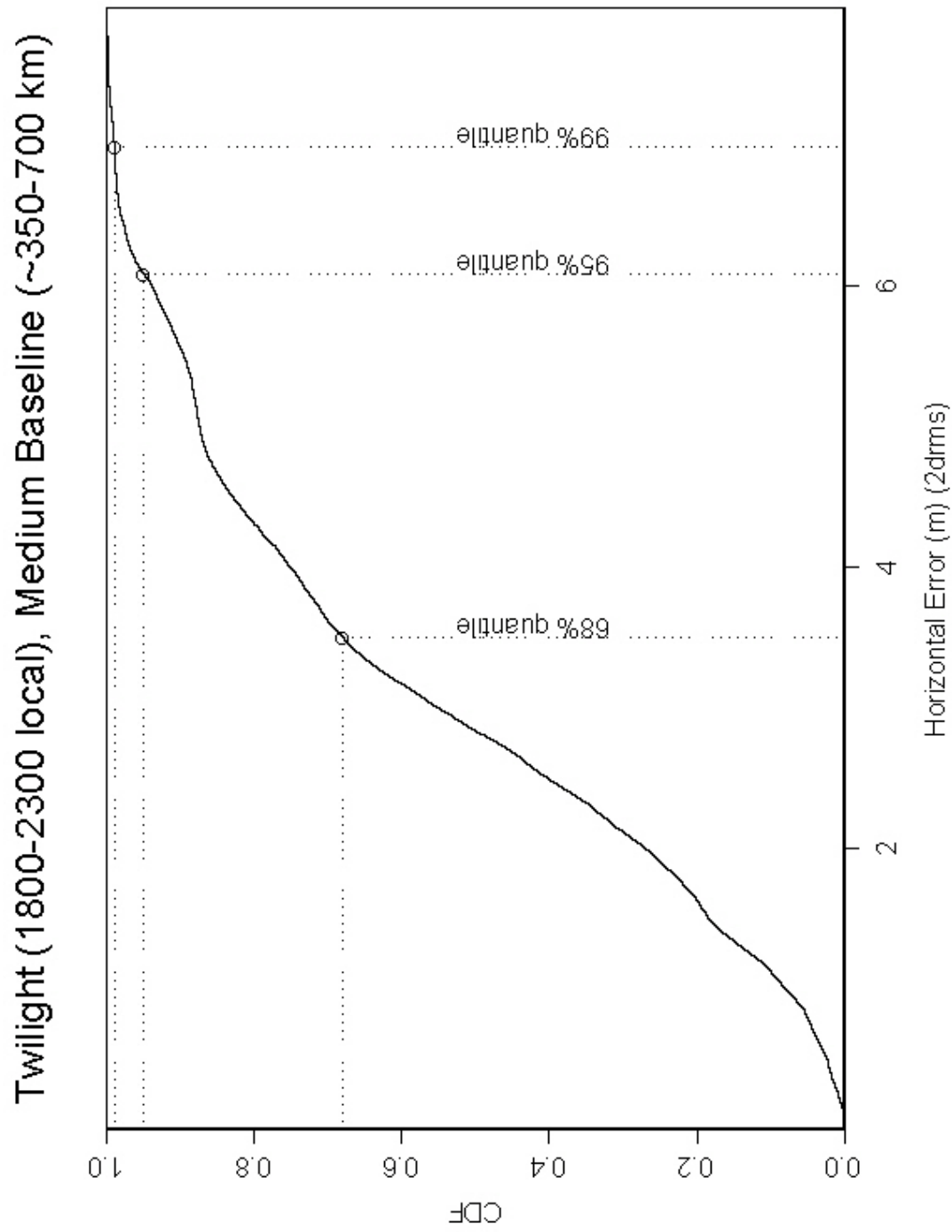Figure 33   Horizontal Error – CDF during *Twilight* with a *Short* Baseline

Figure 34   Horizontal Error – CDF during *Twilight* with a *Medium* Baseline
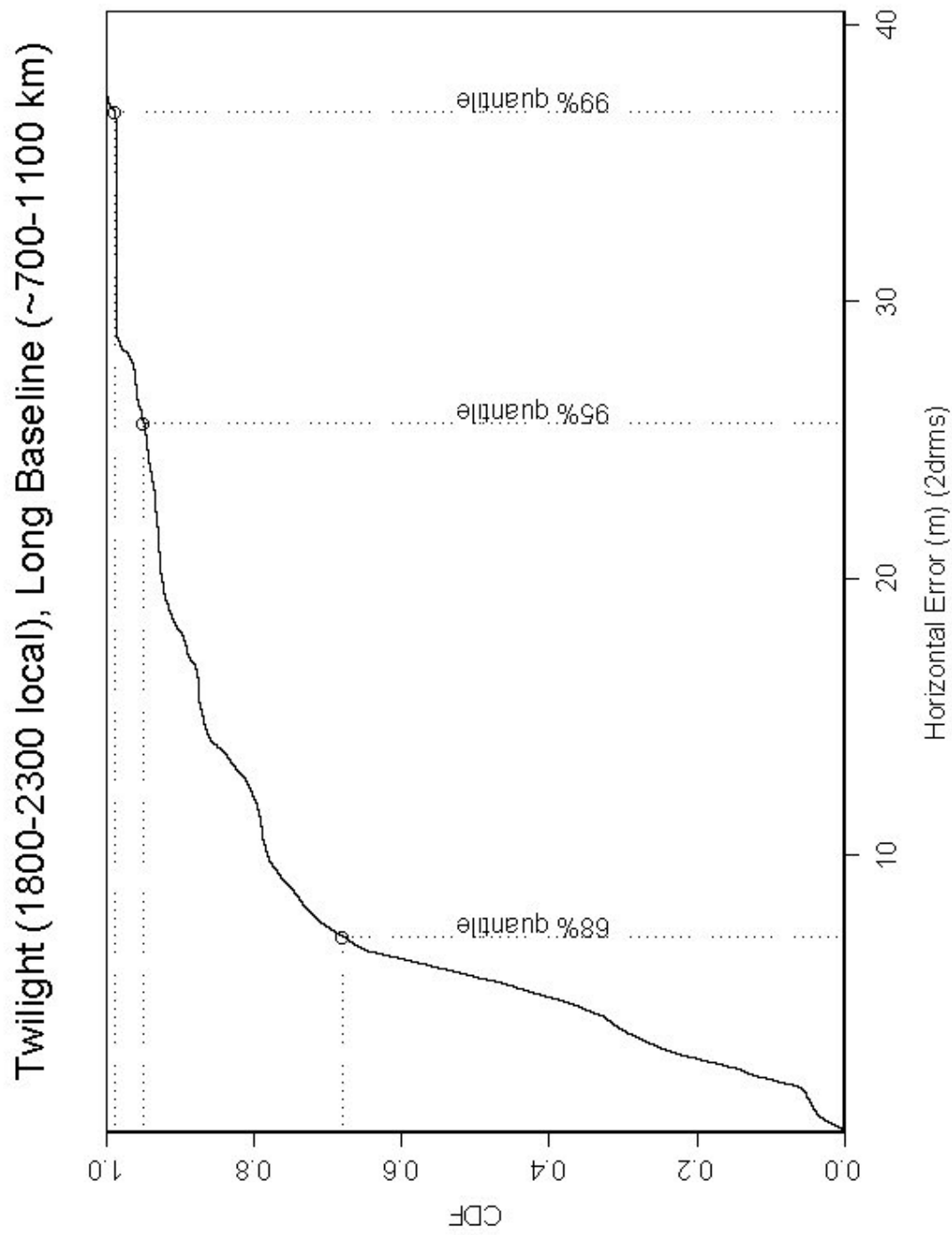
63

Figure 35 Horizontal Error – CDF during *Twilight* with a *Long* Baseline
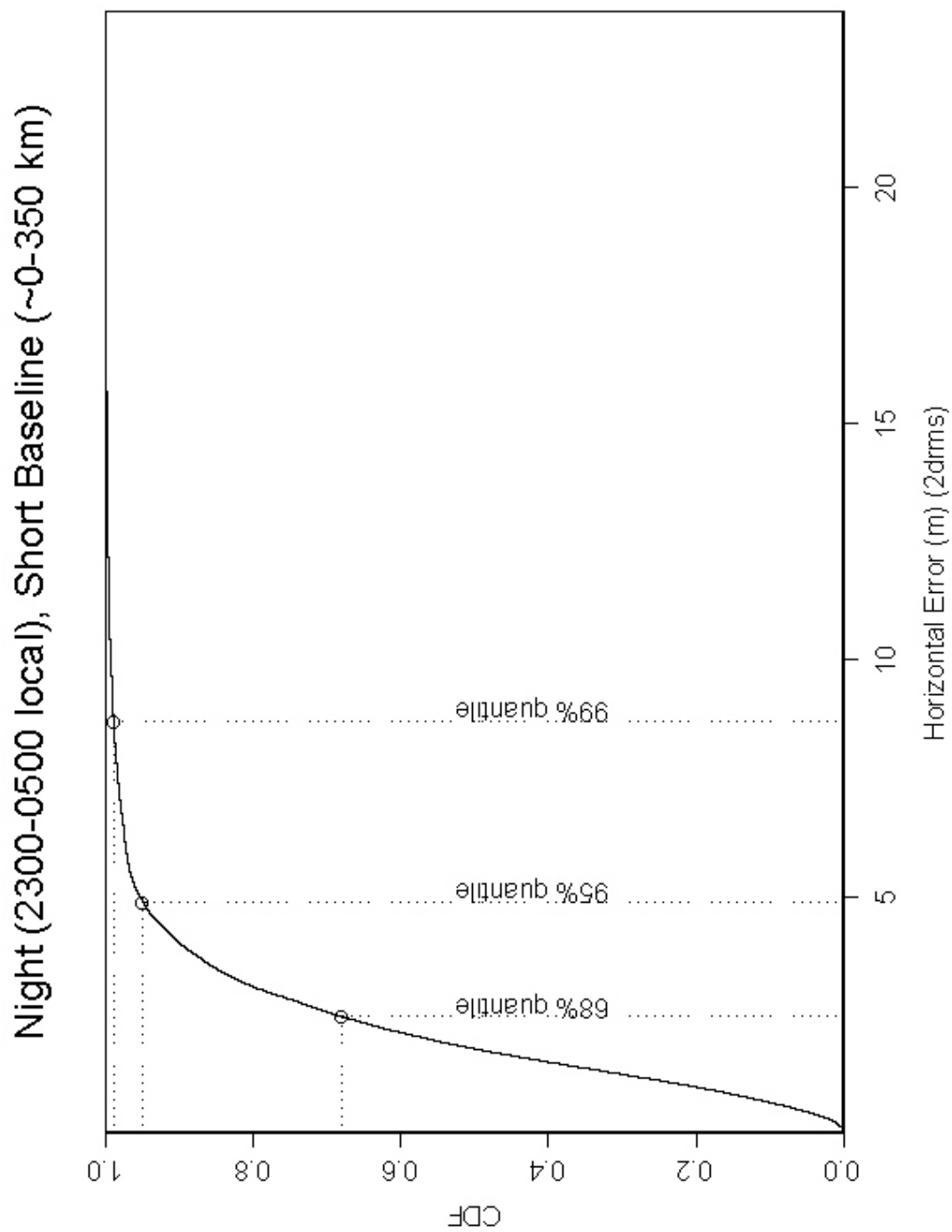
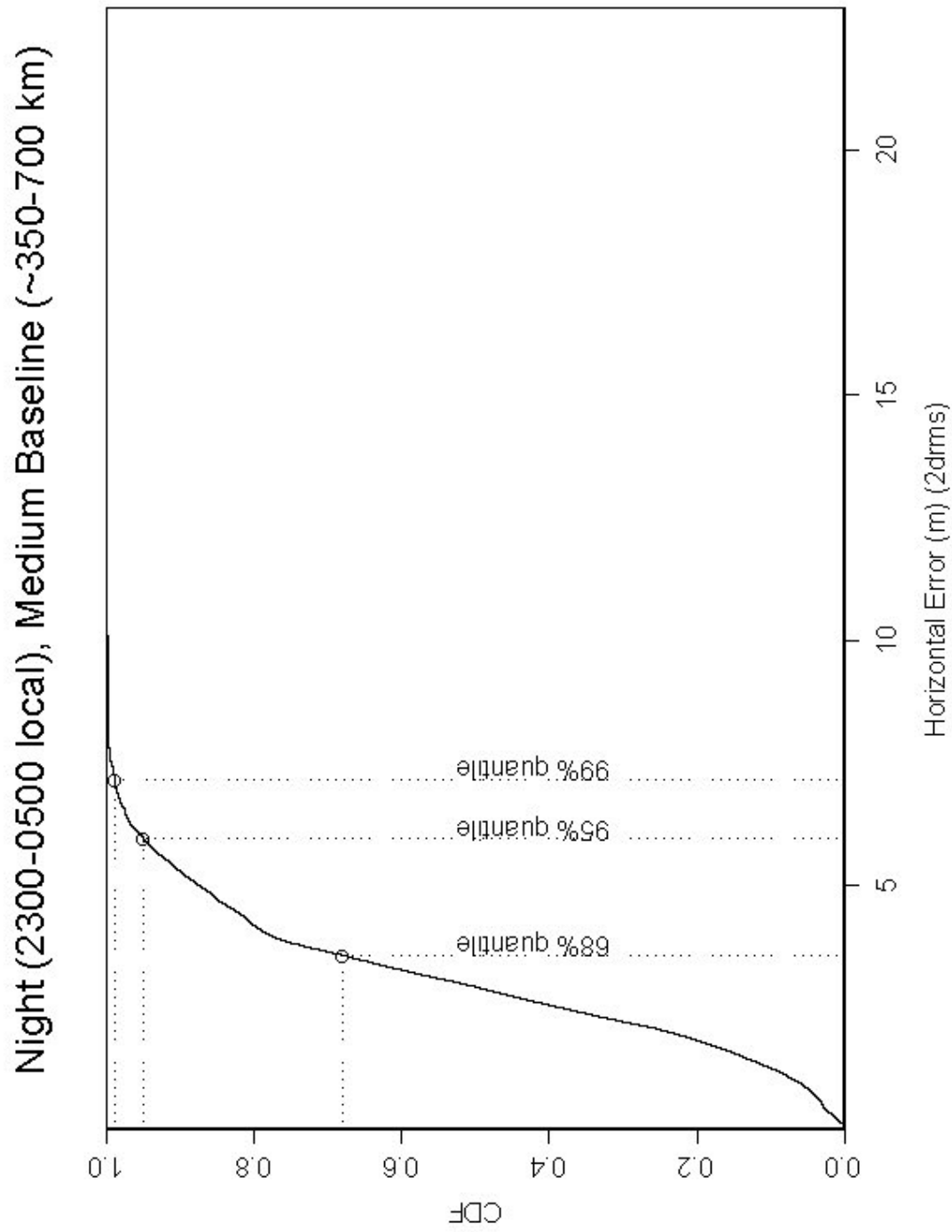Figure 36   Horizontal Error – CDF during *Night* with a *Short* Baseline

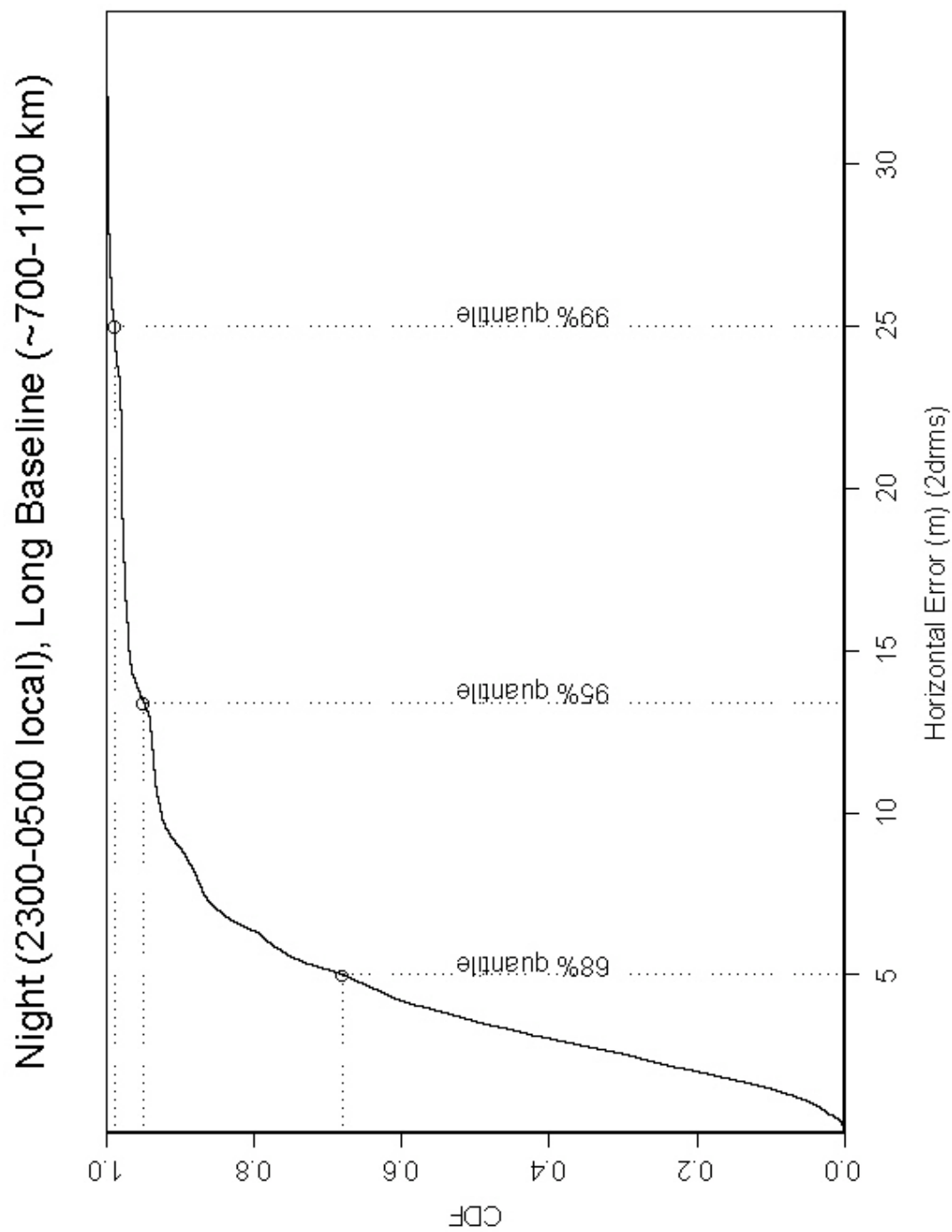Figure 37   Horizontal Error – CDF during *Night* with a *Medium* Baseline

Figure 38   Horizontal Error – CDF during *Night* with a *Long* Baseline

67

THIS PAGE INTENTIONALLY LEFT BLANK

APPENDIX E. CONTOUR PLOTS AND CORRELATIONS FOR USCG DGPS REFERENCE STATIONS

This appendix has each USCG DGPS reference station contour plotted. Included are two plots for each station. The first is an intensity plot and includes the 1σ, 2σ, and 95% error ellipses based upon the residual errors. From closest to the center moving outward, the ellipses are 1σ, then 2σ, and finally 95%. The color of the intensity plot ranges from magenta to light blue, representing least to highest intensity, respectively. The second plot is the contours of the two-dimensional probability density and the values can be read directly from the graph in units of 1/meters².

The final section is the correlation matrices for the data set *Contour*. The matrices represent the correlations between the parameters of the 1σ error ellipses and the statistics describing the mobile-user–reference-station geometry.

During the experiment, the ship's track came very close to Pigeon Point and Point Blunt, California DGPS reference stations. This caused ambiguity in the value of average azimuth to these reference stations. Because of the weak geometry to these two reference stations, they were trimmed from *Contour* but their correlation coefficients are also reported.
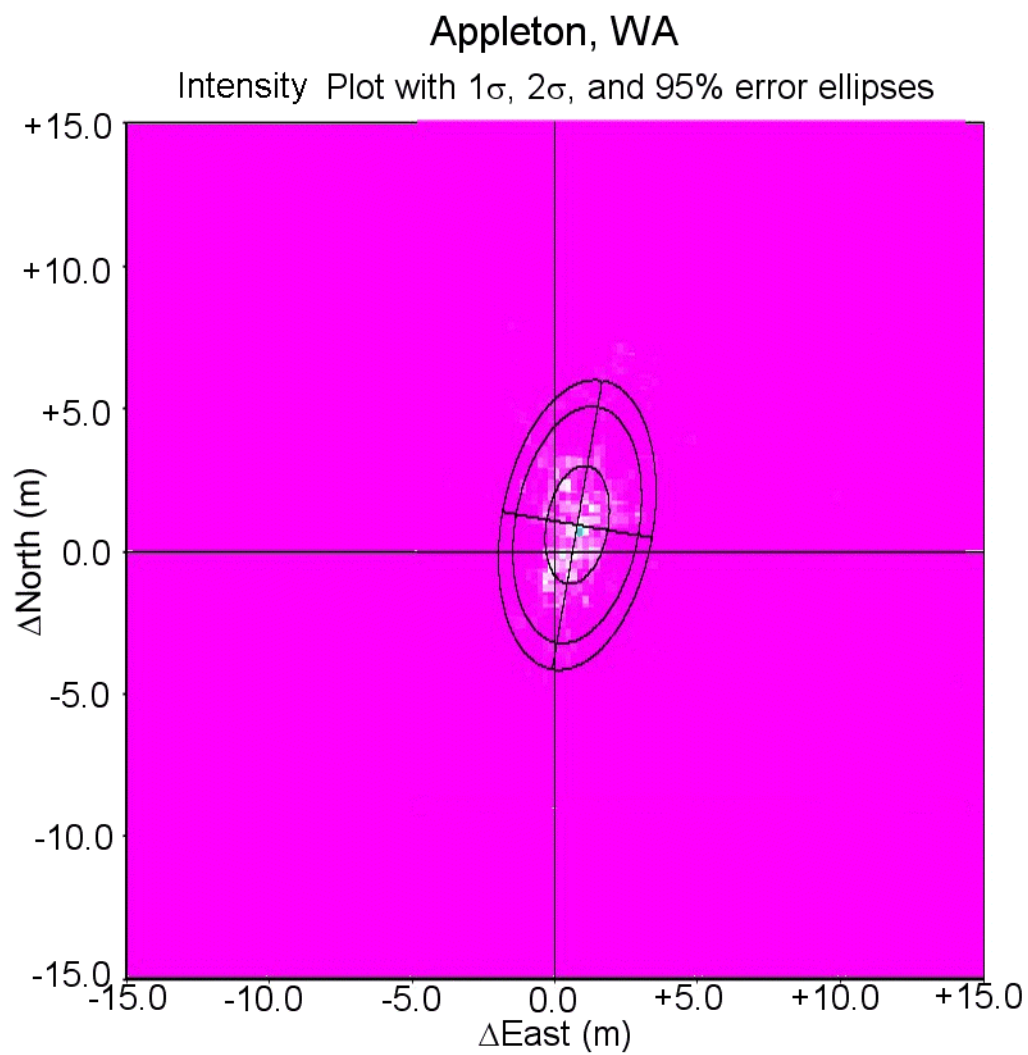
Figure 39   Appleton, WA – USCG DGPS Intensity Plot of Errors with Error Ellipses
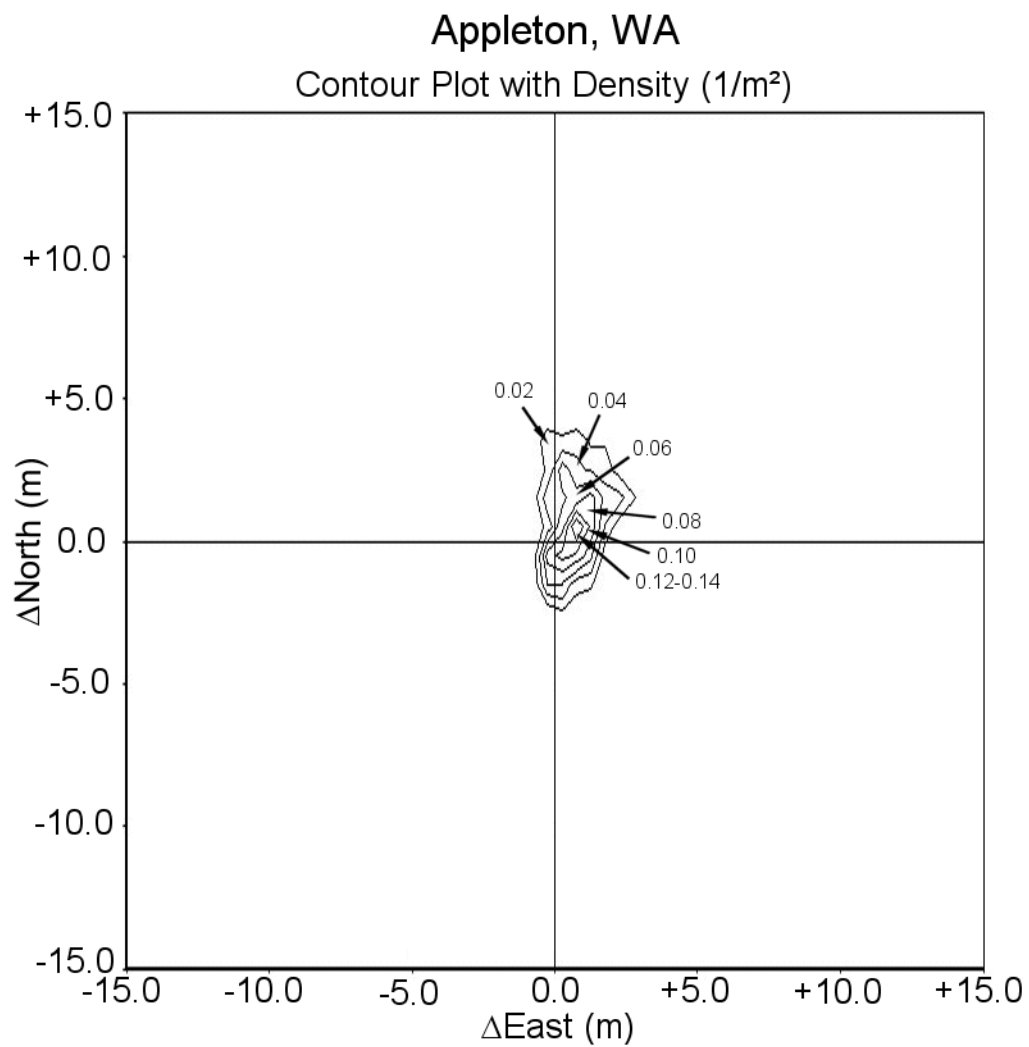
70

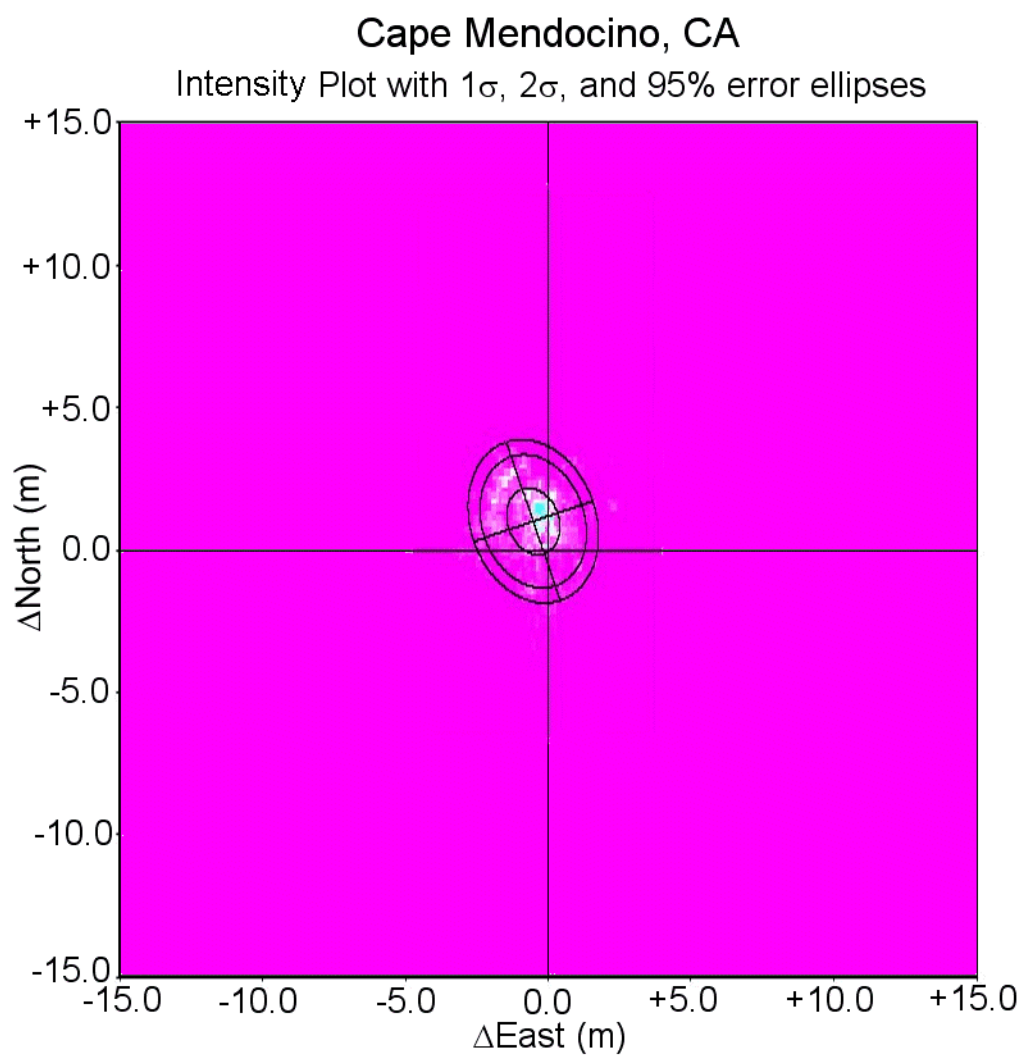Figure 40   Appleton, WA – USCG DGPS Contour Plot of Errors with Density

Figure 41   Cape Mendocino, CA – USCG DGPS Intensity Plot of Errors with Error Ellipses

Figure 42   Cape Mendocino, CA – USCG DGPS Contour Plot of Errors with Density

Figure 43   Chico, CA – USCG DGPS Intensity Plot of Errors with Error Ellipses

Figure 44   Chico, CA – USCG DGPS Contour Plot of Errors with Density

Figure 45   Pigeon Point, CA – USCG DGPS Intensity Plot of Errors with Error Ellipses

Figure 46   Pigeon Point, CA – USCG DGPS Contour Plot of Errors with Density

Figure 47   Point Blunt, CA – USCG DGPS Intensity Plot of Errors with Error Ellipses

Figure 48   Point Blunt, CA – USCG DGPS Contour Plot of Errors with Density

Figure 49   Lompoc, CA – USCG DGPS Intensity Plot of Errors with Error Ellipses

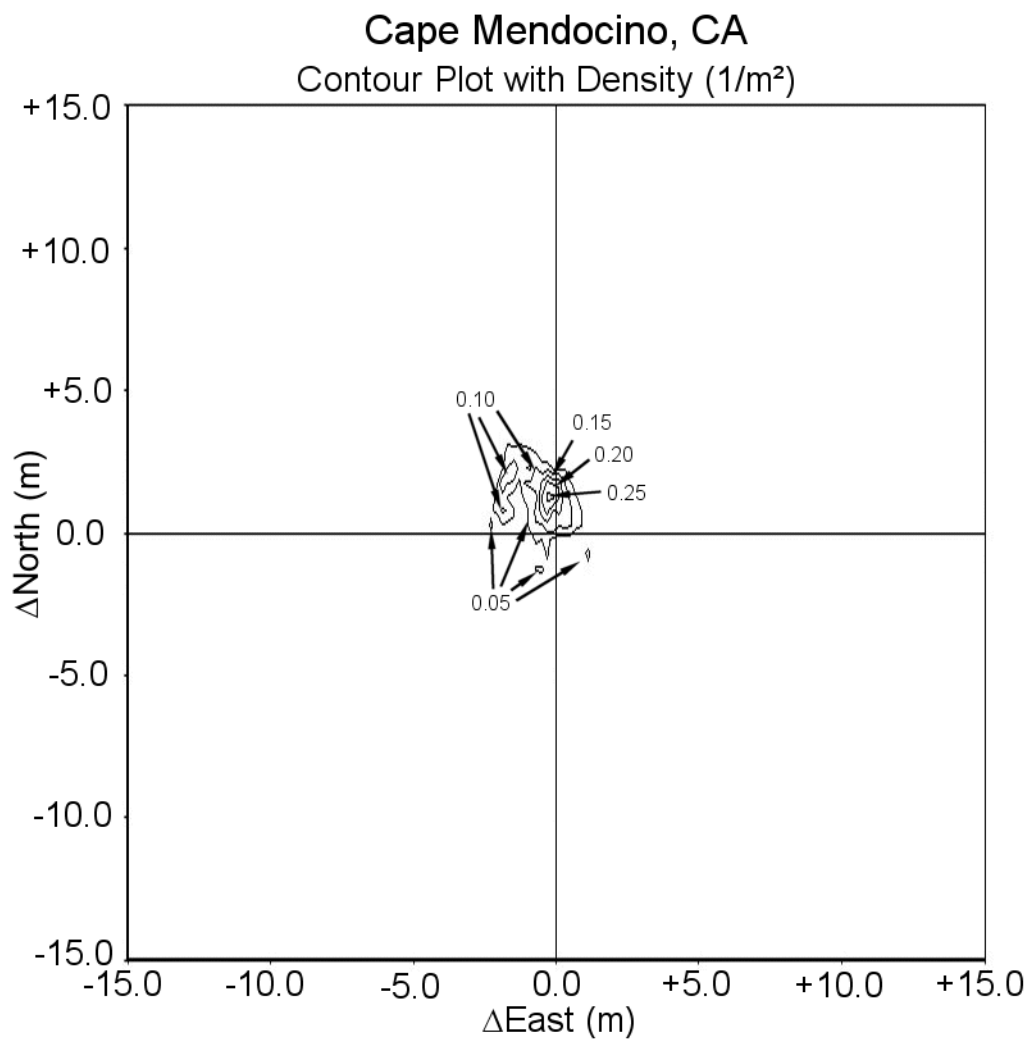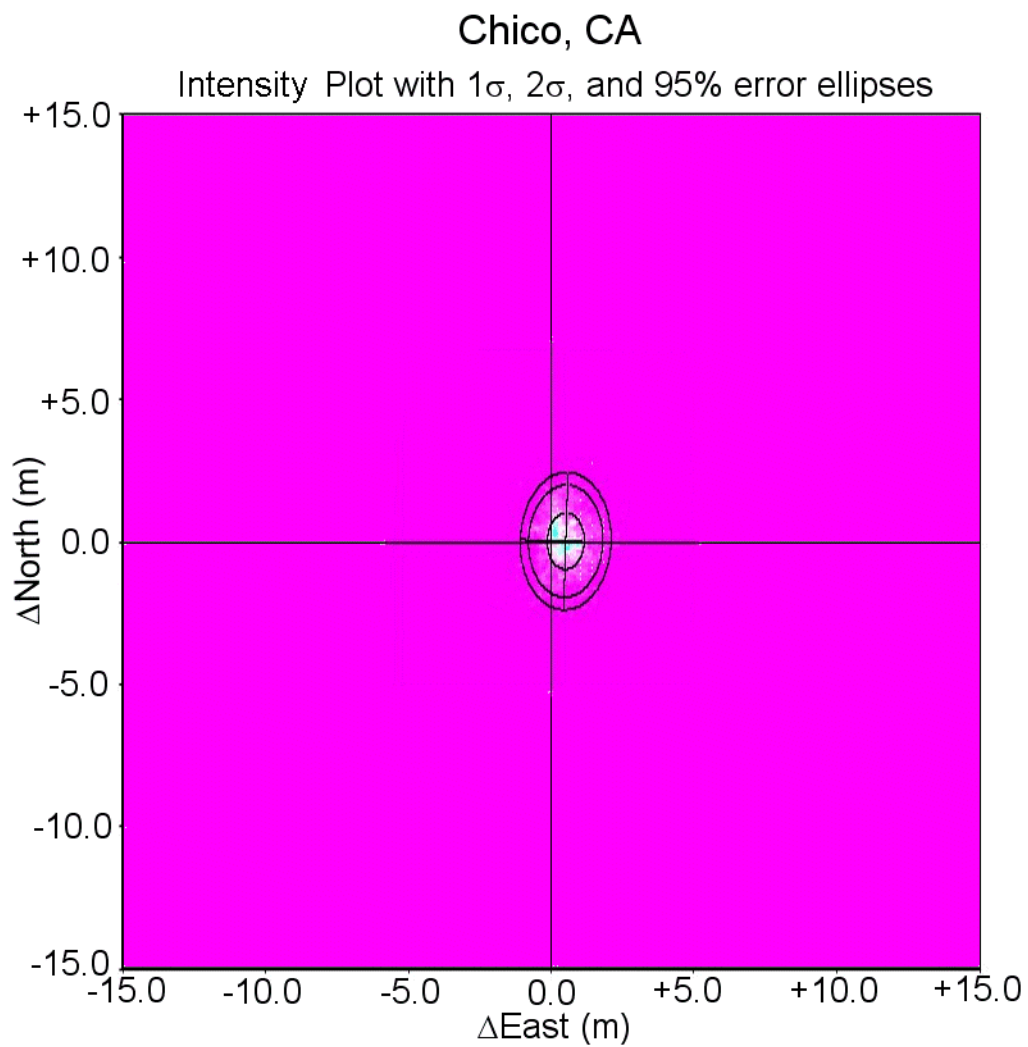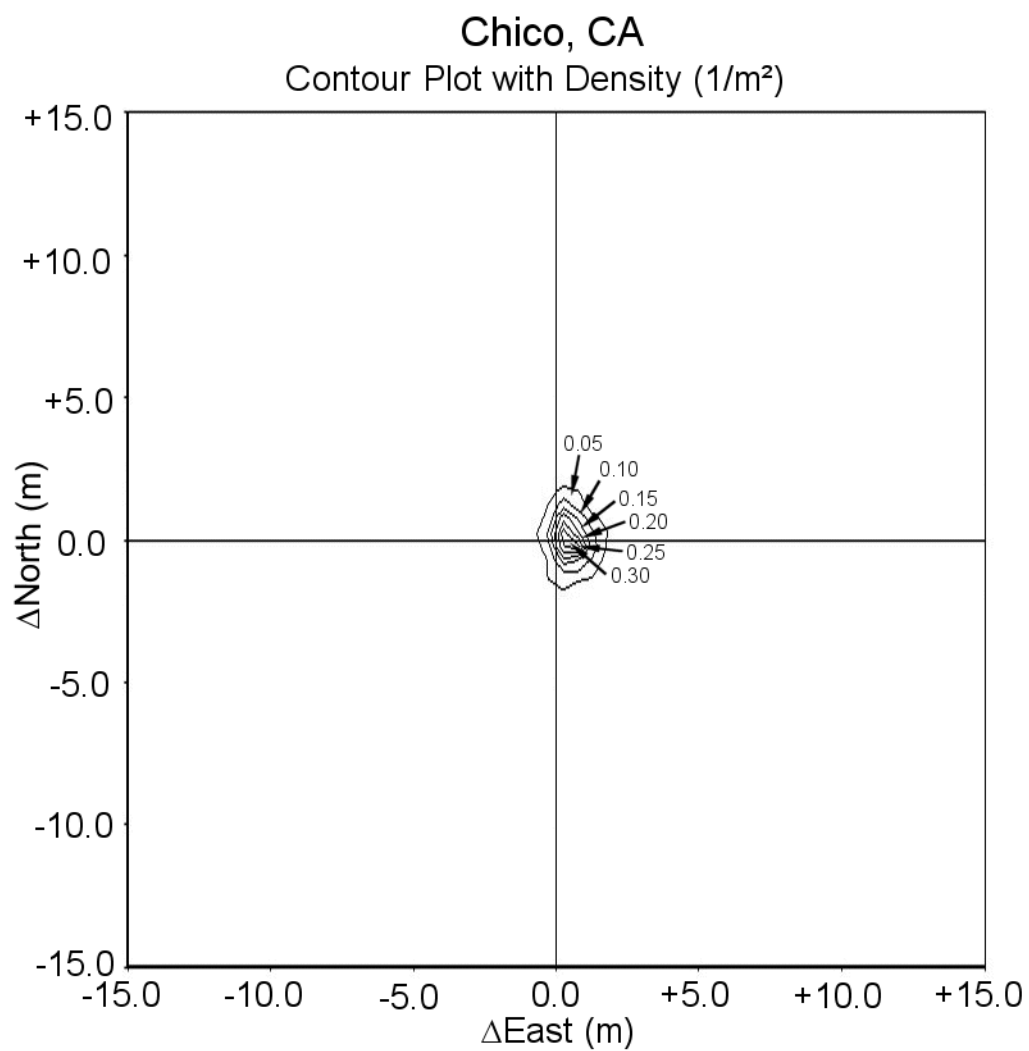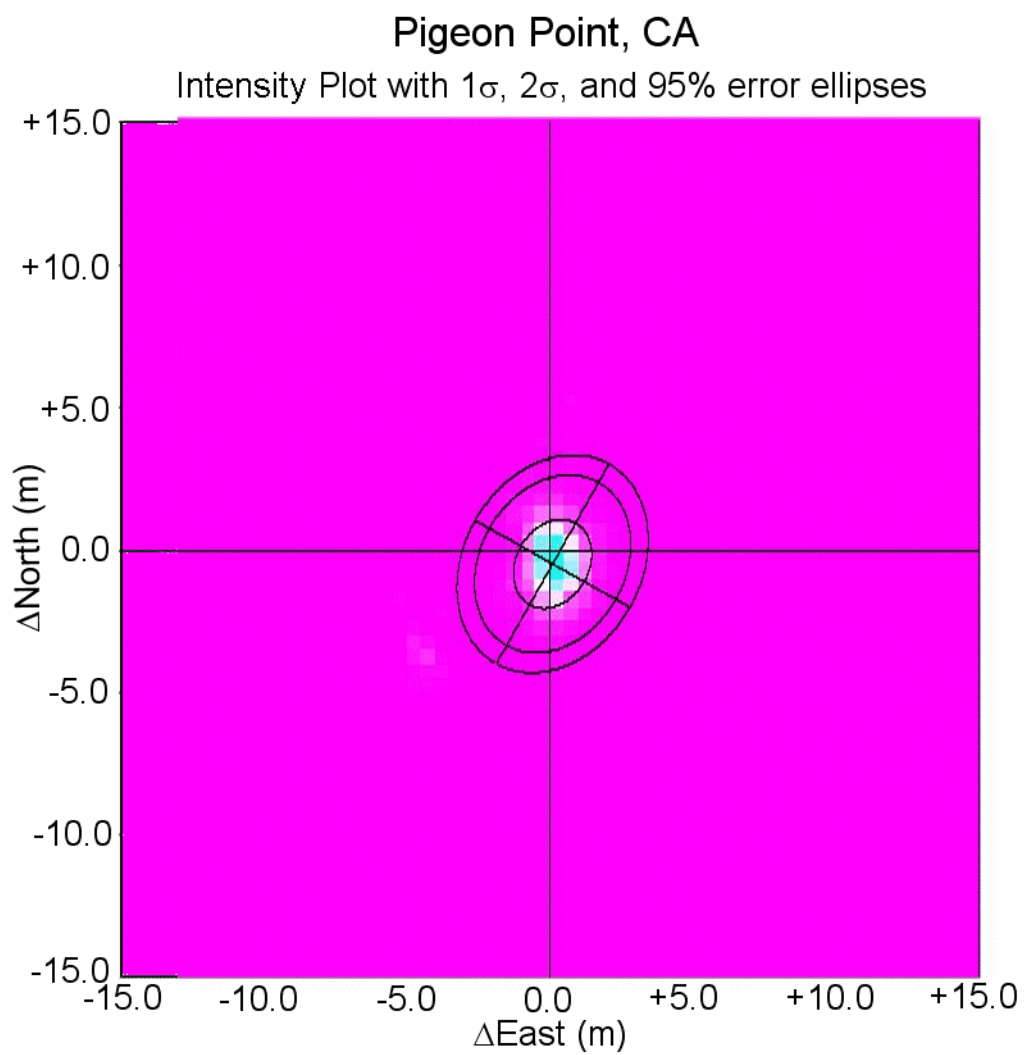Figure 50   Lompoc, CA – USCG DGPS Contour Plot of Errors with Density

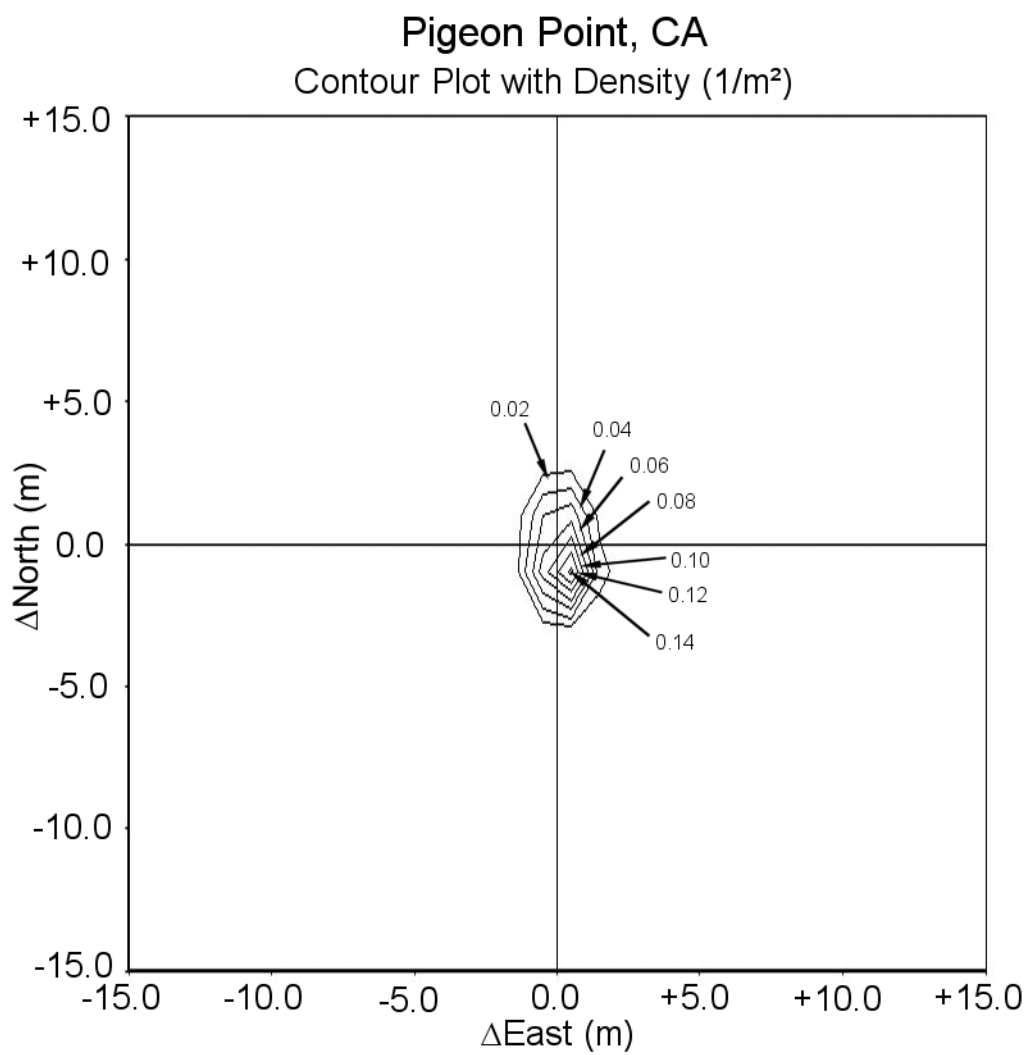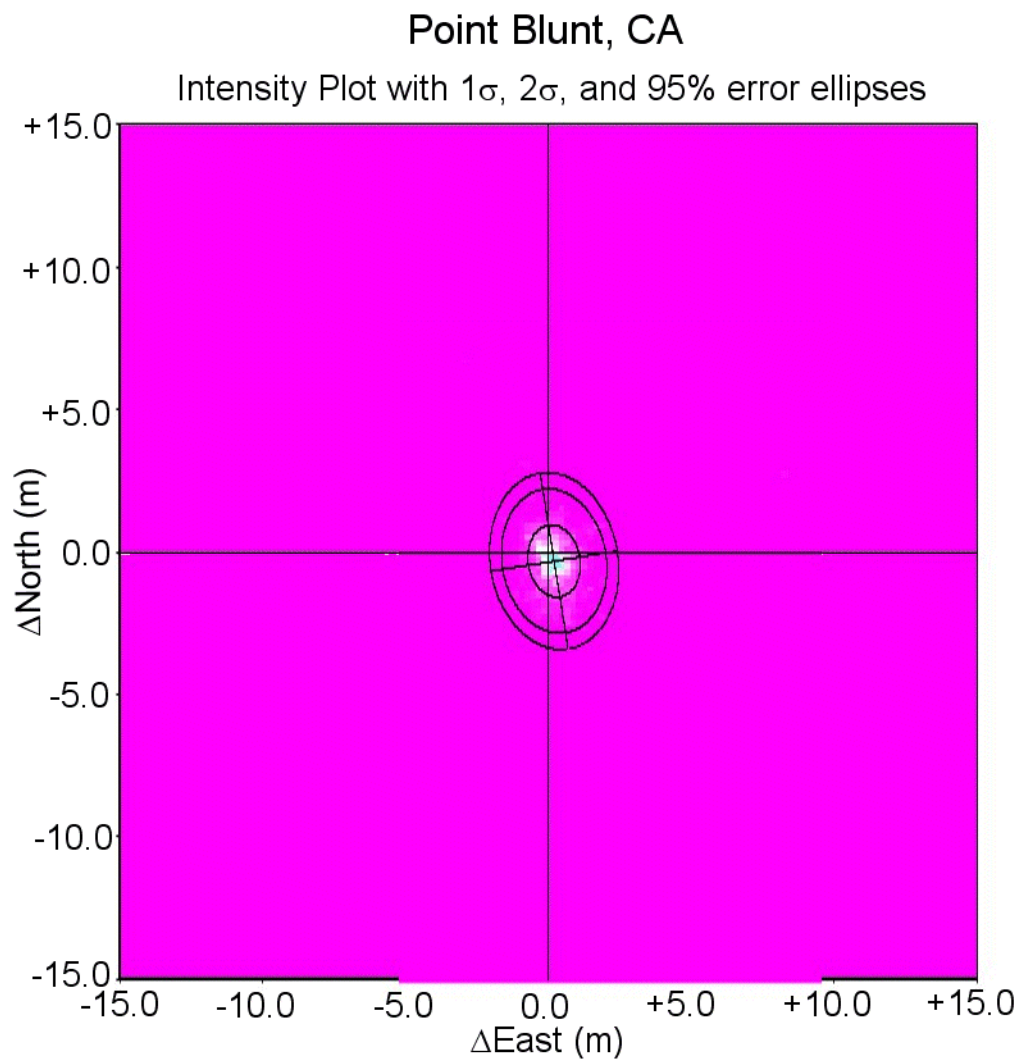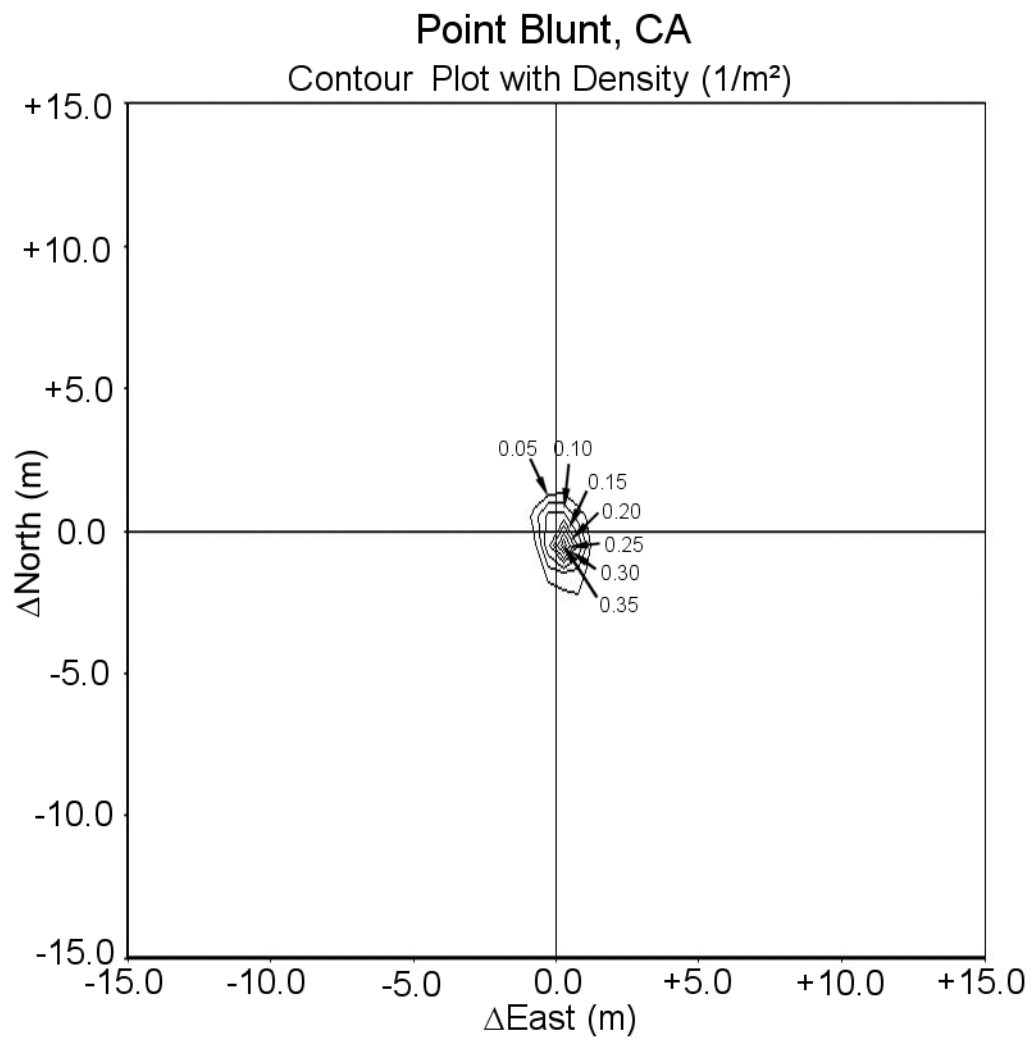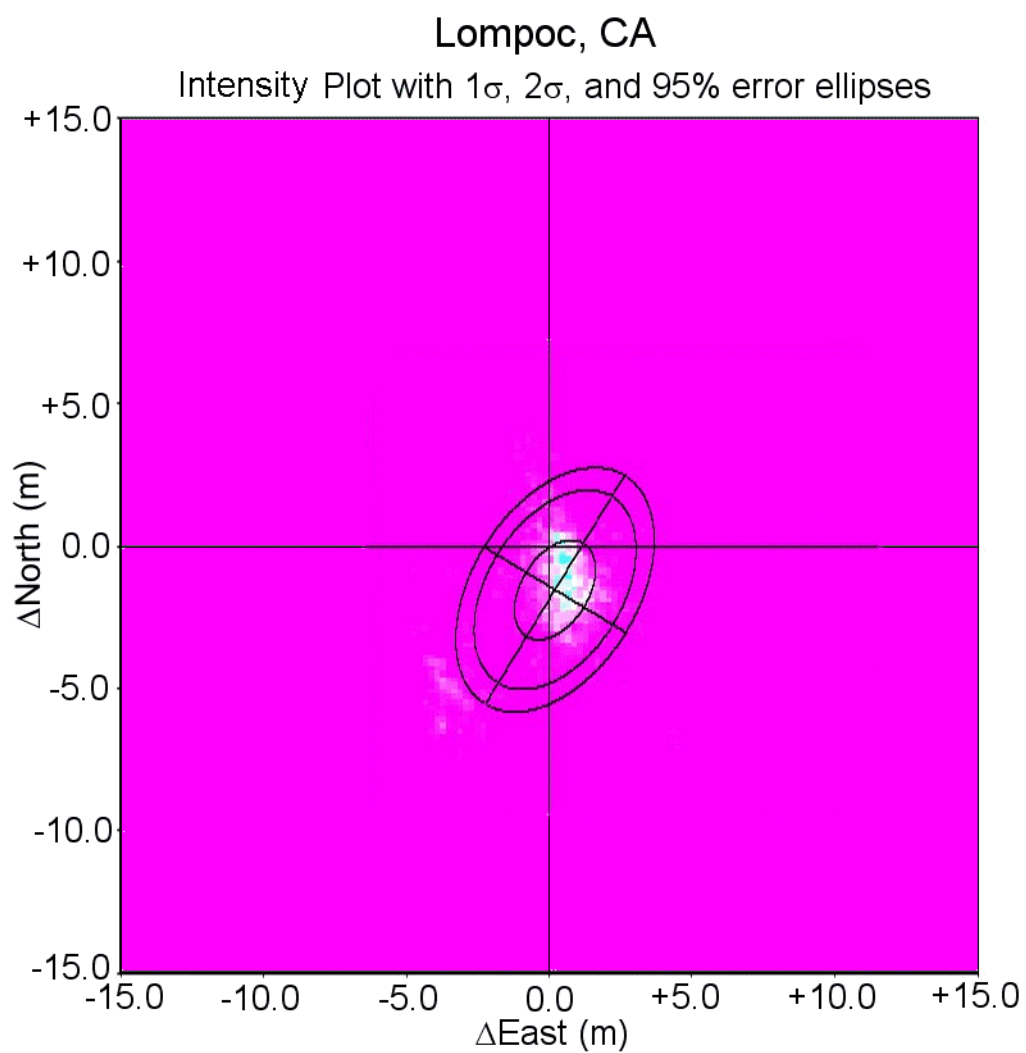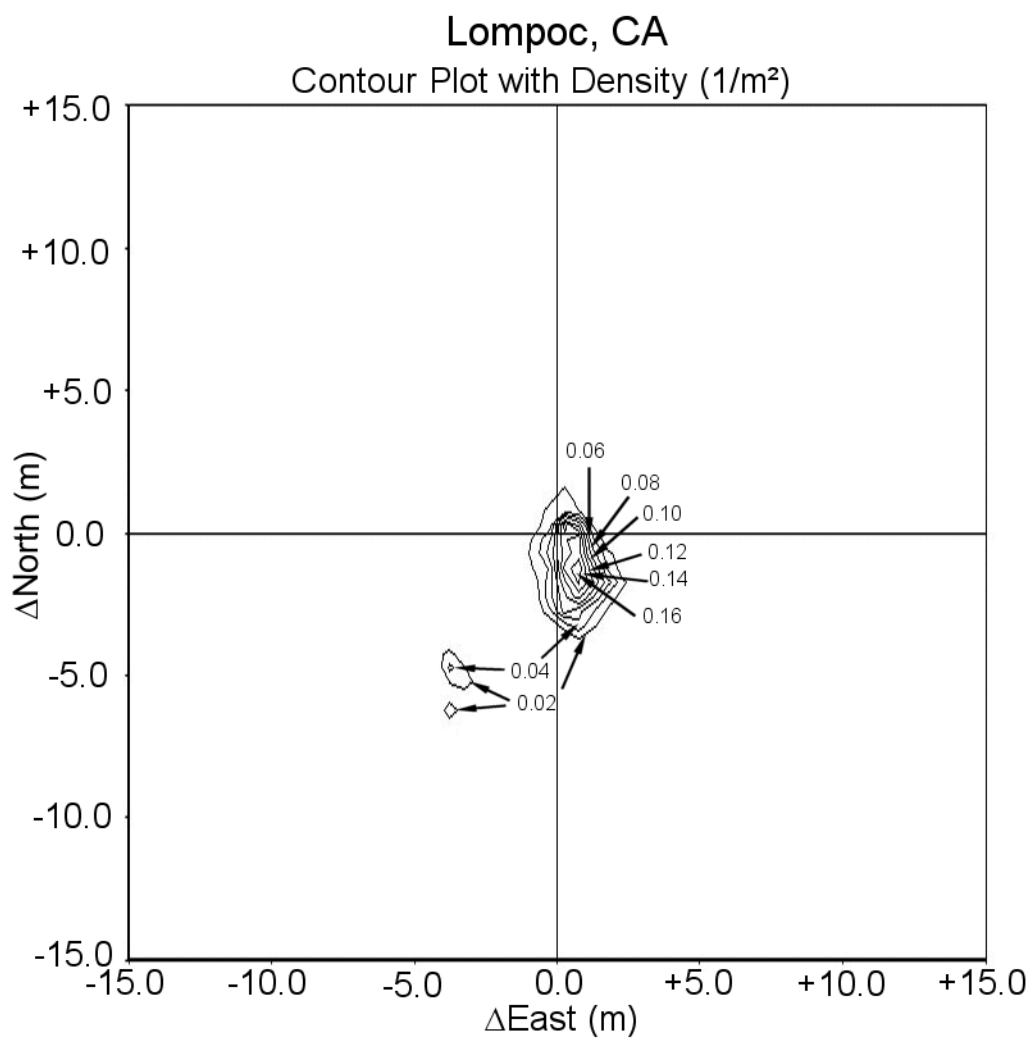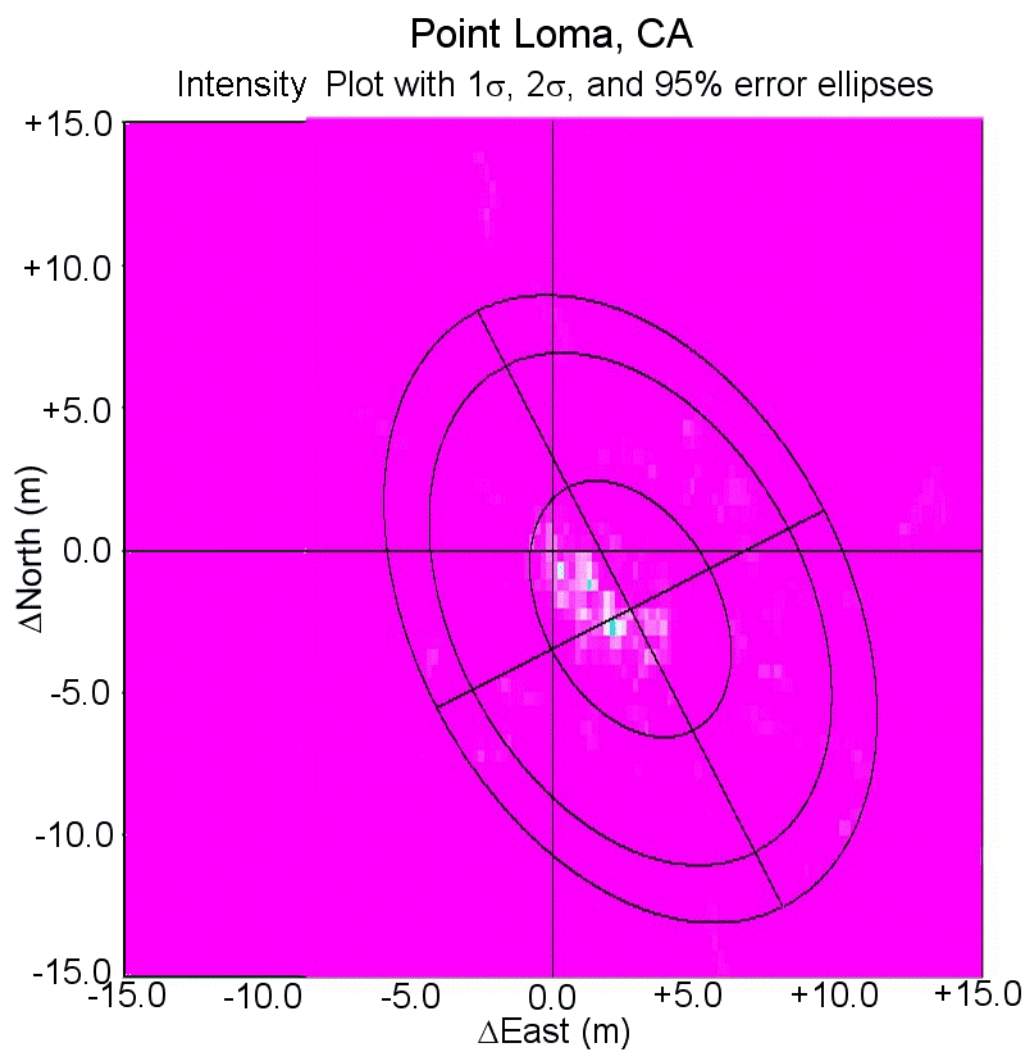Figure 51   Point Loma, CA – USCG DGPS Intensity Plot of Errors with Error Ellipses
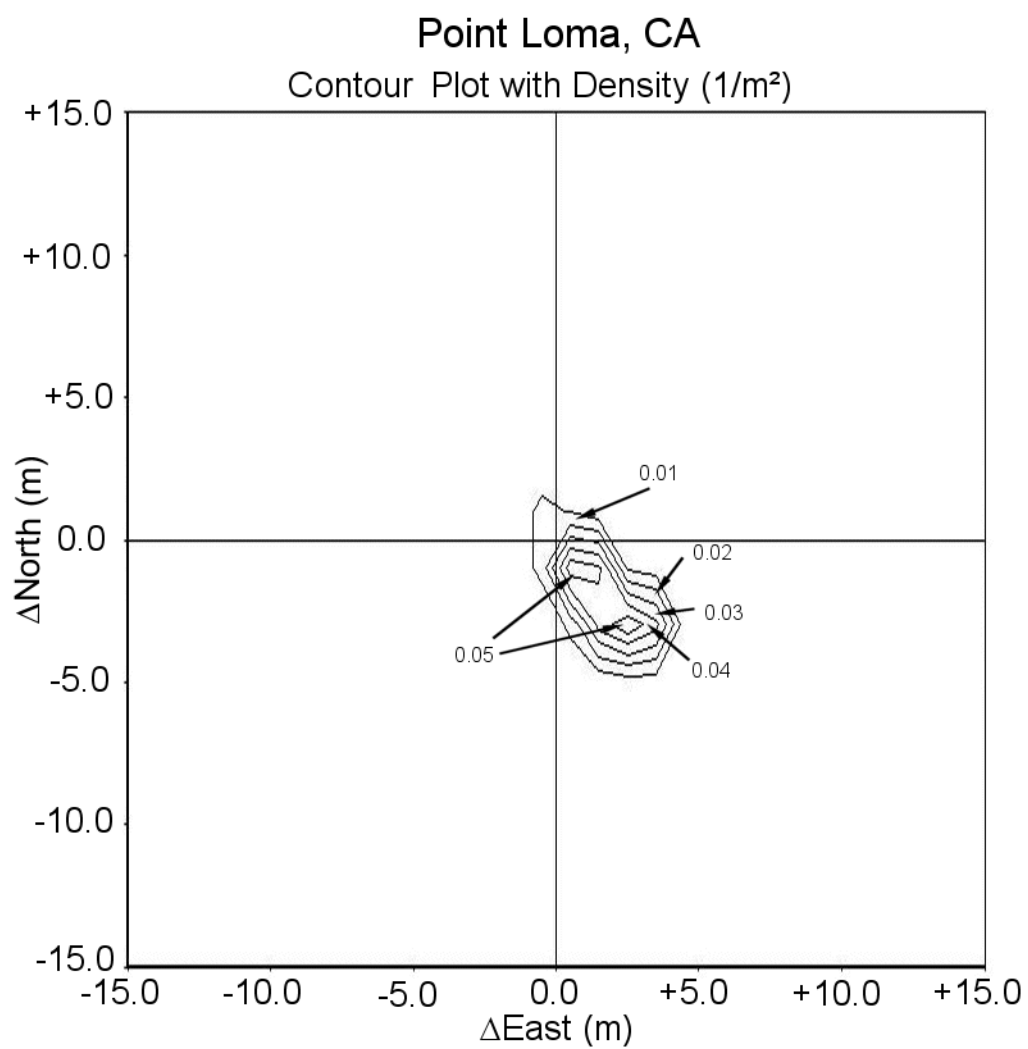
Figure 52   Point Loma, CA – USCG DGPS Contour Plot of Errors with Density

	Semimajor axis	Semiminor axis	eccentricity	orientation	$\overline{azimuth}$	$\overline{distance}$
Semimajor axis	1	0.983	0.309	-0.053	-0.064	0.545
Semiminor axis	0.983	1	0.134	0.065	0.046	0.410
eccentricity	0.309	0.134	1	-0.674	-0.646	0.727
orientation	-0.053	0.065	-0.674	1	0.945	-0.349
$\overline{azimuth}$	-0.064	0.046	-0.646	0.945	1	-0.210
$\overline{distance}$	0.545	0.410	0.727	-0.349	-0.210	1

Table 6   Correlations from Data Set *Contour* Including Pigeon Point and Point Blunt, CA

	Semimajor axis	Semiminor axis	eccentricity	orientation	$\overline{azimuth}$	$\overline{distance}$
Semimajor axis	1	0.989	0.218	-0.008	-0.095	0.499
Semiminor axis	0.989	1	0.076	0.090	0.014	0.397
eccentricity	0.218	0.076	1	-0.735	-0.838	0.584
orientation	-0.008	0.090	-0.735	1	0.976	-0.310
$\overline{azimuth}$	-0.095	0.014	-0.838	0.976	1	-0.323
$\overline{distance}$	0.499	0.397	0.584	-0.310	-0.323	1

Table 7   Correlations from Data Set *Contour*

Table 6 and Table 7 contain the correlation coefficients between the parameters of the error ellipses and the mobile user to reference station geometry. Table 6 includes data from all seven USCG DGPS reference stations used in the experiment. The average azimuth is ambiguous for Pigeon Point and Point Blunt data; Table 7 was compiled without their data.

$\overline{azimuth}$ = average azimuth $\overline{distance}$ = average baseline distance

APPENDIX F. PROBABILITY DENSITY FUNCTIONS (PDF) AND CUMULATIVE DISTRIBUTION FUNCTIONS (CDF) FOR USCG DGPS REFERENCE STATIONS

This appendix includes the Probability Density Functions (PDFs) and Cumulative Distribution Functions (CDFs) for each USCG DGPS reference station used in the experiment. All East errors are plotted in green. All North errors are plotted in Blue. For the PDFs, the dotted lines represent the median of the data set. For the CDFs, the 97.5% and 2.5% quantiles are plotted as dotted lines. Where these dotted lines intercept the X-axis represents the distance in meters of the residual error in position when using this USCG reference station. The interval between the 2.5% and 97.5% quantiles, when read from the CDF's X-axis, represents the 95% prediction interval for the residual error when using that particular reference station. The plots are presented in a north to south order.

The shape and distribution of the data sets is moderately correlated to the average azimuth and the average baseline distance from the mobile user to the USCG DGPS reference station. Table 5 should be referred to when using these plots. Table 6 and Table 7 represent the correlation matrix for the different USCG DGPS reference stations in Table 5.
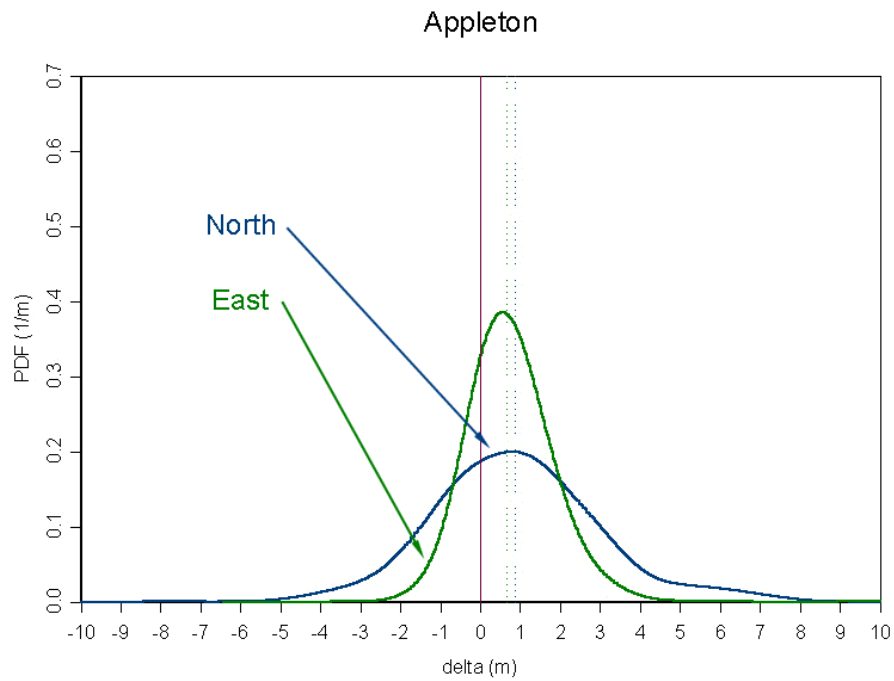
Appleton

Figure 53   Appleton, WA – PDF of ΔNorth and ΔEast Errors
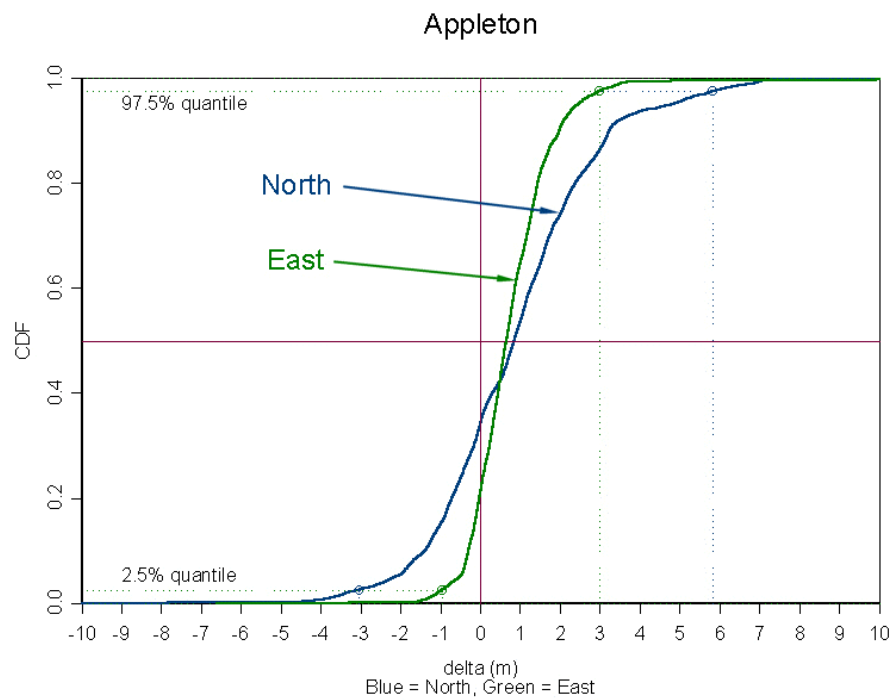
Appleton

Figure 54   Appleton, WA – CDF of ΔNorth and ΔEast Errors with 95% Prediction Interval
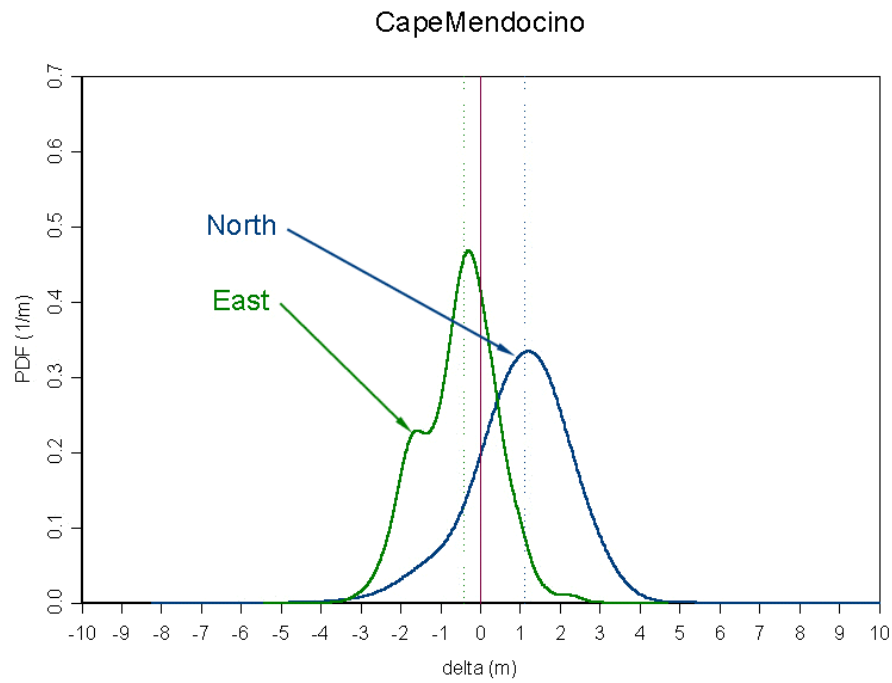
Figure 55   Cape Mendocino, CA – PDF of ΔNorth and ΔEast Errors
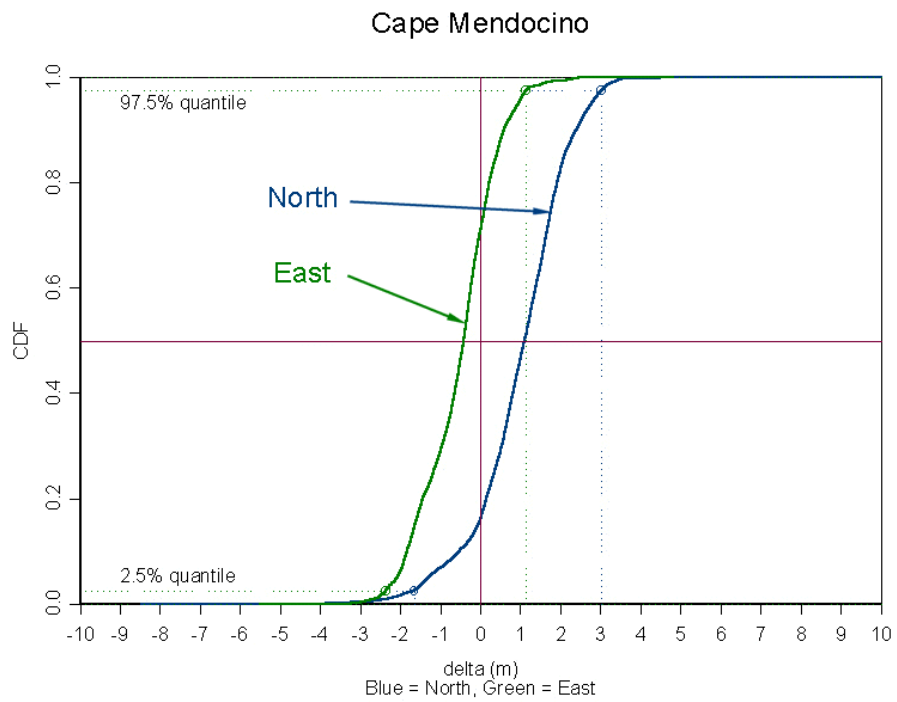
Figure 56   Cape Mendocino, CA – CDF of ΔNorth and ΔEast Errors with 95% Prediction Interval
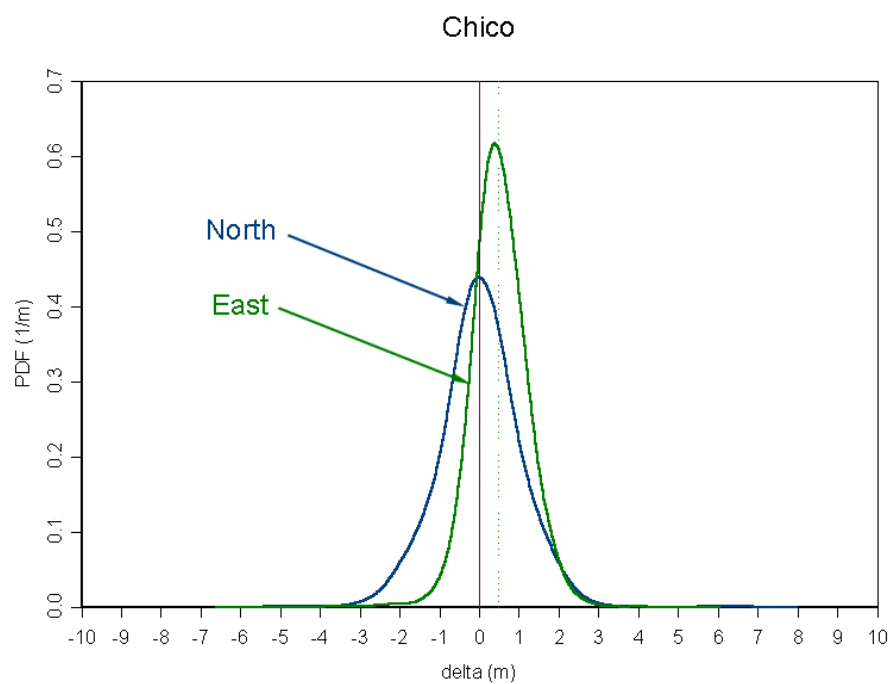
Figure 57   Chico, CA – PDF of ΔNorth and ΔEast Errors
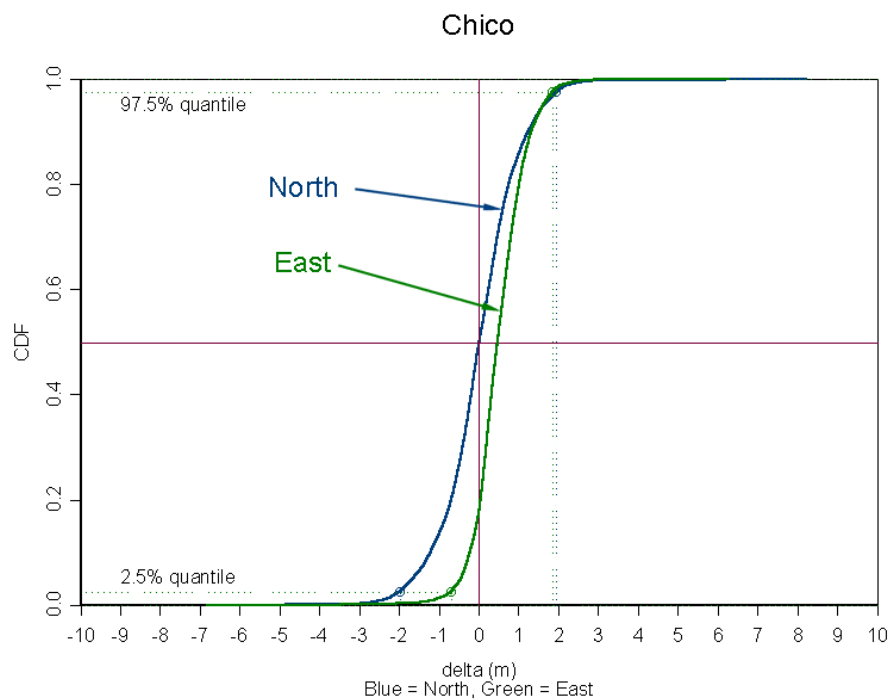
Figure 58   Chico, CA – CDF of ΔNorth and ΔEast Errors with 95% Prediction Interval
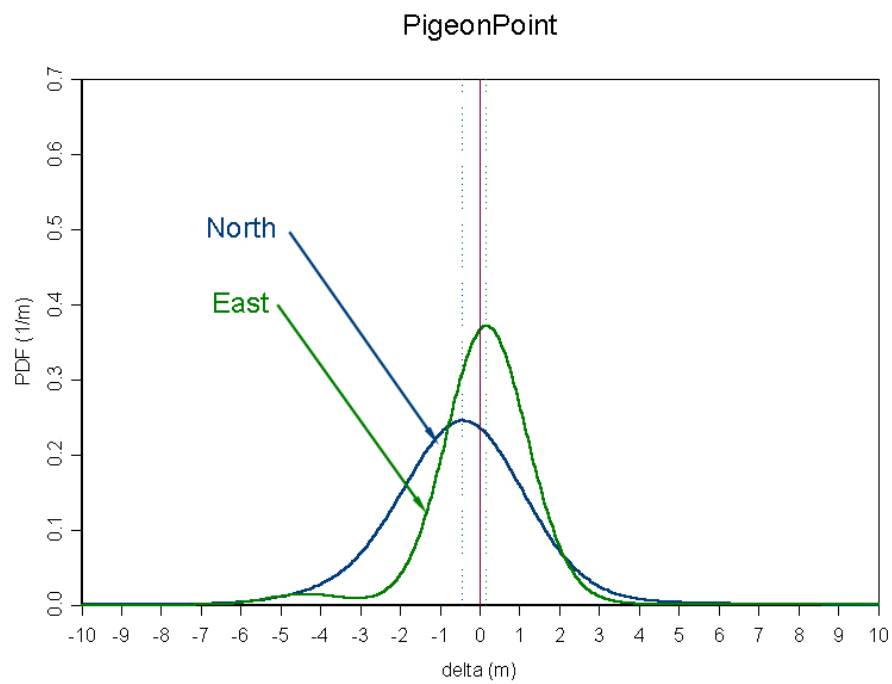
Figure 59   Pigeon Point, CA – PDF of ΔNorth and ΔEast Errors
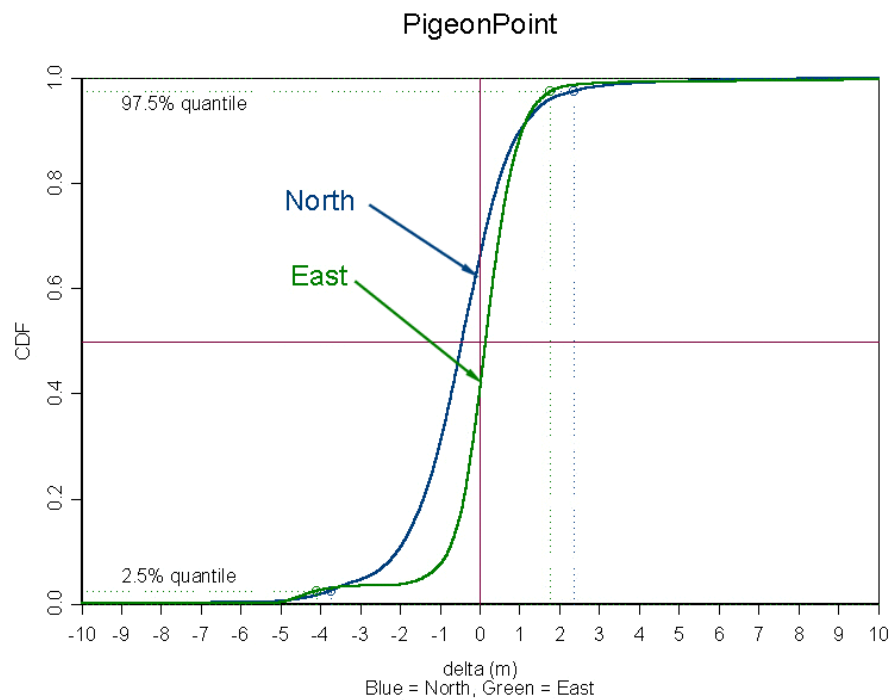
Figure 60   Pigeon Point, CA – CDF of ΔNorth and ΔEast Errors with 95% Prediction Interval
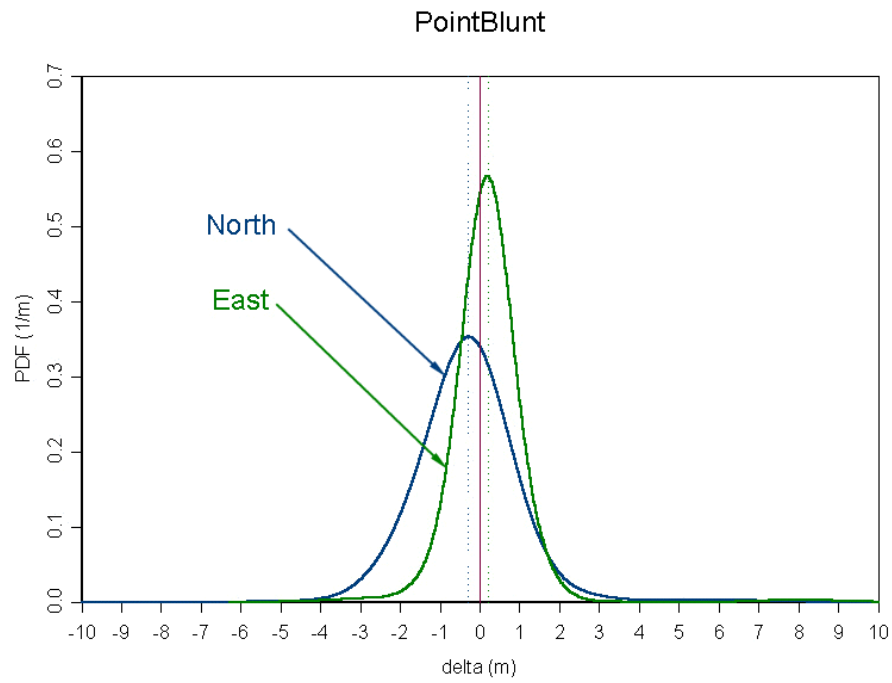
Figure 61   Point Blunt, CA – PDF of ΔNorth and ΔEast Errors
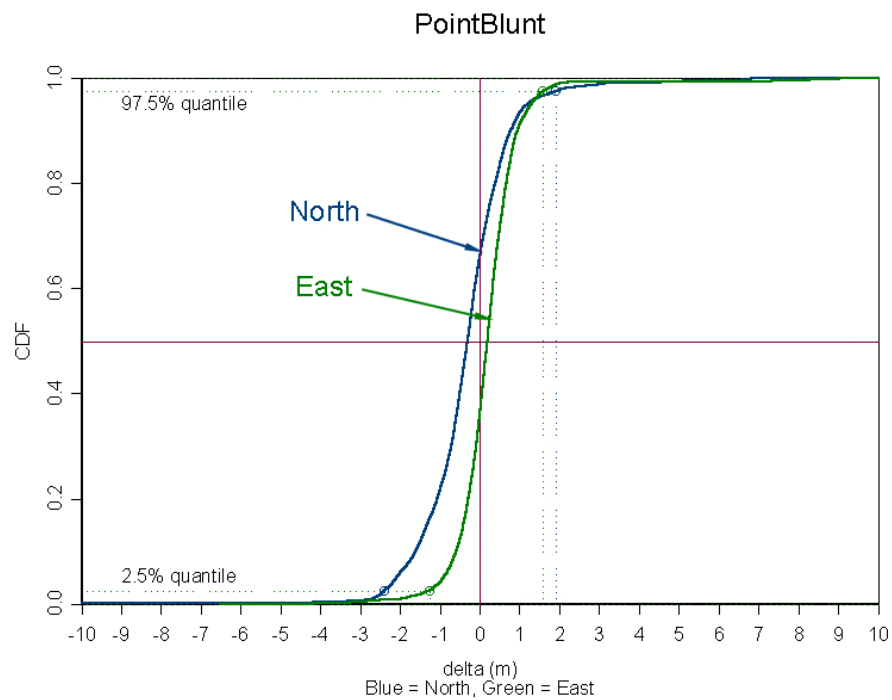
Figure 62   Point Blunt, CA – CDF of ΔNorth and ΔEast Errors with 95% Prediction Interval
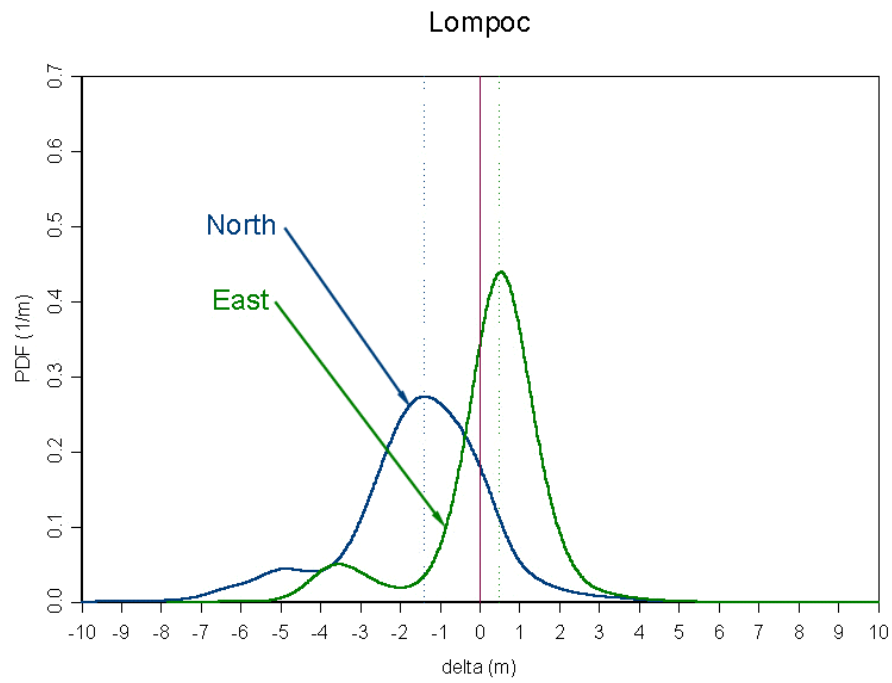
Figure 63   Lompoc, CA – PDF of ΔNorth and ΔEast Errors
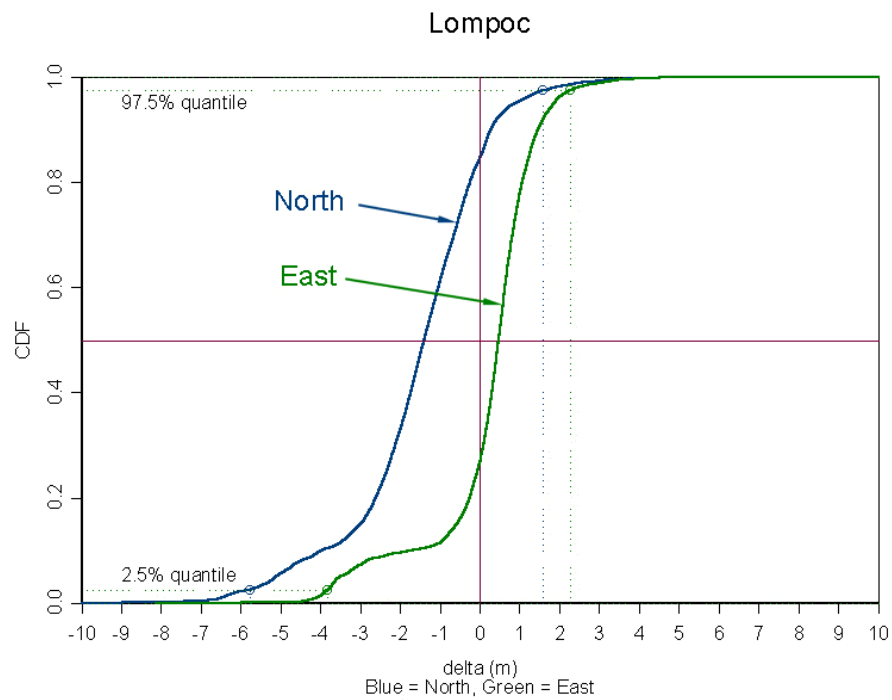
Figure 64   Lompoc, CA – CDF of ΔNorth and ΔEast Errors with 95% Prediction Interval
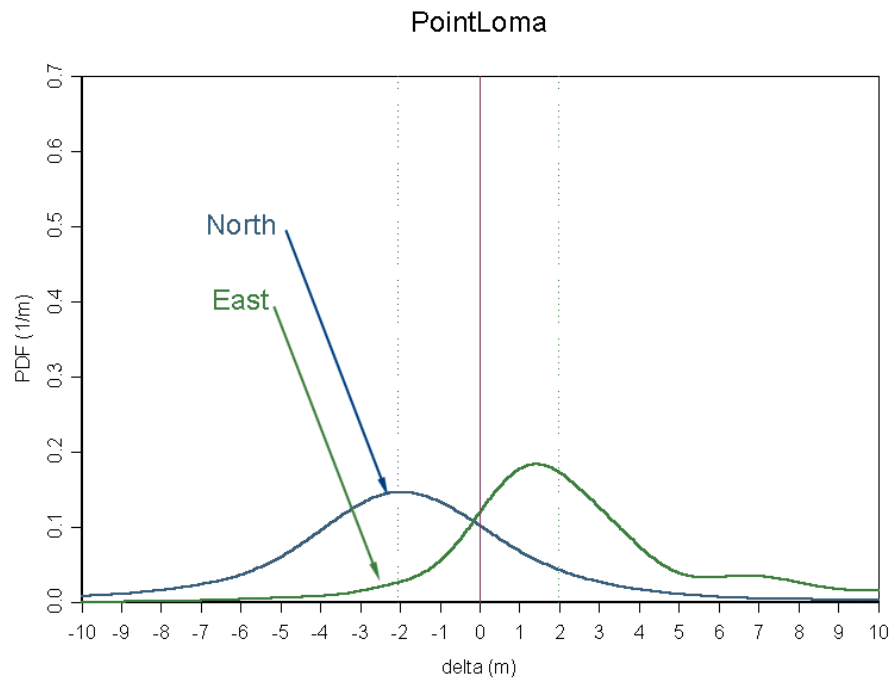
Figure 65   Point Loma, CA – PDF of ΔNorth and ΔEast Errors
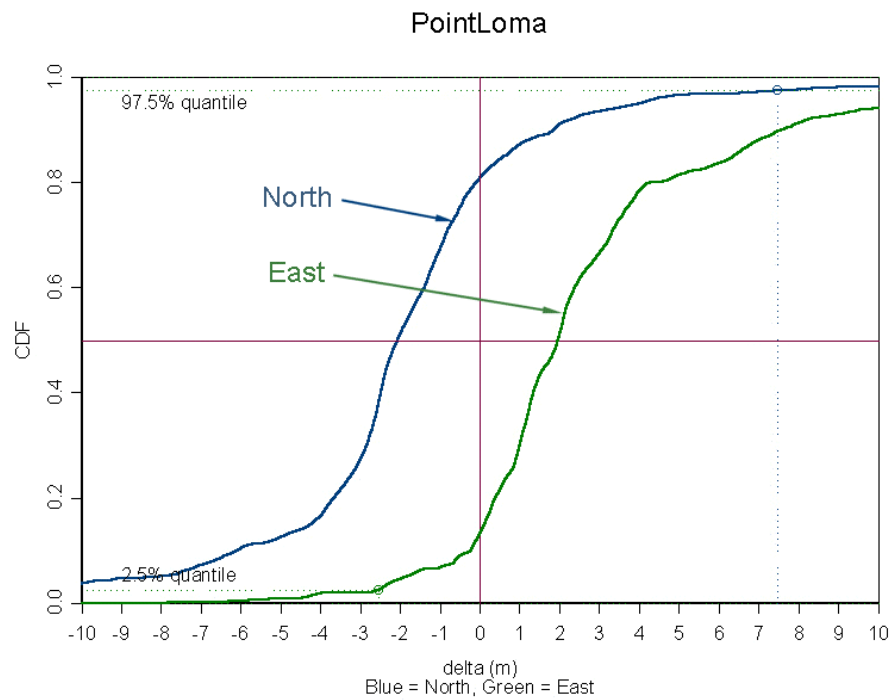
Figure 66   Point Loma, CA – CDF of ΔNorth and ΔEast Errors with 95% Prediction Interval

APPENDIX G. TABLES OF ERRORS FOR USCG DGPS REFERENCE STATIONS

This appendix lists each USCG DGPS reference station summary statistics where $\hat{\mu}$ is the mean and $\hat{\sigma}$ is the standard deviation.

Category (all times local)	ΔNorth (meters)	ΔEast (meters)	ΔUp (meters)	2drms (meters)	3D error (2σ) (meters)	# Observed Satellites	HDOP	PDOP	σ_UERE (meters)
Dawn (0500-1000)	$\hat{\mu}=0.78$ $\hat{\sigma}=2.30$	$\hat{\mu}=0.69$ $\hat{\sigma}=1.87$	$\hat{\mu}=-2.51$ $\hat{\sigma}=4.79$	6.28	12.51	$\hat{\mu}=6.3$ $\hat{\sigma}=0.9$	$\hat{\mu}=1.7$ $\hat{\sigma}=0.5$	$\hat{\mu}=2.9$ $\hat{\sigma}=1.1$	$\hat{\mu}=1.29$ $\hat{\sigma}=1.21$
Day (1000-1800)	$\hat{\mu}=1.31$ $\hat{\sigma}=2.75$	$\hat{\mu}=0.82$ $\hat{\sigma}=0.98$	$\hat{\mu}=-1.51$ $\hat{\sigma}=2.91$	6.61	9.31	$\hat{\mu}=5.9$ $\hat{\sigma}=1.0$	$\hat{\mu}=1.7$ $\hat{\sigma}=0.5$	$\hat{\mu}=3.4$ $\hat{\sigma}=1.3$	$\hat{\mu}=1.56$ $\hat{\sigma}=1.11$
Twilight (1800-2300)	$\hat{\mu}=1.72$ $\hat{\sigma}=1.27$	$\hat{\mu}=1.08$ $\hat{\sigma}=0.97$	$\hat{\mu}=-1.25$ $\hat{\sigma}=2.74$	5.17	7.94	$\hat{\mu}=6.4$ $\hat{\sigma}=1.1$	$\hat{\mu}=1.4$ $\hat{\sigma}=0.4$	$\hat{\mu}=2.6$ $\hat{\sigma}=0.8$	$\hat{\mu}=1.65$ $\hat{\sigma}=0.96$
Night (2300-0500)	$\hat{\mu}=0.28$ $\hat{\sigma}=1.76$	$\hat{\mu}=0.62$ $\hat{\sigma}=0.82$	$\hat{\mu}=-2.38$ $\hat{\sigma}=2.95$	4.11	8.63	$\hat{\mu}=7.0$ $\hat{\sigma}=1.3$	$\hat{\mu}=1.6$ $\hat{\sigma}=0.7$	$\hat{\mu}=2.8$ $\hat{\sigma}=0.9$	$\hat{\mu}=1.14$ $\hat{\sigma}=0.64$

Table 8   Appleton, WA – USCG DGPS Error Table

Category (all times local)	$\Delta North$ (meters)	$\Delta East$ (meters)	ΔUp (meters)	2drms (meters)	3D error (2σ) (meters)	# Observed Satellites	HDOP	PDOP	σ_{UERE} (meters)
Dawn (0500-1000)	$\hat{\mu} = 0.43$ $\hat{\sigma} = 1.43$	$\hat{\mu} = -0.64$ $\hat{\sigma} = 0.72$	$\hat{\mu} = -1.36$ $\hat{\sigma} = 1.88$	3.55	5.85	$\hat{\mu} = 6.5$ $\hat{\sigma} = 1.3$	$\hat{\mu} = 1.4$ $\hat{\sigma} = 0.5$	$\hat{\mu} = 2.5$ $\hat{\sigma} = 0.8$	$\hat{\mu} = 1.20$ $\hat{\sigma} = 0.73$
Day (1000-1800)	$\hat{\mu} = 1.17$ $\hat{\sigma} = 1.28$	$\hat{\mu} = -1.46$ $\hat{\sigma} = 0.71$	$\hat{\mu} = -0.75$ $\hat{\sigma} = 2.12$	4.75	6.54	$\hat{\mu} = 7.3$ $\hat{\sigma} = 1.1$	$\hat{\mu} = 1.3$ $\hat{\sigma} = 0.4$	$\hat{\mu} = 2.3$ $\hat{\sigma} = 0.7$	$\hat{\mu} = 1.98$ $\hat{\sigma} = 0.91$
Twilight (1800-2300)	$\hat{\mu} = 1.28$ $\hat{\sigma} = 0.86$	$\hat{\mu} = -0.06$ $\hat{\sigma} = 0.73$	$\hat{\mu} = -0.17$ $\hat{\sigma} = 2.05$	3.41	5.35	$\hat{\mu} = 7.6$ $\hat{\sigma} = 1.1$	$\hat{\mu} = 1.1$ $\hat{\sigma} = 0.2$	$\hat{\mu} = 2.0$ $\hat{\sigma} = 0.6$	$\hat{\mu} = 1.40$ $\hat{\sigma} = 0.77$
Night (2300-0500)	$\hat{\mu} = 0.87$ $\hat{\sigma} = 1.07$	$\hat{\mu} = -0.08$ $\hat{\sigma} = 0.71$	$\hat{\mu} = -1.24$ $\hat{\sigma} = 2.08$	3.11	5.75	$\hat{\mu} = 7.8$ $\hat{\sigma} = 1.4$	$\hat{\mu} = 1.2$ $\hat{\sigma} = 0.3$	$\hat{\mu} = 2.2$ $\hat{\sigma} = 0.6$	$\hat{\mu} = 1.23$ $\hat{\sigma} = 0.61$

Table 9   Cape Mendocino, CA – USCG DGPS Error Table

Category (all times local)	ΔNorth (meters)	ΔEast (meters)	ΔUp (meters)	2drms (meters)	3D error (2σ) (meters)	# Observed Satellites	HDOP	PDOP	σ_{UERE} (meters)
Dawn (0500-1000)	$\hat{\mu} = -0.08$ $\hat{\sigma} = 0.99$	$\hat{\mu} = 0.41$ $\hat{\sigma} = 0.62$	$\hat{\mu} = -0.23$ $\hat{\sigma} = 1.64$	2.48	4.14	$\hat{\mu} = 6.7$ $\hat{\sigma} = 0.9$	$\hat{\mu} = 1.3$ $\hat{\sigma} = 0.3$	$\hat{\mu} = 2.5$ $\hat{\sigma} = 0.7$	$\hat{\mu} = 0.85$ $\hat{\sigma} = 0.49$
Day (1000-1800)	$\hat{\mu} = 0.01$ $\hat{\sigma} = 1.24$	$\hat{\mu} = 0.34$ $v = 0.63$	$\hat{\mu} = 0.13$ $\hat{\sigma} = 2.16$	2.86	5.19	$\hat{\mu} = 7.2$ $\hat{\sigma} = 1.1$	$\hat{\mu} = 1.2$ $\hat{\sigma} = 0.3$	$\hat{\mu} = 2.3$ $\hat{\sigma} = 0.8$	$\hat{\mu} = 1.03$ $\hat{\sigma} = 0.55$
Twilight (1800-2300)	$\hat{\mu} = 0.11$ $\hat{\sigma} = 0.72$	$\hat{\mu} = 0.65$ $\hat{\sigma} = 0.61$	$\hat{\mu} = 0.22$ $\hat{\sigma} = 1.47$	2.30	3.76	$\hat{\mu} = 7.2$ $\hat{\sigma} = 1.1$	$\hat{\mu} = 1.2$ $\hat{\sigma} = 0.3$	$\hat{\mu} = 2.2$ $\hat{\sigma} = 0.6$	$\hat{\mu} = 0.84$ $\hat{\sigma} = 0.45$
Night (2300-0500)	$\hat{\mu} = 0.03$ $\hat{\sigma} = 0.81$	$\hat{\mu} = 0.68$ $\hat{\sigma} = 0.66$	$\hat{\mu} = -0.43$ $\hat{\sigma} = 1.22$	2.49	3.59	$\hat{\mu} = 8.0$ $\hat{\sigma} = 1.1$	$\hat{\mu} = 1.2$ $\hat{\sigma} = 0.3$	$\hat{\mu} = 2.2$ $\hat{\sigma} = 0.5$	$\hat{\mu} = 0.87$ $\hat{\sigma} = 0.46$

Table 10   Chico, CA – USCG DGPS Error Table

Category (all times local)	ΔNorth (meters)	ΔEast (meters)	ΔUp (meters)	2drms (meters)	3D error (2σ) (meters)	# Observed Satellites	HDOP	PDOP	σ_{UERE} (meters)
Dawn (0500-1000)	$\hat{\mu}=-0.69$ $\hat{\sigma}=1.79$	$\hat{\mu}=-0.21$ $\hat{\sigma}=1.92$	$\hat{\mu}=-0.10$ $\hat{\sigma}=3.36$	5.44	8.65	$\hat{\mu}=6.6$ $\hat{\sigma}=1.0$	$\hat{\mu}=1.4$ $\hat{\sigma}=0.4$	$\hat{\mu}=2.4$ $\hat{\sigma}=0.8$	$\hat{\mu}=1.37$ $\hat{\sigma}=1.52$
Day (1000-1800)	$\hat{\mu}=-0.69$ $\hat{\sigma}=1.76$	$\hat{\mu}=-0.07$ $\hat{\sigma}=1.34$	$\hat{\mu}=0.21$ $\hat{\sigma}=2.64$	4.64	7.04	$\hat{\mu}=7.0$ $\hat{\sigma}=1.2$	$\hat{\mu}=1.3$ $\hat{\sigma}=0.4$	$\hat{\mu}=2.4$ $\hat{\sigma}=0.8$	$\hat{\mu}=1.26$ $\hat{\sigma}=1.13$
Twilight (1800-2300)	$\hat{\mu}=0.06$ $\hat{\sigma}=0.99$	$\hat{\mu}=0.49$ $\hat{\sigma}=0.90$	$\hat{\mu}=-0.03$ $\hat{\sigma}=2.22$	2.85	5.28	$\hat{\mu}=7.0$ $\hat{\sigma}=1.1$	$\hat{\mu}=1.3$ $\hat{\sigma}=0.3$	$\hat{\mu}=2.3$ $\hat{\sigma}=0.7$	$\hat{\mu}=0.80$ $\hat{\sigma}=0.58$
Night (2300-0500)	$\hat{\mu}=-0.38$ $\hat{\sigma}=1.18$	$\hat{\mu}=0.38$ $\hat{\sigma}=0.64$	$\hat{\mu}=-0.56$ $\hat{\sigma}=1.62$	2.89	4.48	$\hat{\mu}=7.7$ $\hat{\sigma}=1.2$	$\hat{\mu}=1.3$ $\hat{\sigma}=0.5$	$\hat{\mu}=2.3$ $\hat{\sigma}=0.7$	$\hat{\mu}=0.87$ $\hat{\sigma}=0.52$

Table 11   Pigeon Point, CA – USCG DGPS Error Table

Category (all times local)	$\Delta North$ (meters)	$\Delta East$ (meters)	ΔUp (meters)	2drms (meters)	3D error (2σ) (meters)	# Observed Satellites	HDOP	PDOP	σ_{UERE} (meters)
Dawn (0500-1000)	$\hat{\mu}=-0.43$ $\hat{\sigma}=1.02$	$\hat{\mu}=-0.05$ $\hat{\sigma}=0.70$	$\hat{\mu}=0.38$ $\hat{\sigma}=1.43$	2.62	3.95	$\hat{\mu}=6.9$ $\hat{\sigma}=0.8$	$\hat{\mu}=1.3$ $\hat{\sigma}=0.3$	$\hat{\mu}=2.2$ $\hat{\sigma}=0.5$	$\hat{\mu}=0.86$ $\hat{\sigma}=0.48$
Day (1000-1800)	$\hat{\mu}=-0.29$ $\hat{\sigma}=1.90$	$\hat{\mu}=0.05$ $\hat{\sigma}=1.32$	$\hat{\mu}=-0.24$ $\hat{\sigma}=4.09$	4.66	9.43	$\hat{\mu}=7.2$ $\hat{\sigma}=1.2$	$\hat{\mu}=1.2$ $\hat{\sigma}=0.3$	$\hat{\mu}=2.3$ $\hat{\sigma}=0.9$	$\hat{\mu}=1.16$ $\hat{\sigma}=1.21$
Twilight (1800-2300)	$\hat{\mu}=-0.23$ $\hat{\sigma}=0.69$	$\hat{\mu}=0.42$ $\hat{\sigma}=0.61$	$\hat{\mu}=-0.10$ $\hat{\sigma}=1.89$	2.08	4.32	$\hat{\mu}=6.9$ $\hat{\sigma}=1.1$	$\hat{\mu}=1.2$ $\hat{\sigma}=0.3$	$\hat{\mu}=2.3$ $\hat{\sigma}=0.7$	$\hat{\mu}=0.65$ $\hat{\sigma}=0.37$
Night (2300-0500)	$\hat{\mu}=-0.41$ $\hat{\sigma}=0.82$	$\hat{\mu}=0.33$ $\hat{\sigma}=0.61$	$\hat{\mu}=-0.31$ $\hat{\sigma}=1.31$	2.30	3.54	$\hat{\mu}=7.9$ $\hat{\sigma}=1.1$	$\hat{\mu}=1.2$ $\hat{\sigma}=0.3$	$\hat{\mu}=2.2$ $\hat{\sigma}=0.5$	$\hat{\mu}=0.73$ $\hat{\sigma}=0.46$

Table 12   Point Blunt, CA – USCG DGPS Error Table

Category (all times local)	ΔNorth (meters)	ΔEast (meters)	ΔUp (meters)	2drms (meters)	3D error (2σ) (meters)	# Observed Satellites	HDOP	PDOP	σ_{UERE} (meters)
Dawn (0500-1000)	$\hat{\mu} = -2.35$ $\hat{\sigma} = 1.93$	$\hat{\mu} = -0.40$ $\hat{\sigma} = 1.89$	$\hat{\mu} = 0.51$ $\hat{\sigma} = 2.07$	7.21	8.37	$\hat{\mu} = 7.0$ $\hat{\sigma} = 1.2$	$\hat{\mu} = 1.3$ $\hat{\sigma} = 0.4$	$\hat{\mu} = 2.3$ $\hat{\sigma} = 0.7$	$\hat{\mu} = 2.56$ $\hat{\sigma} = 2.06$
Day (1000-1800)	$\hat{\mu} = -2.02$ $\hat{\sigma} = 1.58$	$\hat{\mu} = 0.26$ $\hat{\sigma} = 1.43$	$\hat{\mu} = 0.32$ $\hat{\sigma} = 2.31$	5.90	7.52	$\hat{\mu} = 7.2$ $\hat{\sigma} = 1.2$	$\hat{\mu} = 1.3$ $\hat{\sigma} = 0.5$	$\hat{\mu} = 2.4$ $\hat{\sigma} = 0.9$	$\hat{\mu} = 2.11$ $\hat{\sigma} = 1.37$
Twilight (1800-2300)	$\hat{\mu} = -0.62$ $\hat{\sigma} = 0.91$	$\hat{\mu} = 0.83$ $\hat{\sigma} = 0.70$	$\hat{\mu} = -0.57$ $\hat{\sigma} = 1.96$	3.09	5.12	$\hat{\mu} = 7.6$ $\hat{\sigma} = 1.1$	$\hat{\mu} = 1.2$ $\hat{\sigma} = 0.3$	$\hat{\mu} = 2.1$ $\hat{\sigma} = 0.6$	$\hat{\mu} = 1.13$ $\hat{\sigma} = 0.63$
Night (2300-0500)	$\hat{\mu} = -0.46$ $\hat{\sigma} = 1.34$	$\hat{\mu} = 0.41$ $\hat{\sigma} = 0.60$	$\hat{\mu} = -1.21$ $\hat{\sigma} = 2.03$	3.18	5.70	$\hat{\mu} = 7.9$ $\hat{\sigma} = 1.2$	$\hat{\mu} = 1.2$ $\hat{\sigma} = 0.5$	$\hat{\mu} = 2.3$ $\hat{\sigma} = 0.7$	$\hat{\mu} = 1.18$ $\hat{\sigma} = 0.81$

Table 13   Lompoc, CA – USCG DGPS Error Table

Category (all times local)	$\Delta North$ (meters)	$\Delta East$ (meters)	ΔUp (meters)	2drms (meters)	3D error (2σ) (meters)	# Observed Satellites	HDOP	PDOP	σ_{UERE} (meters)
Dawn (0500-1000)	$\hat{\mu}=-3.35$ $\hat{\sigma}=2.57$	$\hat{\mu}=0.13$ $\hat{\sigma}=2.61$	$\hat{\mu}=-6.96$ $\hat{\sigma}=2.61$	9.93	17.88	$\hat{\mu}=5.3$ $\hat{\sigma}=1.1$	$\hat{\mu}=1.8$ $\hat{\sigma}=0.4$	$\hat{\mu}=3.2$ $\hat{\sigma}=1.1$	$\hat{\mu}=2.42$ $\hat{\sigma}=1.27$
Day (1000-1800)	$\hat{\mu}=-3.96$ $\hat{\sigma}=5.25$	$\hat{\mu}=4.26$ $\hat{\sigma}=3.44$	$\hat{\mu}=-3.09$ $\hat{\sigma}=8.28$	17.11	24.60	$\hat{\mu}=6.2$ $\hat{\sigma}=1.0$	$\hat{\mu}=1.5$ $\hat{\sigma}=0.5$	$\hat{\mu}=3.0$ $\hat{\sigma}=0.9$	$\hat{\mu}=4.40$ $\hat{\sigma}=3.00$
Twilight (1800-2300)	$\hat{\mu}=-3.20$ $\hat{\sigma}=4.38$	$\hat{\mu}=5.81$ $\hat{\sigma}=4.75$	$\hat{\mu}=-8.62$ $\hat{\sigma}=7.24$	18.52	29.15	$\hat{\mu}=5.0$ $\hat{\sigma}=0.7$	$\hat{\mu}=2.0$ $\hat{\sigma}=0.5$	$\hat{\mu}=3.5$ $\hat{\sigma}=1.2$	$\hat{\mu}=4.75$ $\hat{\sigma}=3.40$
Night (2300-0500)	$\hat{\mu}=-0.14$ $\hat{\sigma}=3.24$	$\hat{\mu}=1.16$ $\hat{\sigma}=1.66$	$\hat{\mu}=-1.59$ $\hat{\sigma}=2.52$	7.65	9.69	$\hat{\mu}=7.0$ $\hat{\sigma}=1.3$	$\hat{\mu}=1.6$ $\hat{\sigma}=0.7$	$\hat{\mu}=2.8$ $\hat{\sigma}=1.0$	$\hat{\mu}=1.60$ $\hat{\sigma}=0.93$

Table 14   Point Loma, CA – USCG DGPS Error Table

THIS PAGE INTENTIONALLY LEFT BLANK

APPENDIX H. PIGEON POINT VISIT

To examine the equipment setup and receiver settings at a typical USCG DGPS reference station, a visit was completed to the USCG Pigeon Point, California; DGPS reference station on August 19, 2002.

Figure 67   USCG Pigeon Point DGPS Reference Station

In theory and practice, each USCG Differential GPS reference station has the exact same system layout and operation. The following equipment is the standard and can been seen in Figure 67.

Control Building
MF Transmission Tower
Primary Receiver Antenna
Secondary Receiver Antenna

Adapted from marine Radionavigation beacons, which pre-existed DGPS technology, the MF transmission tower and broadcasting equipment were already established and operating as an aid to navigation. Each GPS receiver benchmark (see Figure 68) has two antennas, including a separate integrity monitor to warn if the system has failed. Both primary and secondary receivers and integrity monitors are connected to an Uninterruptible Power Supply (UPS) to prevent system shutdown due to instantaneous power fluctuations.

Figure 68   Typical USCG DGPS Receiver Antenna Layout

During the visit, a close inspection of the base station receiver settings was recorded. These settings exactly matched the NAVCEN webpage reported settings. The settings were capable of being updated remotely via a modem attached to the system. These settings are remotely maintained by the USCG Command and Control Center (C2CEN) in Portsmouth, Virginia.

BIBLIOGRAPHY

Abousalem, M. Development and Analysis of Wide Area Differential GPS Algorithms. Ph. D. Dissertation, Department of Geomatics Engineering, The University of Calgary, Calgary, 1996.

Ashtech Receiver Communication Software *User's Guide*

Bowditch, Nathaniel, LL. D. The American Practical Navigator Defense Mapping Agency Hydrographic / Topographic Center, Bethesda, 1995.

Brown, Alison. Extended Differential GPS Navigation: Journal of The Institute of Navigation, 1989.

Cleveland, William S. Robust Locally Weighted Regression and Smoothing Scatterplots Journal of the American Statistical Association, Volume 74, Number 368, December 1979.

Davies, Kenneth Ionospheric Radio Peter Peregrinus, London, 1990.

Department of Defense / Department of Transportation 2001 Federal Radionavigation Plan National Technical Information Service, Springfield, March 2002.

Forssell, Börje Radionavigation Systems Prentice Hall, Hertfordshire, 1991.

Hoffmann-Wellenhof, Bernhard, et al. GPS Theory and Practice Springer-Verlag, Wein, 1997.

Kaplan, Elliott D. Understanding GPS Principles and Applications Artech House, Norwood, 1996.

Lindy, Fred. Differential Solutions Using Long-Range Dual Frequency GPS Correction Data Naval Postgraduate School, Monterey, 2002.

Logsdon, Tom The NAVSTAR Global Positioning System Van Nostrand Reinhold, New York, 1992.

Martin, E. H. "GPS User Equipment Error Models," Global Positioning System Papers Vol. I, Institute of Navigation, Washington D.C., 1980.

Monroe, Jeffrey W. and Bushy, Thomas L. Marine Radionavigation and Communications Cornell Maritime Press, Centreville, 1998.

NAVSTAR GPS Space Segment / Navigation User Interfaces ICD-GPS-200 rev. C, 4 March 2002.

Parkinson, Bradford W., Spilker James J. Jr., et al. Global Positioning System: Theory and Applications Volume I American Institute of Aeronautics and Astronautics, Washington DC, 1996.

Parkinson, Bradford W., Spilker James J. Jr., et al. Global Positioning System: Theory and Applications Volume II American Institute of Aeronautics and Astronautics, Washington DC, 1996.

RTCM Special Committee No. 104. RTCM Recommended Standards for Differential GNSS (Global Navigation Satellite Systems) Service Version 2.2, Radio Technical Commission For Maritime Services, Alexandria, 1998.

Secretary of Transportation National Civilian GPS Services US Department of Transportation, Washington DC, March 21, 2000.

USCG Commandant Instruction M16577.1 Differential Global Positioning System Broadcast Standard US Department of Transportation, Washington, 21 April 1993.

Valley, Shea L., et al. <u>Handbook of Geophysics and Space Environments</u> Air Force Cambridge Research Laboratories, Bedford, 1965.

INITIAL DISTRIBUTION LIST

1.   Defense Technical Information Center
        Ft. Belvoir, Virginia

2.   Dudley Knox Library
        Naval Postgraduate School
        Monterey, California

3.   James R. Clynch
        Oceanography Department
        Naval Postgraduate School
        Monterey, California

4.   James Eagle
        Operations Research Department
        Naval Postgraduate School
        Monterey, California

5.   Mr. David Deveau
        Naval Undersea Warfare Center
        Atlantic Undersea Test and Evaluation Center
        Andros Island, Bahamas

6.   T. Kelly-Bissonnettee
        Naval Undersea Warfare Center Division Newport
        NWWCDIVNPT Code 7005
        1176 Howell Street
        Newport, Rhode Island 02841-1708

7.   Bryant Wynn
        Global Positioning System – Joint Program Office
        2420 Vela Way, Suite 1467
        El Segundo, CA 90245-4659

8.   Carderock Division, Naval Surface Warfare Center
        9500 MacArthur Boulevard
        West Bethesda, Maryland 20817-5700

9.   United States Coast Guard, NAVCEN
        7323 Telegraph Road
        Alexandria, Virginia 22315

10.   National Geodetic Survey
        NOAA, N/NGS12